GEOPHYSICAL EXPLORATION FOR GOLD IN NORTHERN NEVADA

James L. Wright, Manager, Geophysical Operations, NV, Newmont Mining Corp., Carlin, NV
Chester S. Lide, Managing Geophysicist, Zonge Geosciences Inc., Reno, Nevada

TABLE OF CONTENTS

INTRODUCTION

Gold exploration in northern Nevada spans some 150 years with modern exploration methodologies being applied since gold's deregulation in 1973. Exploration over the last twenty years has generated a tremendous number of discoveries containing reserves in excess of 150 million ounces. The role of geophysics in the early part of this twenty-year period was mainly one of support, confirmation, and testing. Outcropping or thinly covered deposits were readily discovered with geologic and/or geochemical methods leaving little need for application of geophysics. However, in the last five years depletion of shallow targets has forced exploration into covered areas and to depth within bedrock. With this evolution geophysics has assumed a more prominent role. As would be expected, the specific application of geophysics to any exploration effort is completely dependent upon the geologic characteristics of the deposit sought *and* the surrounding rock mass. The recognition that geophysics may map both a deposit and/or its geologic surroundings is very important and leads to the concepts of direct and indirect detection.

GEOPHYSICAL EXPLORATION CONCEPTS

Direct detection is predicated upon the ability of geophysics to map some physical characteristic of a deposit with sufficient resolution as to allow a reasonable chance for discovery. That is, a deposit is *anomalous* in some physical parameter. A fine example is the extremely conductive nature of volcanogenic massive sulfide (VMS) deposits. Indirect detection is defined identically except geophysics in this case maps some feature related to the deposit – not the deposit itself. For example, lead – zinc deposits in southeast Missouri occur near basement uplifts, which can be delineated by both gravity and magnetics. By its very nature indirect detection is generally less successful than direct. The key to successful application of either approach is for the response to be clearly *anomalous* (i.e. deviating from the regular arrangement, general rule, or usual pattern). Direct and indirect detection need not be mutually exclusive. Indeed, a combined application can greatly enhance the exploration program and upgrade a target's anomalous measure. Furthermore, an ore deposit need not be anomalous in only one direct or indirect parameter. Doyle (1990) and Corbett (1991) observe that exploration for gold is one of the most difficult applications for geophysics; one fraught with uncertainty. The uncertainty springs from the wide variety of anomalous responses related to alteration and the geologic environment. However, with this variety comes unprecedented opportunity for geophysics to contribute to an exploration program. A number of examples are presented which span the direct versus indirect detection spectrum and clearly demonstrate the advantage of a combined approach.

Application of geophysics to any exploration program must first, and foremost, be based upon an understanding of the geologic setting and characteristics of the target deposit. Outlined in the following section are characteristics of several deposit types found in northern Nevada. As to the geologic setting in northern Nevada, a multitude of references covers this subject. Nonetheless, some observations concerning the geologic setting as pertaining specifically to geophysics are of merit. Tabulated below are some generalized observations, which are applicable in most cases; but exceptions are possible.

- Paleozoic sediments are non-magnetic, thus all magnetic anomalies are caused by volcanics, intrusives, alteration or Tertiary / Quaternary sediments.
- Volcanic units are often strongly remanently magnetic and can occur within basin fill sediments.

- Carbonate units are denser than clastic or siliciclastic sediments with dolomite being denser than limestone. Facies variations, to be expected westward, may invalidate this assumption.
- Basin and Range extension has reactivated older structures.
- Sediments filling valleys are derived locally and of recent (i.e. Tertiary and/or Quaternary) origin.
- Variations within basin fill sediments can be mapped with geophysics and reflect variations within the bedrock at considerable depth.
- The topography is robust, both above and below basins, and can have a profound effect on anomaly shapes. This is particularly true of volcanic lithologies.
- Alteration can manifest itself in a multitude of ways (Corbett, 1991): decreased or increased density, decreased or increased resistivity, decreased or increased IP measure, decreased or increased magnetic susceptibility, decreased or increased resistance to weathering, etc. The style of alteration, and thus its geophysical response, depends upon the type of mineralization and host rocks.
- Carbonaceous and/or sulfidic sediments are abundant in northern Nevada. Proper application of electrical techniques *must* take into consideration the distribution and thermal history of these sediments.

Given a particular style of mineralization and associated alteration it is very feasible to design a geophysical program to detect the alteration ***and*** map associated structures or contacts. This dual approach will optimize exploration for targets in which the alteration is not totally definitive (i.e. indirect detection). Reactivation of older structures and variations of physical properties in overlying sediments are critical to being able to map all structures / contacts associated with mineralization. Delineation of structures and/or alteration is the first step in a process which must include ***strong geologic input***. ***Application of geophysics in a geologic vacuum is dangerous.***

EXPLORATION CONCEPTS AND OBJECTIVES WITH RESPECT TO DEPOSIT TYPE

Four deposit types are discussed: Carlin – Sediment Hosted, Porphyry Related, Volcanic Hosted, and Hot Springs Related. These groupings are defined to span most significant gold deposits in northern Nevada, but are not based upon rigorous geologic definitions. The grouping is loosely modeled on Shawe's (1991) deposit codification. Division of volcanic deposits as either volcanic hosted or hot springs related runs somewhat contrary to Bonham's (1988) classification of low sulfur, high sulfur, and alkalic. Such a scheme does accommodate deposits such as Florida Canyon, which is classified as hot springs related but hosted in non-volcanic sediments (Hastings, et. al., 1988).

CARLIN – SEDIMENT HOSTED

Sediment hosted deposits, as a class, contain the vast majority of gold reserves in northern Nevada. Host rock and structural conduits/preparation are considered essential to formation of these deposits (Teal and Jackson, 1997). Mineralization is commonly classified as stratigraphic or structural depending upon the relative contribution of these two factors (Groves, 1996). Bakken (1990), among others, notes alteration varies depending upon magnitude of the system, host rock, and structural preparation. Carbonate dissolution, argillization, silicification, and sufidation of reactive iron are the primary alteration types associated with a sediment hosted deposit (Christensen, 1993). Teal and Jackson (1997) apply summarize exploration methodology for

these deposits as based upon the concepts of *system*, *structure*, and, *host*. Geophysics, in turn, has been applied to detecting or mapping these features. Direct detection would target the system and it's associated alteration signature. Indirect detection targets the host and structure, or more specifically the intersection of the two.

Structural mapping is the principal application for geophysics in exploration for Carlin-type gold deposits. Lithologic and alteration mapping are important secondary applications. North-to-northwest trending faults are described as the primary conduits for gold mineralization in all sub-districts on the Carlin Trend (Teal and Jackson, 1997) and intersections of these features with northeast trending faults are important on the deposit scale. Mineralization in the Twin Creeks (Bloomstein, et al, 1991), Lonetree (Braginton, per. comm.), Archimedes (Dilles, et al., 1996), Pipeline (Foo, et al., 1996) and Jerritt Canyon (Daly et al., 1991) deposits is also strongly controlled by folding and faulting. **Every major ore controlling fault, in every major sediment hosted deposit in northern Nevada, can be delineated with proper application of the available geophysical tools, provided good geologic support is available.** Of course, there are a multitude of structures unrelated to gold deposits**.** Geologic control is essential to unraveling this complexity.

Geophysical methods have met with little success in directly detecting Carlin-type deposits for several reasons. The classic Carlin-type deposit is an oxidized, strata-form ore body. The oxidized ore bodies are generally devoid of pyrite and carbonaceous material while the unaltered host rocks often contain syngenetic pyrite and carbonaceous material making application of IP a questionable endeavor. In addition, prior to the discovery of deeper high-grade sulfide mineralization, the presence of sulfides was undesirable. A notable exception is Barrick's (Bettles and Kornze, 1996) reported IP contribution to the discovery of the Betze and Screamer deposits. Numerous EM methods were attempted in the 1970's, but most were frequency-domain systems designed for massive sulfide exploration in resistive terrain. These systems were capable of mapping shallow structure in areas of thin alluvial cover. As exploration moved out into areas of moderate to thick alluvial cover, these systems quickly became obsolete. As with IP, the mapping of resistivity to directly detect the deposit must contend with overburden variations, variation of oxidation levels and complex lithologic/structural relationships, all of which can produce resistivity anomalies indistinguishable from that generated by an ore body. Finally, Carlin-type deposits do not exhibit anomalous densities or magnetic susceptibilities. The initial failure of geophysics to *directly* detect Carlin-type deposits lead to a perception that geophysics was generally inapplicable to such exploration efforts. At Newmont, in the early 1990's, it became clear geophysics offered great potential for indirect detection, specifically as a structural mapping tool to aid the geologist; and in certain cases direct detection was possible, if sufficient constraints could be imposed to limit target possibilities. Application of geophysics to Carlin-type deposits has evolved from a simplistic anomaly finding exercise to an integrated multi-technique approach requiring rigorous integration of geology, geochemistry and geophysical.

CARLIN – SEDIMENT HOSTED SUMMARY

- Indirect detection methods predominate the use of geophysics for sediment hosted deposits.
- Structure, lithology, and alteration, in descending order, are the features delineated by geophysics.
- Specific targets can be developed only with tight integration of geology and geochemistry with the geophysics.
- Direct detection is possible, if geologic controls are good and multiple data sets can constrain target possibilities.

PORPHYRY RELATED

Gold mineralization related to intrusive rocks, specifically porphyritic intrusions, is certainly a broad and complex topic; one for which a complete technical understanding is still forthcoming. One can crudely categorize gold mineralization associated with such intrusions as skarn hosted, vein hosted, or lodes and breccias (Sillitoe, 1988). Structural elements can control intrusive placement and channeling of mineralizing fluids (Wotruba, 1988). Kuyper (1988) notes faults controlled emplacement of the Brown Stock at the McCoy deposit and played an important role in localizing both high and low grade mineralization.

The intrusion provides a large detectable target, which can focus the exploration effort. Magnetic surveys are an obvious choice; however, the assumption that all intrusions will respond as compact magnetic highs should be avoided. In northern Nevada, a number of intrusions are weakly to non-magnetic while others are remanently magnetized. A number of the weakly magnetic ones exhibit donut shaped highs surrounding the intrusion. These high rims are reflecting alteration proximal to the intrusion. The Fortitude skarn was discovered by drilling a localized high within a magnetic rim. Volcanic rocks can have a highly variable, large amplitude magnetic signature, making intrusions emplaced into predominately volcanic hosts difficult to delineate magnetically. The intrusions may also weather recessively to produce bedrock depressions detectable by electrical, seismic, or gravity methods. When a positive magnetic anomaly does accompany an intrusion, it is desirable for the response to be complex. Smooth uniform anomalies generally indicate little hydrothermal activity, only one intrusive surge, and/or lack of retrograde alteration. All these factors tend to increase the complexity of a magnetic anomaly. Skarns can contain significant amounts of both magnetite and pyrrhotite (Kuyper, 1988). Both inductive and remnant effects can be present. Strong magnetic responses, of either polarity, proximal to an intrusion are likely candidates for indicating skarn mineralization.

Electrical methods have played a premier role in porphyry copper exploration and, as such, are excellent tools for delineation of sulfides associated with disseminated gold mineralization. Certainly, a detailed IP survey will map both sulfide and clay distributions aiding greatly in defining the zonation of alteration. Ivosevic and Theodore (1996) note that limits of the Au/Ag zone coincide with limit of iron sulfide mineralization at Upper Paiute Canyon. Skarn mineralization usually contains abundant sulfides, both disseminated and, less commonly, massive. IP and electromagnetic surveys find great utility in mapping these two styles of sulfide emplacement. Indeed, Wotruba et. al. (1988) notes sulfides in the Lower Fortitude ore zone average 10% with localized concentrations reaching 50%. Kuyper (1988) notes disseminated pyrite locally comprising 15-20 % of the exoskarn at McCoy. At McCoy high grade gold occurs as lenses and pods located along intrusive margins, faults, and at intersections of these features. Economic ore bodies can be as small as 10 by 50 by 100 feet. Borehole IP finds great utility for detecting these small bodies. Application of electrical techniques to sulfide mapping in a skarn system is a good example of direct detection. Resistivity mapping, by either electromagnetic or galvanic methods, can also define the various alteration halos associated with a porphyry system. Potassic alteration, under limited cover, will produce strong anomalies detectable with radiometric surveys.

PORPHYRY RELATED SUMMARY

- Direct detection is quite feasible with electrical and magnetic methods, particularly for skarn deposits.
- Mapping of the relatively predictable alteration can lead to near direct detection.

- Owing to extensive alteration and contrasting rock types (i.e. intrusive versus host), structural mapping is very effective.

VOLCANIC HOSTED

Volcanic hosted deposits, as defined herein, would include Rosebud, Sleeper, and Hollister in northern Nevada. These deposits are hosted within volcanics with structural and lithologic controls (Bartlett, et. al., 1991) to mineralization. Variations within the basement, either local highs or offsets, also play a role in localizing mineralization. Mineralization styles include veins, stockworks and breccias (Nash et. al., 1991) with extensive alteration halos extending to considerable distance from the deposits. Alteration suites include propylitic, phyllic, silicic, argillic and opaline. Significant volumes of sulfides ranging up to 25% (Van Nieuwenhuyse, 1991) can occur within certain mineralization/alteration types.

The sulfide and extensive alteration systems present attractive targets for electrical surveys. Induced polarization/resistivity provide a combined survey ideal for sulfide and alteration mapping. In addition, the volcanic host rock would be expected to produce a limited number of spurious background IP anomalies. Generally the presence of pyrite indicates a hydrothermal system, but specific IP targets are less likely to be directly associated with gold. Electromagnetic techniques can map the resistivity as well, but no IP information is produced. However, strong geologic input will be required to aid in unraveling the complex resistivity section produced by overlapping alteration assemblages. Magnetics hold the potential for mapping alteration within enclosing volcanics; however, the magnetic character of volcanics is generally quite variable making recognition of alteration effects problematic. Alteration would manifest itself in the magnetics as localized zones where the magnetics return to background levels, and the internal structure is smooth or muted. Potassium mapping by way of radiometric surveys is idea for delineation of potassic alteration. Unfortunately, depth penetration is limited to the top few inches of surficial material. In northern Nevada, exposed areas of altered material sufficient in size to produce a radiometric anomaly will have already been explored.

Basement delineation is relatively more important in the lower sulfide systems (i.e. Hollister) and in areas with extensive cover, which might render direct detection techniques less definitive. Electromagnetics (i.e. CSAMT), gravity, and to a lesser extent magnetics, all find application in basement mapping. Obviously surveys applied to direct detection will find utility in basement/structural mapping concurrent with the direct detection effort. A well planned exploration program should consider this dual role.

VOLCANIC HOSTED SUMMARY

- Electrical and methods can yield very specific targets, provided sulfides related to the overall hydrothermal system do not produce too many anomalies unrelated to gold.
- Indirect detection via basement mapping and/or alteration is somewhat less definitive.
- Indirect detection based upon mapping of near surface structures can be quite successful.

HOT SPRINGS RELATED

Nelson (1988) identifies eight deposits within Nevada classified as hot springs related. Among these are Florida Canyon, Buckhorn, and Sulfur (i.e. Crowfoot-Lewis). Paradise Peak and Sleeper

are also noted, but the critical sinter association is questionable. Hot springs gold deposits can be typified as silicified breccias and vein stockworks, which contain several volume percent sulfides. Alteration includes silicification, argillization, and adularia proximal to veins and vents. The alteration systems can be extensive covering 20 square km in one instance (Bussey, 1988). Structural control is essential and provides conduits for the ascending hydrothermal fluids. Basin bounding faults are a common local for such deposits. A feature of these deposits, one with important exploration implications, is their very young age. This means most will be near surface or buried beneath limited cover with relatively clear structural features. The limited cover and lack of subsequent structural overprint greatly enhances the chances for successfully applying geophysics.

Most comments concerning the volcanic hosted deposits apply equally well for hot springs related ones. Alteration and sulfide associations are similar, thus electrical and radiometric surveys will find applicability for direct detection. Monroe et. al. (1988) presents a fine example of direct detection with electrical methods at the Buckhorn Deposit. The sinter will provide a very definitive resistivity target, very likely detectable by airborne electromagnetic surveys. Ground surveys will also be excellent for detecting and mapping the sinter. As expected, magnetic methods can be applied in volcanic hosts as with the volcanic hosted deposits. In other hosts the magnetics response would likely be very subtle, probably a weak magnetic low if the host contained some minor magnetic constituent.

HOT SPRINGS RELATED SUMMARY

- Very young age of these deposits implies relatively shallow depth and immunity from structural overprinting. Both features which greatly enhance successful application of geophysics.
- Electrical methods can be applied with excellent chances for direct detection.
- Indirect detection by way of structural mapping is also very effective.
- Probably the deposit class most amenable to direct geophysical detection.

DEPOSIT TYPE EXAMPLES:

Figure 1 presents locations for seven deposits within northern Nevada. These examples demonstrate geophysical methods as applied to the four deposit categories previously defined. Each example includes a number of geophysical products with supporting geology. Observations are drawn concerning the technical and cost effectiveness of a given technique, restrictions upon application, and likely problems to be encountered.

CARLIN – SEDIMENT HOSTED

NORTH AREA

Figures 2, 3, 4 from Wright (1996) present gravity, aeromagnetic, and topography over a twenty kilometer square covering the northern portion of the Carlin trend. Figures 5 and 6 present geology and a generalized stratigraphic column for the area. Some 50 million ounces of reserves are contained within the survey area. Figure 7 presents selected geologic features, ore deposit outlines (Teal and Jackson, 1997), and line/area designators pertinent to the following review.

The stratigraphic column, specific to the Carlin mine, is also applicable to the northern Carlin trend. The lower carbonate section (i.e. Roberts Mtn. and Popovich Fm.) is generally denser than

the overlying siliciclastic units (i.e. Rodeo Creek and Vinini Fm.). In turn, the tertiary cover and basin fill unit (i.e. Carlin Fm.) are less dense than either. All bedrock units are essentially non-magnetic with the Carlin Fm. being weakly inductively magnetic. Intrusive lithologies (i.e. Goldstrike Int.) are moderately inductively magnetic. Tertiary volcanic units, located to the west and northwest of the trend, can be strongly remanently magnetic. Wright (1996) gives further details concerning the density and magnetic susceptibility of these units. Both the carbonate and overlying siliciclastic units are carbonaceous and contain syngenetic sulfides. This coupled with the intrusive activity in the northern Carlin trend has had a profound effect upon the effectiveness of electrical methods in the northern and central Carlin trend. The intrusive activity mobilized carbon pushing substantial portions into "carbon fronts" proximal to intrusive bodies and maturating the carbon to graphite. Couple this with a complex structural setting, differential weathering along structures, addition of sulfides and remobilization of existing sulfides by hydrothermal activity related to gold mineralization and what has resulted is an area of extreme electrical variability (i.e. IP & resistivity). It has proven difficult to employ electrical methods for direct detection of sulfides related to gold mineralization in such a chaotic electrical environment.

Tabulated below are various features noted in the aeromagnetic and gravity data sets.

AEROMAGNETIC

- Intrusive Mapping: Goldstrike, Little Boulder Basin (LBB), and Vivian intrusions; as well as the northern extremes of the deep-seated Mary's Mountain intrusive complex.
- Volcanic Mapping: Remnantly magnetized volcanics southwest of the Goldstrike.
- Fault Mapping: Post - Beast – Genesis fault corridor and Basin Bounding fault.
- Basin Fill Mapping: LBB, Brush Creek Basin, and Upper Boulder Basin.

GRAVITY

- Lithologic Mapping: Shallow carbonate hosts along the Tuscarora and Tuscarora Spur ranges.
- Basin Fill Mapping: LBB and Brush Creek basin.
- Fault Mapping: Post – Beast – Genesis fault corridor, Basin Bounding fault, and Castle Reef fault.
- Metamorphic Aureoles Mapping: LBB and Vivian intrusions.
- Alteration Mapping: Decalcification along Castle Reef Fault.

Structural mapping by both the aeromagnetics and gravity is obvious; also obvious is the alignment of deposits along these structures or their intersections. Decalcification, resulting in a decrease in density and increase in porosity and permeability, is described as a pre-ore stage of the mineralizing process (Teal and Jackson, 1997; Kuehn, 1989; Bakken, 1990). The gravity low extending along the eastern portions of the Castle Reef fault is produced by decalcification of the Roberts Mtn. Formation (Evans, 1974); a good example of alteration mapping sometimes possible with geophysics. Lithologic delineation of carbonates, intrusives, and basin fill are also important contributors to an exploration program.

A detailed analysis of these data can yield considerably more information. Two examples follow which demonstrate the surprising information found in these data. Figure 8 presents topography and gravity for a portion of the area's southeast corner (see Figure 7) and Figure 9 the

aeromagnetics and gravity. The prominent gravity high (see southeast portion Figure 8) traces a contact along the topography, which is nearly a constant elevation, contour, suggesting a possible sub-horizontal stratigraphic control. Furthermore, weak gravity highs protrude up several drainages along the gravity contact and, conversely, weak lows extend up ridges. This suggests a shallow northwesterly dip to the sub-horizontal feature. On Figure 8 three elevations (m) are picked along the gravity contact from which a three point problem can be solved, yielding a strike of N35E and dip of 5 deg. NW for the gravity contact. Geologic mapping places silty limestones against upper plate clastic units along the Copper Stone Thrust. The strike is in agreement with geologic mapping; however, mapped dips are steeper averaging 30 deg. This disparity reflects the thrust's flatter aspect as compared to the highly contorted bedding. Silty limestone is the preferred host for gold mineralization in the northern Carlin trend. Its delineation is of primary exploration importance.

Figure 9 compares gravity and aeromagnetics for example area #1. The Rodeo Creek Structure, Basin Bounding Fault, and Lynn Fault, three important ore controlling faults (Teal and Jackson, 1997), are delineated to varying degrees in both data sets. Geometry of Little Boulder Basin (LBB) is clearly mapped by the gravity with areas of deeper fill corresponding to lower gravity (i.e. purple & blue areas). A gravity low matches the LBB stock as mapped by the aeromagnetics. This is interpreted and confirmed by drilling as preferential weathering of the intrusive lithology. The northwest oriented gravity high crossing LBB and bounded to the northeast and southwest by the intrusion and Rodeo Creek Structure respectively reflects a buried bedrock ridge bridging the valley. This ridge represents weather resistive hornfels bounding the intrusion. The gravity data, while not as complete, indicates a similar situation along the intrusive's northern edge. Hydrologically this is important as ground water exits the basin via alternate routes depending upon its location relative to the bedrock ridge. A rectangular, weak gravity high corresponds to the general area of the Vivian Intrusion. The high maps the slightly high density of the intrusive relative to surrounding upper plate rocks and a slight increase in density associate with hornfels of the encompassing units. Both the LBB and Vivian Intrusions are well delineated by the aeromagnetics. A comparison with the gravity reveals the magnetics mirror the gravity within the basin. Deeper basin fill as mapped by the gravity correlates perfectly with positive magnetic responses. Such a condition indicates fairly uniform magnetic basin fill. Perhaps derived from weathering of the proximal intrusions.

Figure 10 presents topography and ground magnetics for detailed example area #2 (see Figure 7). Note the much higher resolution of the ground data as compared to the airborne data. Nonetheless, even minor features in the airborne survey are confirmed by the ground follow-up. The prominent magnetic low surrounding anomalies related to the Vivian Intrusion indicate a limited depth extent to the intrusion. Indeed, the Vivian Intrusion is sill like and often referred to as the Vivian Sill. A series of northeast oriented faults drop the sill's western portion into Little Boulder Basin (LBB). The sill's eastern extreme is terminated by erosion along the Tuscarora Mountain's eastern slope. In addition, a number of drainages into LBB have incised the tabular intrusive and removed material to produce magnetic lows. However, contrary to this pattern is a northeast oriented low corridor interpreted as being fault bounded. Figure 11 shows an idealized exploration model applicable to the Carlin Mine approximately three miles to the south. Of note is the concentration of mineralization in horsted blocks at the plate boundary being fed by NE and NW faults. This same target concept is applicable near the Vivian sill where the lower plate is at increased depth. The magnetic low corridor reflects a horsted block between two northeast bounding structures. The lack of magnetic anomaly within the block reflects removal by erosion, just as in the case of the incised streams and eastern range slope. Somewhat surprising since the horst occurs within a set of down to the west fault blocks. In fact, this horst block is an important ore control at the Turf Deposit.

Electrical methods also play an important role in exploration along the northern Carlin trend. As with the gravity and magnetic techniques, the primary contribution has been in indirect detection. Figures 12 presents a geologic section and two-dimensional smooth-model inversion of a CSAMT line across the Meikle Mine area. The line's location can be found on Figure 7. The Post fault zone is expressed as a broad gradient in the resistivity data, which corresponds to a series of step faults. Thickness of the Carlin Formation increases markedly to the east of the fault at station 2W. The Carlin Formation exhibits low resistivities, which are typical of clay-rich tuffaceous rocks. Massive carbonate rocks in the lower plate are locally mapped as a high-resistivity layer at depth on the CSAMT line.

In conductive, highly carbonaceous rocks, increased resistivity may be observed in areas of deeper oxidation along structures that host deeper mineralization. Figure 13 is a CSAMT section along line 12100N (see Figure 7), extending from west of the Screamer Deposit to the central part of the Betze deposit. Graphitic carbon occurring along bedding planes within the Rodeo Creek formation is interpreted to cause the low-resistivity layer. Removal of carbon by supergene oxidization over the Betze ore body is interpreted to cause the increased depth to the low resistivity. The top of the low-resistivity zone at a depth of approximately 600 feet is the approximate depth of the redox boundary. A narrow zone of higher resistivity is observed at 7400E in the hanging wall of the Buzzard Fault that hosts the Screamer Deposit. Deeper oxidation along fractures related to this fault is also interpreted to partly cause this high-resistivity. This location is just north of the West Bazza Pit, which was a shallow oxide deposit. These types of features are likely to be observed over faults or fracture zones that cut carbonaceous rocks, allowing deeper circulation of meteoric waters.

Pyrite is associated with the mineralization in deep deposits on the Carlin trend, suggesting that IP may be useful in detecting these deposits. Bettles and Kornze (1996) site the contribution of IP in the discovery of the Betze and Deepstar deposits at Goldstrike. In addition, IP data is described as part of the target development for the discoveries of the Screamer and Rodeo-Goldbug deposits (Teal and Jackson, 1997). Wright (1996) shows an IP response observed on a down-hole IP survey that is attributed to the Deep Star orebody. This survey was used to search for sulfides located lateral to the drill hole, but below the interfering effect of near-surface lithologies.

As stated earlier, while deep gold deposits are expected to have an intrinsic IP response due to sulfides, the depth of target, combined with presence of other IP sources makes target recognition problematic. In general, in the Carlin-type deposit environment, IP anomaly amplitudes from sulfides are lower (approximately 15 to 30 milliseconds) than those for graphitic carbon. Graphitic carbon has amplitudes often exceeding 100 milliseconds (Freeman, 1996). Graphitic carbon and syngenetic pyrite are common in this environment, and can create numerous IP anomalies that are unrelated to gold mineralization.

NORTH AREA SUMMARY

- Structural mapping by gravity and aeromagnetics is obvious. Almost every major ore controlling structure in the north area is delineated in either data set.
- Decalcification and hornfels are mapped either directly or via associated weathering characteristics.
- Lower plate carbonate geometries are mapped either directly by gravity or indirectly by basin offsets.
- Detailed carbonate delineation is demonstrated leading to important structural inferences (i.e. apparent right lateral offset of Castle Reef Fault).

- Intrusive margins and internal structure clearly mapped by magnetics with structural inferences leading directly to drill targets.
- Total cost to cover the north area with gravity (1000' square grid) and aeromagnetics (200m line spacing) is on the order of $250000, yielding 400 sq. km. of coverage.

MIKE DEPOSIT

The Mike Deposit is located in the central Carlin Trend approximately 2.5 miles northwest of the Gold Quarry Deposit (see Figure 1). A good geologic review can be found in Teal and Branham (1997). While hosted within sediments, geologic features of the deposit suggest an intrusive relationship.

Figures 14 presents aeromagnetic data and geology over a 40 square kilometer area surrounding the Mike Deposit. Outlines for the Mike, Tusc and Mac deposits are located on the geophysical portion. DIGHEM acquired the data along 200m spaced lines oriented N35E. A circular magnetic anomaly underlies the Mike Deposit, which is covered by 500 – 800' of Carlin Formation. Carlin Formation can produce weak magnetic anomalies owing to either transported clastic sediments or, more commonly, magnetite bearing tuffs in lacustrine sediments. A good example is the north – south magnetic linear extending south from the circular high. This is a sediment filled paleo channel bounded by faults, which affords an empirical measure of the Carlin Formation's magnetic response. While weak, a sufficient amount of Carlin Formation could produce a response comparable in magnitude to the circular anomaly found over the Mike Deposit. However, the shape of the response does not match the overall thickness of Carlin Formation. The Carlin thickens approximately as a wedge to the northwest into Maggie Creek basin. In fact, beneath the circular high Carlin is actually known to thin.

Figures 15 presents a regional – residual decomposition of the airborne magnetic data using a depth slicing approach. The pole reduced data (i.e. UL) is upward continued to 500m and designated the regional (i.e. LR), these data are then subtracted from the pole reduced data to obtain the residual (i.e. UR). Such a procedure separates the data into a long wavelength regional and shorter wavelength residual. Long wavelengths correspond to deep sources and shorter to shallow sources. Relative amplitudes between the regional and residual are nearly equal indicating contribution to the total magnetic response is fairly evenly split from deep and shallow sources. The regional indicates a deep seated magnetic source centered approximately one-kilometer northwest of the Mike Deposits. Half width estimations applied to the response indicate a depth of roughly two kilometers. More refined computer modeling agrees with this estimate. A buried intrusive is the inferred source. The residual data are presented along with the 385 Hz airborne resistivity in Figure 16. Shown on the figure is a profile along which depth of overburden (i.e. Carlin Formation) and the residual magnetics have been extracted. These profile data are presented in Figure 17. Examination of the profile reveals an inverse relationship between basin depth and magnetic response. Higher magnetics in areas of thicker basin fill supports the hypothesis that volume of Carlin Formation could account for the circular magnetic anomaly, but is contradicted by the overall basin geometry. Magnetic gradients associated with the circular anomaly suggest a shallow source. Figure 18, modified from a text on stratigraphy and sedimentation provides a mechanism to reconcile these disparate observations. In a lacustrine sedimentation environment, elevated bedrock will winnow coarser sandy sediments along their margins as the basin fills. This winnowing process can even extend some distance into the sediments above the buried bedrock high. The flanking magnetic highs would represent magnetite black sands winnowed along the edges of the bedrock high known to occur over the Mike Deposit. Mapping or detection of the bedrock high has important implications for exploration.

The bedrock high is produced by resistive jasperoid directly related to mineralization at Mike. In fact, drill testing of the bedrock high would have discovered the deposit.
Figure 19, presents airborne resistivity data and geology for the same 40 square kilometer area. Detailed mapping of the bedrock overburden contact is evident. More important is mapping of lithologies in areas of exposure. Units of Dp, Drc, and Roberts Mtn. Formation are well mapped in the eastern corner of the survey. Patches of Carlin Formation perched atop the Roberts Mtn. are also mapped. Depth penetration into covered areas is suggested along the north – south oriented graben. However, penetration in areas of deeper cover to the north is not indicated. A large powerline extends along the survey's northeast edge and badly contaminated data along its length. The DIGHEM system can record three frequencies simultaneously, from which three resistivity maps are produced. Figure 20 presents a composite of these three resistivity maps. Color ranges for all plots are identical to allow easy comparison. Depth penetration via frequency sounding is possible with lower frequencies (i.e. 385 Hz) looking deeper. The paleo channel mentioned previously is better delineated at lower frequencies where some penetration to bedrock is indicated. However, the major proportion of covered areas show little variation with frequency. This lack of variation indicates these areas of the survey are near or at the inductive limit and no additional information can be obtained by varying the frequency. Exposed bedrock in the east does show variation. The most dramatic and important feature detected by the airborne survey is the Good Hope Fault, an important ore controlling structure. Placement of more resistive Roberts Mtn. formation against relatively more conductive Roberts Mtn. and Dp along the fault produces a sharp resistivity demarcation. The Good Hope Fault does not produce well-defined anomalies in any other geophysical technique. A possible extension northwest under extensive cover is also evident. Limited depth penetration by the system in the 10 – 20 ohm-m cover and known depths in excess of 500' would strongly suggest this extrapolation might not be valid. As with the aeromagnetic survey, features within the Carlin Formation can produce resistivity anomalies that map structures at depth. Figure 21 presents the 385 Hz resistivity with the bedrock – overburden contact and a prominent gravity gradient both outlined. The gravity gradient, facetted by a number of structures, marks the limits of deeper basin versus shallower basin. A close correlation between elevated resistivities and deeper portions of the basin is clearly evident. This pattern is mapping stratigraphy within the Carlin Formation. Two major divisions are mapped in the Carlin: an upper 100 – 200 foot interbedded conglomerate and sandstone (Tcu), and a lower 250 – 450 foot lacustrine sandstone and mudstone (Tcm). The Tcm unit contains significant quantities of clay and would produce lower resistivities as compared to the Tcu unit. It is the Tcm unit which is interpreted to produce the circular magnetic anomaly via winnowing of magnetite sands. The airborne electromagnetic survey maps the Tcm as a low resistivity fringe along the basin's edge where the Tcm laps on to the bedrock. Basinward the more resistive Tcu begins and thickens into the basin. The northeast extension of the Good Hope Fault has placed Tcu and Tcm abruptly against each other, thus allowing the faults delineation beneath extensive cover with airborne resistivity mapping.

MIKE SUMMARY

- Airborne magnetic survey delineates buried intrusion, basin-bounding faults, and sediments reflecting bedrock topographic variations related to alteration (i.e. jasperoid).
- Airborne EM survey maps the major ore controlling Good Hope Fault, its extension under extensive cover, exposed geology, and basin stratigraphy.
- Exploration for the Mike Deposit would have been expedited by the airborne EM and, perhaps, discovered by drilling the bedrock high indicated by the magnetics after confirmed by additional work (i.e. CSAMT, IP, or gravity).
- Total survey costs are on the order of $12000.

TWIN CREEKS

The Twin Creeks Deposit is located approximately 35 miles northeast of Winnemucca (see Figure 1) at the extreme northern end of the Getchell Trend. Twin Creeks is an amalgamation of two deposits discovered by Goldfields and Sante Fe Minerals, and referred to as Chimney Creek and Rabbit Creek respectively. Gold at Twin Creeks (Rabbit Creek portion) is intimately associated with sulfides (Simon et al, 1997), usually pyrite and to a lesser extent arsenian pyrite. The arsenian pyrite post dates the low arsenic pyrite and hosts the gold mineralization. Concentrations of the gold bearing arsenian pyrite can range up to 4.4 wt%. Mineralization is hosted within calcareous black shales and interlayered volcanic rocks of the Ordovician Comus Formation. Application of electrical methods to delineation of the sulfides is an obvious choice. In contrast to the North Area of the Carlin Trend, no large intrusive bodies are interpreted near the deposit. The Osgood Stock's margin is located approximately seven miles to the west; sufficient distance to mitigate thermal effects and minimize maturation of carbon within the Comus to graphite. This should minimize spurious anomalies related to the thermal overprint. Presumably mineralizing process would increase sulfide content above the background diagenetic sulfides. Mapping of sulfide content would then be a viable direct detection tool.

Figure 22 presents self-potential (SP) data over an eleven square mile area centered on the Vista Pit. The Vista Pit is developed on the original Chimney Creek Deposit. Oxidation of sufides has been proposed as a source mechanism for self-potentials (Sato and Mooney, 1960). Although the original hypothesis by Sato and Mooney relies upon massive sulfides to provide return current paths; it is reasonable to assume a large volume of oxidizing disseminated sulfides within highly broken rock could generate a similar electrochemical cell. In fact, Osterberg and Guilbert (1991) note the ore body is currently oxidizing and thus a redox reaction is in progress. Induced polarization work by Goldfields outlined a sulfide halo surrounding the observed self-potential low (Knox, per. comm.) suggesting some form of oxidation cell. Widely spaced regional data extending to the northeast, covering approximately 104 square miles, confirms the highly anomalous nature of the Vista Pit low. However, additional surveys conducted over many properties in northern Nevada proved the Vista Pit survey to be unique. Some relatively specific set of physiochemical processes might be required to produce SP anomalies as observed at the Vista Pit.

An enlarged view of the Vista Pit with geology and self-potential contours superimposed is presented in Figure 23. A number of major northeast oriented faults are seen to bound the internal structure of the low. These are major ore controlling structures within the deposit, and their relationship to the SP anomaly indicates not only deposit detection by SP, but also some internal delineation. The SP anomaly shape appears to be controlled by the ore controlling structures.

Figure 24 presents geology and section 49200N location for the Mega Pit area of the more southerly Rabbit Creek Deposit. Observed induced polarization (msec) and resistivity data taken along section 49200N are presented in Figure 25. The array used was dipole-dipole with A=1000' and N=1-6. Chargeabilities clearly outline a broad response at depth in the middle portion of the line. Internal structure of the anomaly suggests multiple sources with superposition of responses dominating the section. The resistivities define a thin low resistivity surface layer (i.e. overburden) extending from approximately station 16000E off the section to the east. Thinning of the overburden is noted near 20000E. Geology for the section is presented in Figure 26. Comparison of the geologic and resistivity sections reveals good mapping of overburden distribution and some indication of the higher resistivity Valmy Formation on the section's

western extreme. Interestingly, the interpreted thinning of overburden east of station 20000E may reflect a bedrock rise along the Fiber Line Fault.

Figure 25 presents a composite of two products: inverted chargeabilities with drill holes and qualitative sulfide content, and geologic section with approximate gold grade outlines. The inverted chargeability model does a good job of mapping the redox boundary beneath overburden. Also, qualitative sulfide estimates agree very will with the model. Note elevated chargeability correlating with large volumes of sulfides on the section's eastern portion. Weaker or thinning of sulfide volume is modeled beneath station 17000E; this also is confirmed by holes bottoming in no sulfides.

TWIN CREEK SUMMARY

- A large redox cell 2.5 miles in diameter is clearly mapped by SP and would have lead to discovery, if drill tested. SP data is customarily gathered along with IP data and provides a valuable additional parameter.
- Induced polarization data over the Mega Pit mapped sulfides related to gold mineralization and would have lead to discovery, if drill tested.
- Both SP and IP, while giving very definitive responses over the deposits, would be expected to yield a number of anomalies not related to gold in the Twin Creeks geologic environment. Coupling these surveys with geology, geochemistry, and additional indirect geophysical techniques would eliminate the majority of spurious anomalies.

RAIN DEPOSIT

The Rain district is located approximately eight miles southwest of the town of Carlin at the southern limit of the Carlin Trend. Figure 1 presents the district's location relative to other deposits. Thoreson (1991) reviews the structural, lithologic, and alteration assemblages found at Rain and several smaller satellite deposits. Exploration in the district has focussed upon tracking the Rain Fault to the northwest from the deposit. To date, discontinuous mineralization has been defined for over two miles northwest along the fault. Figures 28 and 29 present the complete Bouguer gravity (CBA) at 2.50 g/cc and idealized ore shapes along the fault. As is obvious from Figure 28, gravity can clearly map the Rain Fault, which forms the northeast boundary to a large horst block – the Rain horst. Mineralizing fluids have migrated along the Rain Fault to bleed out along favorable contacts. Figure 29 shows several ore zones and their distribution relative to the fault. Ore grade mineralization is very tightly constrained to within a few hundred feet of the fault. Figure 30 presents a typical section depicting the mineralization's limited separation from the fault. The mineralization is concentrated at the Devils Gate – Webb Formation contact. As with the north area, this contact is a major demarcation between clastic over carbonate sediments, and as in the north area, also marks a major density contrast. Up section are more clastic units such as the Chainman sandstone and Diamond Peak Formation. Down section a large dolomitic unit referred to as the Nevada dolomite underlies the Devils Gate. The gravity expression of the Rain Horst results from bringing this denser carbonate section up. Figure 31 presents a longitudinal section along the horst's eastern extreme. The horst is successively dropped to the northwest by cross cutting northeast faults. These northeast faults are also mapped by the gravity as offsets and thinning in the gravity pattern. Overall, the gravity is seen to diminish in magnitude and thin to the northwest, reflecting increased depth of cover.

Gravity has been used successfully at Rain to map the horst and accurately place drill holes within a few hundred feet of the Rain Fault at depths in excess of 2000'. Figure 30 shows two of the early holes targeted at the deep mineralization. On previously undrilled sections, holes are

placed within 400’ of the fault then followed-up with offsets closer to the fault to “sharp shoot” the high grade core.

RAIN SUMMARY

- Gravity successfully maps the Rain horst, northeast bounding Rain fault, and secondary cross cutting faults.
- Gravity is utilized to place drill intercepts within 300’ of the Rain fault at depths in excess of 2000’.
- Survey cost to acquire gravity data in Figure 28 on a square 500’ station spacing is $78000.

PORPHYRY RELATED

COVE DEPOSIT

The Cove deposit is located in the McCoy Mining District, approximately 45 km south of the town of Battle Mountain, in Lander County, Nevada. Pre-mine reserves at Cove were approximately 3.6 million ounces of gold and 164.3 million ounces of silver. The Geology and mineralization of the McCoy District are presented in Emmons and Eng (1995). The geologic background included here is summarized directly from their paper. The McCoy district is located in the northern Fish Creek Mountains and occurs in Triassic carbonate and siliciclastic rocks, which have been intruded by Jurassic, and Tertiary igneous rocks. Locally extensive Tertiary volcanic rocks are locally present in the district and are post-mineral in age. Post-mineral volcanics and alluvial material concealed much of the Cove deposit.

The McCoy district comprises the McCoy and Cove deposits. The McCoy deposit is a proximal skarn genetically related to the Tertiary Brown Stock, which is a biotite and hornblende granodiorite. The Cove Deposit is tentatively interpreted to be a distal metasomatic replacement deposit. Both the McCoy and Cove deposits are thought to be related to a large buried porphyry intrusive system that is inferred to lie beneath the district.

The Cove deposit is hosted by the Smelser Pass, Panther Canyon and Home Station Members of the Triassic Augusta Mountain Formation. Figure 32 is a portion of the Emmons and Eng, (1995) map covering the immediate vicinity of the Cove Deposit. Figure 33 is a stratigraphic column, also taken directly from Emmons and Eng that shows the relationship of the different types of mineralization to the various host rock lithologies. The Home Station Member consists predominantly of dolomite with lesser amounts of dolomitic limestone and limestone. The Panther Canyon Member comprises two submembers, the lower unit being predominantly dolomite with the upper submember, a quartz pebble conglomerate and sandstone with lesser siltstone and mudstone. The Smelser Pass Member is a monotonous, medium bedded to massive gray limestone and makes up most of the Augusta Mountain Formation.

The Triassic rocks are intruded by numerous dikes and sills of felsic composition and range in age from 39.4 to 40.3 Ma. These rocks are unconformably overlain by the Caetano Tuff (33.5 Ma) and locally by tuffaceous sediments. These rocks are post-mineral in age.

The Triassic rocks exhibit gentle folds along northwest trending axes. The Cove anticline, which is considered to be an important ore control, has limbs which dip approximately 30 degrees and plunges to the southeast.

One of the important faults in the Cove area is the Lighthouse Fault. This is a major north-south striking normal fault, which dips 65 degrees to the east. It exhibits both pre- and post-mineral movement totaling up to 500 feet. It is thought to have been a conduit for mineralization. Intrusive rocks at Cove include the Southeast Intrusive located beneath alluvial cover at the southeast edge of the Cove pit and the Bay and Cay dikes, which intrude northeasterly striking structures.

Mineralization at Cove extends over a vertical range of over 1200 feet. The Cove deposit consists of two distinct orebodies. These are an upper, oxide orebody and a deeper sulfide orebody. The upper oxide orebody is hosted mainly in the lower portion of the Smelser Pass Member. It consists of a central jasperoid zone which is stratigraphically and fault controlled. The jasperoid contains an abundance of manganese minerals, predominately Psilomelane-group minerals and pyrolusite. The jasperoid grades outward into manganese-flooded and decalcified limestone. Bleached and argillized limestone forms a broader halo.

The sulfide orebody at Cove is hosted by the Panther Canyon and Home Station Members. The sulfide orebody contains most of the gold and silver reserves of the Cove deposit. Alteration consists of sulfidation, silicification and sericitization. Alteration occurs as stockwork veinlets and as replacement in the clastic and dolomitic units with many of the veinlets being sub-parallel to bedding. Pyrite is the dominant sulfide and occurs as disseminations and veinlets. Sulfide veins are up to nine inches thick. Two high grade zones are contained within the sulfide orebody, which are generally strata-bound

EXPLORATION HISTORY

The Cove deposit was discovered in 1987 by Echo Bay Mines Ltd. This was the result of a systematic district exploration program consisting of sediment, rock and soil sampling, geologic mapping and drilling (Emmons and Coyle, 1988). Prior to the discovery of the Cove deposit, exploration work was concentrated in the vicinity of the McCoy deposit, located approximately one mile to the southwest. Geophysical work consisted of IP/resistivity surveys conducted mostly around the vicinity of the McCoy deposit, however, three dipole-dipole lines were surveyed in the alluvial covered area to the east of the Cove deposit in 1982. A moderate increase in IP response observed at the extreme western limits of data coverage for one of these lines, is now recognized as being caused by sulfide mineralization related to the Cove sulfide orebody. A comprehensive IP/resistivity survey was conducted over the Cove deposit in 1987 by Mining Geophysical Surveys Inc. of Tucson Arizona. The data from this survey show a broad area of anomalous IP response at depth which is roughly centered on the Cove orebody. The IP response is shallowest and strongest near the center of the Cove orebody and defines a roughly circular zone of anomalous IP effects approximately 1500 to 2000 feet in diameter. Anomalous IP effects extend outward from the deposit for a considerable distance and appears to be stratigraphically controlled. Some of this response may be formational in nature. The shallower oxide ore body is characterized by low resistivity and low IP effects.

Line 1-87

Figure 32 shows the locations of selected IP/resistivity lines that were run over the Cove deposit. Figure 34 shows the results of two-dimensional smooth-model inversions of the IP and resistivity,

as well as, raw data pseudosections for 400 foot dipole-dipole data acquired along this line. Figure 35 show the model results with a drilling result summary from Eng (1991) that coincides with this line.

The raw IP data exhibit a broad zone of moderate amplitude IP effects at depth reaching a maximum apparent amplitude of 22 milliseconds at an n-spacing of 6. The two-dimensional smooth-model results of this data define a zone of anomalous IP effects at depths below approximately 400 feet. Intrinsic IP values of over 40 milliseconds are indicated. The limits of the model IP effects correspond very well with the extent of the drill-defined sulfide mineralization. The shallowest and central portion of the IP anomaly corresponds to the high grade sulfide zone.

The shallower oxide deposit is expressed as a zone of relatively low resistivity of 20 to 40 ohm-meters. This may be enhanced by tuffaceous sediments that lie beneath the Caetano tuff, however, argillic alteration of the Augusta Mountain limestone appears to be responsible for at least part of the low resistivity.

The deeper sulfide ore body appears to be associated with relatively high resistivity rock of approximately 100 ohm-meters, which is somewhat surprising given the high percentage of sulfides and the vein-like nature of the sulfide mineralization.

The Caetano Tuff is expressed as relatively high resistivity rock of approximately 100 ohm-meters which forms the volcanic ridge in the northern half of the section. Northerly dipping normal faults displace the stratigraphy down to the north. While the individual faults are not resolved with the 400 foot dipoles, the resistivity model identifies the sense of displacement, and the general dip of the structures reasonably well.

Line 3-87

This is an east west line that crosses near the central portion of the Cove deposit. Figure 36 shows the modeled IP section along with a geologic section taken directly from Emmons and Eng (1995). The geologic section lies approximately 400 feet to the north of the IP line. A pronounced IP response is associated with the Cove mineralization. An intrinsic IP response of 30 to 40 milliseconds is estimated at depths below 400 to 500 feet. This agrees well with the depths and intrinsic IP response interpreted by Wieduwilt, (1987) from curve matching. The top of the IP response is closely correlated with the top of the Panther Canyon Member and the axis of the IP high is roughly coincident with the axis of the Cove anticline. Weaker IP effects are observed at greater depth to the west of the Cove deposit and are indicated at depths of 800 to 1000 feet beneath the western half of the line. The estimated depth to the top of sulfides corresponds closely with the top of the Panther Canyon Member. Exploration drilling has encountered sulfides associated with mineralization in the Panther Canyon Member at these depths to the west of the Cove deposit.

Figure 37 shows the modeled resistivity results with the geologic section for Line 387. A zone of low resistivity of less than 20 ohm-meters is observed in the upper 200 feet, which is associated with the upper oxide orebody and probably reflects argillic alteration of the Smelser Pass Member. Low resistivity of 30 to 50 ohm-meters appears to be associated with intrusive units, particularly the Southeast Intrusive.

COVE DEPOSIT SUMMARY

- Sulfide mineralization associated with the Cove sulfide orebody produces a broad, moderate amplitude IP response.
- Estimated depth to the top of sulfides derived by manual curve fitting, Wiedawuilt, (1997) are in good agreement with the drill-determined depth to sulfides.
- Depth and lateral extent of the IP source derived from two-dimensional inversion of the IP and resistivity data agree well with the drill-determined limits of the sulfide orebody on line 1-87.
- The highest intrinsic IP effects and shallowest interpreted depth to the top of sulfides is in close spatial association with the axis of the Cove anticline.
- Relatively low resistivity is associated with the oxide mineralization and is interpreted to reflect a halo of argillized rock surrounding the deposit.
- Two-dimensional smooth-model IP results provide a good estimate to the top of the Panther Canyon Formation to the west of the Cove deposit and reflect sulfides associated with weaker mineralization.

VOLCANIC HOSTED

TALAPOOSA DEPOSIT

The Talapoosa deposit is located in the Virginia range in Lyon County, Nevada approximately 50 km east of Reno (see Figure 1). The Talapoosa deposit is an epithermal quartz-adularia, low-sulfidation-type stockwork vein system hosted in intermediate volcanic rocks.

GEOLOGY

The following geological interpretation is based on information and data from various exploration and development programs that have occurred at Talapoosa from the late 1970s to 1997. The geologic map (Figure 38) and the drill section (Figure 39) were provided by Miramar Mining Corporation. The geologic work at Talapoosa is condensed into the following summary by Ann Carpenter (Miramar Gold Corp., unpublished company report).

Stratigraphy

The volcanic and sedimentary rocks in the Talapoosa District are Miocene to Pliocene age, based on stratigraphic interpolation and limited age-dating. Figure 38 is a generalized geologic map of the district, and Figure 39 is a geologic section through the central portion of the deposit.

The oldest rocks in the district are aphanitic, and commonly amygdular basalts and basaltic sediments and are referred to as the Lower Pyramid Sequence (LPS) basalts. These rocks are exposed in a canyon north of the Main District and are encountered in drilling in the footwall of the Talapoosa Fault in the Main District and Dyke Adit.

The LPS basalts are overlain by volcanic and sedimentary rocks of the Upper Pyramid Sequence (UPS). The oldest UPS unit currently identified is a massive porphyritic dacite flow or flow dome. This dacite unit is overlain by a sequence of tuffaceous and sedimentary units of the

Upper Pyramid Sequence, comprised mainly of lithic-rich rhyolitic ash flow tuff and poorly sorted, coarse-grained conglomerate of the same composition. These rocks are exposed north of the Talapoosa District, and are encountered in the footwall of the Talapoosa Fault within the district.

Conformably overlying the Pyramid Sequence rocks is the Kate Peak Formation (KPF), divided into lower and upper units. The Lower Kate Peak Formation hosts the bulk of mineralization at Talapoosa and consists of porphyritic andesite flows, flow breccias and lahars. Unconformably overlying the Lower Kate Peak Formation is a package of lahars, flows and volcaniclastic sediments of dacitic composition of the Upper Kate Peak Formation.

Overlying the KPF are the Coal Valley (CVF) and the Lousetown (LF) Formations. The CVF consists of unaltered tuffaceous sediments with weakly welded to unwelded tuff. The overlying LF consists of black, aphanitic and vesicular basalts, which cap most of the ridges in the region.

Structure

Talapoosa is located at the eastern end of the east-west trending Virginia Range, and is situated between two left-lateral shear zones (Olinghouse Fault Zone to the north and Carson Lineament to the south), and within the northern confines of the Walker Lane, a regionally encompassing northwest trending structural zone.

Mineralization at Talapoosa is structurally controlled and complex, influenced by NW, NE, and EW trending structures. Shallow-dipping stratigraphy appears to be a secondary control for alteration and mineralization. The key mineralizing trend is currently interpreted as N60-70W. High-grade mineralization appears to be localized along N60-70W trending structures at intersections with E-W cross-cutting features. Multi-stage quartz veins, which may attain thicknesses exceeding 10 feet, occupy the Talapoosa Fault in the main district, East Hill and Dyke Adit. All faults contain gouge zones suggestive of significant post-mineral movement.

Alteration and Mineralization

The Talapoosa deposit is an epithermal quartz-adularia, low-sulfidation-type stockwork vein system hosted in intermediate volcanic rocks. Silicic and sericitic alteration host the bulk of gold mineralization, overprinting regional propylitic alteration in the Lower Kate Peak Formation. Intense argillic alteration is confined to the Upper Kate Peak Formation and the upper portions of the Lower Kate Peak Formation. Thin argillic zones may be present between quartz-sericitic and propylitic zones deeper in the deposit. Pyrite (up to 3%) is weakly disseminated in pervasive silicification and quartz veins, but also occurs as banded veins with quartz, marcasite and/or hypogene hematite.

GEOPHYSICS

Geophysical data presented here consists of gradient array and dipole-dipole IP/resistivity surveys and ground magnetic surveys. Gradient array IP/resistivity data were acquired using 100 foot receiver dipoles along lines oriented N40E and spaced 200 feet apart. Multiple transmitter dipoles, ranging in length from 9000 to 12000 feet were used to acquire the data. Dipole-dipole data were acquired on selected lines using 200 and 400 foot receiver dipoles.

Figure 40 shows the gradient array apparent resistivity as a color image. A pronounced zone of high resistivity is observed over the Bear Creek Zone and Main Zone mineralization, as well as, an area of Upper Kate Peak rocks located to the west of the deposit. The edges of the resistivity high correspond closely in plan view to the grade-thickness contours for the Main and Bear Creek Zones as published in Van Nieuwenhuyse, (1990). The southwestern edge of the high resistivity zone coincides with the Road Fault that is a northwest striking and southwest dipping normal fault. Very strong clay alteration of the Upper Kate Peak in the hanging wall of this fault is expressed as a pronounced low resistivity zone. Within the broad area of high resistivity, a pronounced narrower and higher resistivity zone is observed along the 10000NE baseline. Drill results indicate a zone of massive silicification is responsible for this feature. This feature is associated with some of the highest gold grades at shallow depths, (refer to Figure 39).

Figure 41 shows the gradient array chargeability data. The data are relatively noisy due to the general low resistivity environment related to the clay alteration, as well as, tuffaceous sedimentary rocks of the Upper Kate Peak Formation and the overlying Coal Valley Formation. The IP data exhibit a weak high that lies within the zone of high resistivity over the Bear Creek Zone. This zone is distinguished from the immediate surroundings by its continuity and slightly broader expression, however, the amplitude does stand out as particularly anomalous with respect to the rest of the survey area. An extensive area of elevated IP values is observed in the northern portion of the survey area. While numerous narrow variations, largely attributed to noise are observed, the data have a longer wavelength component, suggesting a source at depth. Drilling in this area encountered mineralization and associated sulfides at depths of 200 to 300 feet beneath the post mineral cover (Ann Carpenter, Pers. Comm. 1998).

Ground magnetic coverage of the grid is shown in Figure 42. The basalts of the Lousetown Formation are characterized by numerous short-wavelength variations. Several linear lows occur along the edges of the basalt outcrops reflecting their geometry as a relatively flat-lying cap. The area overlying the Bear Creek and Main Zones is expressed as a magnetically quiet zone with intermediate to low values of magnetic intensity. The strong low observed immediately to the south of the Bear Creek Zone is largely an effect from the edge of the ridge-capping basalts located to the south. This low follows the Ripper-Hill Fault, which forms the northern edge of the basalts. Strong magnetic lows are caused by magnetic rocks, either resulting from the geometry of the source with respect to the earth's magnetic field (north-side, edge or up dip magnetic lows) or by remanence. Note that, as in this case, a strong magnetic low does not preclude the area within the low from being altered.

A relatively broad magnetic high is observed over the dacite unit that lies immediately west of the Main Zone. The magnetic data suggest that the source extends to the east, along the footwall of the Talapoosa Fault, beneath the Lower Kate Peak Andesite. The dacite has been intersected in drill holes in the footwall of the Talapoosa Fault (refer to Figure 39).

Figure 43 shows dipole-dipole IP data for line 10400NW, using a 200 foot dipole. A resistivity-depth section produced from results of two-dimensional smooth-models inversions are shown with the raw data pseudosections and gradient array profiles. The raw data indicate a weak IP response of 10 to 11 milliradians in apparent amplitude centered between 9800NE and 10200NE. The model results define a zone with an intrinsic IP response of 15 to 20 milliradians at depths below approximately 50 feet beneath 10000NE and 10200NE. This location coincides with the weak gradient array IP high. The model results suggest that anomalous IP effects exist at greater depth to the southwest as far as the Road Fault. Depth to the top of the source is approximately 200 feet. This is in good agreement with the depth to the top of the Upper Bear Creek

mineralization located in the foot-wall of the Road Fault (refer to Figure 39). Weakly elevated IP effects are suggested in the hanging wall of the Talapoosa Fault where shallow mineralization is intersected. Near-surface increases in pyrite are noted in both locations from drilling.

Figure 44 shows the resistivity data for the same line. The dipole-dipole data show a high resistivity zone at near surface between 9600NE and 10600NE which is coincident with the broad zone observed in the gradient array data. The two-dimensional inversion results define a zone of higher resistivity with values of over 100 ohm-meters at a shallow depth beneath 10000NE to 10200NE. This is coincident with the high resistivity zone observed along the baseline in the gradient array data. The highest resistivity corresponds to a location where massive silicification is frequently noted in drill logs. The zone is correlative with increased gold values at depths of less than 100 feet (refer to Figure 39). The Talapoosa Fault is observed as a marked resistivity gradient with low resistivity to the northeast. Drilling indicates dominantly argillic alteration to the north of the Talapoosa Fault.

Figure 45 shows the IP and resistivity data with the smooth model results for Line 10400NW using a 400 foot a-spacing. A broad southwesterly-dipping zone of anomalous IP effects corresponds to the Bear Creek mineralization. The maximum IP effects from below the 4800 foot elevation agrees well with the deepest mineralization encountered in drilling. The resistivity inversion defines an approximately 60 degree southwest dipping dike-like resistive zone enclosed within low resistivity material.

TALAPOOSA SUMMARY

- Quartz adularia stockwork mineralization at near-surface is expressed as a zone of high resistivity within a zone of low resistivity related both to intense clay alteration and low resistivity tuffs and sediments.
- A pronounced high resistivity zone and coincident low amplitude IP anomaly is observed at shallow depths overlying the Bear Creek mineralization. This feature does not correspond to any mapped features but coincides with zones of massive silicification, residual sulfides, and higher gold values at shallower depths over much of its length. This is very likely related to vein mineralization in a through-going structure.
- The extent of anomalous IP response, as indicated by two-dimensional inversions, coincides with the Bear Creek mineralization as defined by drilling along a section though the central portion of the deposit
- Two-dimensional inversion of dipole-dipole data suggests the resistive zone associated with the Bear Creek Zone dips at approximately 60 degrees to the southwest.
- Two-dimensional inversions, relatively new and unproven in exploration geophysics, appear to be providing a subsurface image that is consistent with drill results.

HOT SPRINGS RELATED

MULE CANYON DEPOSIT

The Mule Canyon Mine, is located 14 miles east-southeast of Battle Mountain, in the northern Shoshone Range, Lander County, Nevada (see Figure 1). The deposit was discovered by Gold Fields Mining Company in July 1986 during a grass-roots reconnaissance program. No prospecting or mining activities were documented in the area prior to that time.

The following geologic discussion and exploration history is provided by Eric Saderholm, Mine Geologist at the Mule Canyon Mine. Mule Canyon is an epithermal gold/silver system with a total (pre-mining) reserve of 990,000 ounces of gold and an average grade of 0.111 ounces per standard ton. Six discrete ore bodies will be mined from five open pits during the projected five-year mine life. The alteration and mineralization geochemistry indicates that the Mule Canyon deposits are virtually intact, high-level, epithermal systems of the quartz-adularia, low-sulfidation type. Gold mineralization is found in strongly sulfidic ores (up to 20% sulfur) associated with strong argillic alteration and lesser silicification. Gold ore is localized along NNW striking high-angle faults and dikes cutting Miocene basaltic andesites. The ore bodies tend to be narrow and high-angle but the grade of the ore can be quite high (up to 36 opt). Trace element geochemistry is typical of upper level hot spring precious metal systems, displaying elevated Ag, As, Sb, and Se.

EXPLORATION HISTORY

Gold Fields geologist, Andy Schumacher, initiated a grass-roots exploration program, in June 1986, consisting of stream sediment and float sampling. Anomalous float samples (up to 3400 ppb Au) were obtained from the Mule Canyon drainage and were subsequently followed upstream to the source area. Silicified float samples assaying up to 1.06 opt were collected along a north-trending color anomaly, and defined the original surface manifestation of the Main Zone ore body. Further prospecting, geologic mapping, and detailed rock and soil sampling resulted in the discovery of the West, North, Ashcraft, and South Zones. A first-pass drilling program commenced in October, 1986 and demonstrated gold mineralization in the Main, North, West, and South Zones (refer to Figure 46). The discovery hole, MC-1, was collared in the Main Zone and intersected 135 feet averaging 0.721 opt from surface. IP/resistivity surveys were conducted by Gold Fields geophysical crews in 1991. IP anomalies roughly defined the known ore bodies due to the associated sulfides. Additional geophysical studies and interpretation identified a potential target with no outcropping surface expression located south of the South Zone. The Section 9 ore body was discovered in early 1992 as a result of drilling into this strong IP anomaly.

STRATIGRAPHY

Figure 47 shows the stratigraphic section for the Mule Canyon area. Mineralization is hosted in Miocene basaltic andesite flows and dikes of the Northern Nevada Rift. Basement rocks in the area are complexly folded siltstones, sandstones and cherts of the Ordovician Valmy Formation, Silurian Elder Formation, and the Devonian Slaven Formation. These siliceous assemblages, exposed along the western foothills of the Shoshone Mountain Range, are associated with the Roberts Mountain Allochthon. On the east flank, in the Mule Canyon area, the basal volcanic units of the Tertiary sequence unconformably overlie the Paleozoic sediments. At the rift margin, west of Mule Canyon, the Paleozoic-Tertiary contact is a complex set of high-angle, NNW striking, east-dipping normal faults and dikes which locally have significant displacements. Tertiary volcanic successions range in age from Oligocene (Caetano Tuff) to Late-Miocene (Mule Canyon Sequence) and collectively form a southeast-dipping cuesta on the east flank of the range. The ore host stratigraphy consists of Miocene basaltic andesite extrusive and pyroclastic flows, vent-facies rocks and numerous feeder dikes.

Gold mineralization at Mule Canyon is strongly structurally controlled with very limited stratigraphic influence. The ore bodies appear to be virtually intact, near-surface epithermal systems with roughly “funnel” shaped geometries. Gold is localized at the margins of high-angle dikes and structures and locally in vesicular, lava flow tops and pyroclastic vents. The dikes vary

in texture, thickness and continuity. Preferred host dikes are very fine-grained to glassy in texture with distinctive perlitic chill margins or dikes that are strongly vesiculated. Bomb fields, cinders and other vent facies rocks are present where dikes reached the paleo-surface. These highly vesicular, permeable zones are locally preferential sites for gold deposition.

The predominant ore controlling dikes and structures strike between N15W and N25W and ore is generally elongated in this direction. Lesser control is found along N5E to N15E striking dikes and N70E and N70W striking faults and fractures.

High-grade ore is localized at multiple fault or dike intersections and within vent complexes where primary brecciation and structural preparation are the most intense. Six discrete ore zones have been modeled along the 2.5-mile strike-length of known mineralization: the North, Ashcraft, West, Main, South, and Section 9 zones.

GEOPHYSICS

Geophysical work conducted since 1992 has consisted of gradient array IP/resistivity, airborne magnetic and EM surveys, and ground magnetic surveys. Gradient IP surveys have been found to be an effective exploration tool in the district. Figure 46 shows a generalized geologic map of the Mule Canyon Area. Figures 48 through 54 show selected geophysical data on the same base for a 20,000 foot by 30,000 foot exploration surrounding the Mule Canyon Mine.

Figure 48 shows a colored image of the chargeability data from dipole-dipole data acquired with a 100 foot a-spacing. Also shown on this plot are the planned pit outlines, as well as, the location of the Microwave Zone. The plotted value represents the result of a “pant-leg” filter that averages data down the two 45 degree plotting diagonals from each dipole. Distinct IP highs are observed over the Mule Canyon orebodies. The IP highs show elongation in the north-northwest structural direction. A well defined anomaly is also observed over the microwave zone. Broad areas of anomalous IP effects are observed to the west of the mine area that appear to suggest several northwesterly trends. High IP effects are also observed at the north end of the grid and are related to alteration and associated sulfides in the Water Canyon area.

Figure 49 shows an image of the filtered apparent resistivity values from the 100 foot dipole-dipole data. Broad areas of relatively low resistivity (<50 ohm-meters) are observed. Areas of less than 10 to 20 ohm-meters are associated with the economic orebodies. Several gradients can be observed which correlate with structural features. The northwest trending gradient which lies along the eastern side of the Main and Ashcraft Zones corresponds to the Muleshoe Fault, which displaces the pre-mineral stratigraphy down to the east to depths greater than 700 feet. Higher resistivity values are generally correlated with younger stratigraphic units.

Figure 50 shows gradient array IP data. Data were acquired in the time-domain using 100 foot receiver dipoles. Two initial grids were surveyed in the area covering the area of the South, Main, West, North, and Ashcraft Deposits. Lines for these grids were oriented N 70 E and were spaced at 200 feet. The remainder of the data were acquired along east-west lines spaced 300 feet apart. The data were acquired in roughly square grids with dimensions ranging from 3600 feet to 4200 feet. Transmitter dipoles were approximately 9000 to 12000 feet in length. Data were acquired along common lines between grids and the overlap data were used to level the grids for this composite plot.

The gradient array IP data show well defined anomalies associated with the orebodies. The limits of the narrow IP highs correspond well with the limits of the shallow structurally-hosted

mineralization. Considerable structural detail is also evident in the data. The Microwave Zone is seen to be part of a continuous linear IP high, with over 6000 feet of strike length. The data have also defined several linear IP highs with the broad area of high IP observed in the dipole-dipole data to the west of the Mule Canyon Mine area. Most of these zones have been determined to be altered and/or mineralized zones.

Figure 51 shows the apparent resistivity data for the gradient array coverage. An important aspect to note is that the Mule Canyon Deposits are associated with relatively low resistivity values. Subtle linear resistivity highs are observed which are thought to be caused by dikes, but these highs tend to be relatively discontinuous. This is in contrast to the Microwave Zone and several of the linear IP highs located to the west of the Mule Canyon Deposits. Many of these zones are coincident with resistivity highs. These are interpreted to reflect relatively massive and continuous dikes within the structure. The gradient array is particularly sensitive to vertical resistive features relative to other arrays.

Figure 52 shows airborne magnetic data. Data show high magnetic relief, typical of intermediate to mafic volcanic rocks. The magnetic highs in the central portion of the area are observed over topographic highs and appear to largely be related to younger stratigraphic units. Generally low magnetic relief is observed along the western edge of the survey area in the Paleozoic rocks. Broad magnetic highs observed within the Paleozoic rocks indicate dikes.

The mineralization at the Main Zone, South-Zone and Section-9 orebodies occur within relative magnetic lows, although many other lows are observed in the survey area. The Section 9 deposit is associated with a pronounced magnetic low; however, the deposit lies beneath a topographic low that is incised through surrounding younger, more magnetic units. The microwave zone also appears to lie along a linear magnetic low.

An interesting feature is the northeast trending high located in the northeast corner of the map. This coincides with the drainage that forms an erosional window through the capping basalts that are interpreted as having a reversed remanent magnetization.

Figure 53 shows the calculated first vertical derivative for the airborne magnetic data. This provides higher resolution of the dikes in the northwest corner of the property. Orebodies are more clearly associated with magnetic lows here, but there is nothing particularly significant to these lows with respect to the numerous other lows observed throughout the survey.

Figure 54 shows the ground magnetic data conducted over a section of the survey area. Data were acquired along the gradient grid at a 25 foot station spacing. The data show a total variation on the order of 2000 nT. The data show numerous, narrow linear highs associated with some areas of high IP and high resistivity. This is suggestive of the presence of dikes. Some of the broader features observed on the airborne survey are seen to comprise numerous narrow highs, suggesting a swarm of narrow dikes at surface.

A narrow magnetic feature is observed along the Microwave Zone. This feature is coincident with the zone of high IP and resistivity. The airborne data detects this feature at the north end of the zone, but to the south, this feature is not resolved. A review of the ground magnetic profile data show the linear high along the dike is 100 to 200 feet in width with an amplitude of approximately 1000 nT. In the southern portion of the Microwave Zone, this high is located along the western flank of a broader magnetic high. Figure 55 shows a comparison of the airborne data with the ground data which has been upward continued to an altitude of 150 feet above the surface. The southern portion of the magnetic high is not resolved in the upward continued

ground data. This indicates that the two features are too close together to be resolved at a 150 foot terrain clearance.

Figure 54 shows a dipole-dipole line, with 100 foot a-spacings across the West Zone and Main Zone, with a geologic section derived from the mine model. Note the IP data are in the original geophysical grid coordinate system. The corresponding mine grid coordinate is shown on the geologic section. Red areas on the geology section indicate sulfide mineralization and the black zone represent dikes. Mineralization is closely confined to the structure except in the ashflow tuff units, where it extends outward from the structure. With the exception of the Main Zone, significant sulfide mineralization is generally absent in the FBBM unit (Eric Saderholm, Pers. Comm).

Two zones of anomalous IP effects are evident in the IP pseudosections that correspond to localized zones of shallower sulfides that are associated with the West Zone and Main Zone deposits. The apparent IP amplitude of the west zone anomaly is lower due to the increased depth to the top of sulfides. The IP anomaly observed for the Main Zone indicates a shallower source; although the shape of the anomaly and the inversion results indicate that the bulk of the sulfides are at a depth of one-half the a-spacing or 50 feet.

Figure 57 shows the resistivity data for the same section shown in Figure 56. The FBBM unit is defined as an upper resistive cap suggesting that it is relatively massive. Resistivity values of less than 10 ohm-meters are associated with strong argillic alteration below the FBBM. The two-dimensional inversion results suggest that argillic alteration extends to the east of the large dike in the west zone, which is consistent with the location of gold mineralization. The two-dimensional model results suggest the presence of a high-angle resistive zone at the location of the dike beneath 50900E.

Pervasive pyrite is present in the Lower Latite Ashflow Tuff unit (LLAT) and extends a great distance laterally down-dip to the east from the deposits. Sulfides hosted in this unit are the source of the broad high IP background that is observed in the gradient IP data in the mine area. The sulfides in the LLAT unit are indicated to be at depths of 800 and 1000 feet some 3000 feet to the east of the deposits. IP data can be used to infer the depth of the ore host stratigraphy.

MULE CANYON SUMMARY

- IP data clearly define known mineralization at Mule Canyon.
- IP anomalies include the orebodies, as proposed by Nelson (1988), for gold deposits in the hot springs environment.

- PRESENTLY ECONOMIC OREBODIES
  - Closely associated with structures that are interpreted to have been volcanic vents.
  - Characterized by high IP effects at relatively shallow depths that are caused by sulfides hosted within high-angle structural zones.
  - Generally associated with low resistivity values of less than 10 to 20 ohm-meters caused by strong argillic alteration.
  - Generally associated with relative magnetic lows.

- WEAKLY DEVELOPED MINERALIZATION
  - Characterized by existence massive dikes.
  - Characterized by high IP effects with coincident high resistivity and magnetic highs.

- The combination of high IP effect, low resistivity and secondly, low magnetic intensity is considered to be a key exploration criteria.

SUMMARY

- There is no “bright spot” geophysical technique for finding gold, regardless of deposit type. A multidisciplinary approach dramatically raises the chances for success.
- Physical properties of the geologic environment, alteration, and mineralization must be understood to properly apply geophysics.
- Geologic integration is crucial; geophysics applied in a geologic vacuum is dangerous.
- A close working relationship between the geologist and geophysicist must develop, if full benefit is to be realized from an exploration program.

LIST OF FIGURES

ACKNOWLEGEMENT

The authors would like to express their appreciation to the following corporations for permission to use the data presented herein.

Barrick Goldstrike Mines Inc.
Echo Bay Mines Ltd.
Miramar Gold Corporation
Newmont Gold Company

Special appreciation is extended to:

Dave Emmons for providing geological information on the Cove Deposit;
Ann Carpenter, Nevada Colca Gold Inc. for providing the geological summary for Talapoosa;
Eric Saderholm, Jon Brummer, and Reed Kofoed for geologic information on the Mule Canyon and Twin Creeks Deposit.

REFERENCES

Bakken, B.M., 1990, Gold mineralization, wall rock alteration and the geochemical evolution of the hydrothermal system in the main ore body, Carlin Mine, Nevada: PhD Thesis Stanford University, 200p.

Bartlett, M. W., Enders, M. S., and Hruska, D. C., 1991, Geology of the Hollister gold deposit, Ivanhoe District, Elko County, Nevada, *in* Raines, G. L., Lisle, R. E., Schafer, R. W., and Wilkinson, W. H., Eds.,Geology and ore deposits of the Great Basin – Symposium Proceedings: Geological Society of Nevada, v. 1, p.957-978.

Bettles, K., and Kornze, L, 1996, Geology and exploration history of the Goldstrike Property, Carlin Trend, Nevada, Ralph Roberts Distinguished Lecture, April 26, 1996.

Bonham, H. F., 1988, Models for volcanic-hosted epithermal precious deposits, *in* Schafer, R. W., Cooper, J. J., and Vikre, P. G., Eds., Bulk mineable precious metal deposits of the western United States, Symposium Proceedings: Geological Society of Nevada, p 259-271.

Bussey, S. D., 1988, Gold mineralization and associated rhyolitic volcanism at the Hog Ranch District, northwest Nevada, *in* Schafer, R. W., Cooper, J. J., and Vikre, P. G., Eds., Bulk mineable precious metal deposits of the western United States, Symposium Proceedings: Geological Society of Nevada, p 181- 207.

Christensen, O. D., 1993, Carlin trend geologic overview, *in* Christensen, O. D., Ed., Gold deposits of the Carlin Trend, Nevada: Society of Economic Geologists Guidebook, v. 18, p. 12-26.

Corbett, J. D., 1991, Overview of geophysical methods applied to precious metal exploration in Nevada, *in* Raines, G. L., Lisle, R. E., Schafer, R. W., and Wilkinson, W. H.,

Eds.,Geology and ore deposits of the Great Basin – Symposium Proceedings: Geological Society of Nevada, v. 1, p.1237-1251.

Daly, W. E., Doe, T. C., and Loranger, R. J., 1991, Geology of the northern Independence Mountains, Elko, County, Nevada, *in* Raines, G. L., Lisle, R. E., Schafer, R. W., and Wilkinson, W. H., Eds., Geology and ore deposits of the Great Basin – Symposium Proceedings: Geological Society of Nevada, v. 1, p. 583-602.

Dilles, P. A., Wright, W. A., Monteleone, S. E., Russell, K. D., Marlowe, K. E., Wood, R. A., and Margolis, J., 1996, The geology of the West Archimedes Deposit: a new gold discovery in the Eureka mining district, Eureka County, Nevada, *in* Coyner, A. R., and Fahey, P. L., Eds, Geology and ore deposits of the American Cordillera – Symposium Proceedings: Geological Society of Nevada, v. 1, p. 159-171.

Doyle, H. A., 1990, Geophysical exploration for gold – A review: Geophysics, v. 55, p. 134-146.

Eaton, D. W., Milkereit, B., and Adam, E., 1997, Paper 7, 3-D Seismic exploration, in, Proceedings of Exploration 97, Fourth Decennial International Conference on Mineral Exploration, Gubins, A. G., ed., published by the Prospectors and Developers Association of Canada, p. 65-78.

Emmons, D. L. and Eng, A. L., 1995, Geologic map of the McCoy Mining District, Lander County, Nevada: Nevada Bureau of Mines, Geologic Map 103.

Eng, A.L., 1991, Unpublished exploration report, Echo Bay Exploration Inc.

Evans, J. G., 1974, Geologic map of the Rodeo Creek NE Quadrangle, Eureka County, Nevada, Map GQ-1116, United States Geological Survey.

Foo, S. T., Hays, R. C., and McMormack, J. K., 1996, Geology and mineralization of the Pipeline Gold Deposit, Lander County, Nevada, *in* Coyner, A. R., and Fahey, P. L., Eds., Geology and ore deposits of the American Cordillera – Symposium Proceedings: Geological Society of Nevada, V. 1, p. 95-109.

Freeman, K., 1996, Gold Quarry in-pit geophysical data review, induced polarization, VLF resistivity, radiometrics, *in* Wright, J. L., Freeman, K., and Phillips, N., Eds., Geophysical field trip guide, Carlin Trend, Nevada: Society of Exploration Geophysicists, section I.

Groves, D. A., 1996, End members of the deposit spectrum on the Carlin Trend, Examples from recent discoveries: New Mineral Deposits of the Cordillera, 1996 Cordilleran Roundup Short Course, British Columbia Geological Society, p. 2.

Hajnal, Z., Annesley, I. R., White, D., Mathews, R. B., Sopuck, V. Koch, R., Leppin, M., and Ahuja, S., 1997, Sedimentary hosted mineral deposits: A high resolution seismic survey in the Athabasca Basin, *in* Gubins, A. G. Ed., Proceedings of Exploration 97, Fourth Decennial International Conference on Mineral Exploration: Prospectors and Developers Association of Canada, Paper 53, p. 421-432.

Hastings, J. S., Burkhart, T. H., and Richardson, R. E., 1988, Geology of the Florida Canyon gold deposit, Pershing County, Nevada, *in* Schafer, R. W., Cooper, J. J., and Vikre, P. G., Eds., Bulk mineable precious metal deposits of the western United States, Symposium Proceedings: Geological Society of Nevada, p. 433-452.

Ivosevic, S. W., and Theodore, T. G., 1996,Weakly developed porphyry system at Upper Paiute Canyon, Battle Mountain Mining District, Nevada, *in* Coyner, A. R., and Fahey, P. L., Eds, Geology and ore deposits of the American Cordillera – Symposium Proceedings: Geological Society of Nevada, v. 3, p. 1573-1594.

Jones B.K, 1992, Application of metal zoning to gold exploration in porphyry copper systems, Journal of Geochemical Exploration, v.43, p. 127-155

Kuehn, C.A., 1989, Studies of disseminated gold deposits near Carlin, Nevada: Evidence for a deep geologic setting of ore formation: PhD Dissertation, Pennsylvania State University.

Kuyper, B. A., 1988, Geology of the McCoy gold deposit, Lander County, Nevada, *in* Schafer, R. W., Cooper, J. J., and Vikre, P. G., Eds., Bulk mineable precious metal deposits of the western United States, Symposium Proceedings: Geological Society of Nevada, p173-185.

Miller, R. D., and Steeples, D. W., 1995, Applications of shallow high resolution seismic reflection to various mining operations, Mining Engineering, vol. 47, p. 355-361.

Monroe, S. C., Godlewski, D. W., and Plahuta, J. T., 1988, Geology and mineralization at the Buckhorn Mine, Eureka County, Nevada, *in* Schafer, R. W., Cooper, J. J., and Vikre, P. G., Eds., Bulk mineable precious metal deposits of the western United States, Symposium Proceedings: Geological Society of Nevada, 273-291.

Nash, J. T., Utterback, W. C., and Saunders, J. A., 1991, Geology and geochemistry of the Sleeper gold deposit, Humboldt County, Nevada, An interim report, *in* Raines, G. L., Lisle, R. E., Schafer, R. W., and Wilkinson, W. H., Eds.,Geology and ore deposits of the Great Basin – Symposium Proceedings: Geological Society of Nevada, v. 1, p. 1063-1084.

Nelson, C. E., 1988, Gold deposits in the hot springs environment, *in* Schafer, R. W., Cooper, J. J., and Vikre, P. G., Eds., Bulk mineable precious metal deposits of the western United States, Symposium Proceedings: Geological Society of Nevada, 417-431.

Osterberg, M. W., and Guilbert, J. M., 1991, Geology, wall-rock alteration, and new exploration techniques at the Chimney Creek sediment-hosted gold deposit, Humboldt County, Nevada, *in* Raines, G. L., Lisle, R. E., Schafer, R. W., and Wilkinson, W. H., Eds., Geology and ore deposits of the Great Basin – Symposium Proceedings: Geological Society of Nevada, v. 2, p. 805-819.

Sato, M., and Mooney, H. M., 1960, The electrochemical mechanism of sulphide self potentials: Geophysics, vol. 25, p. 226-249.

Shawe, D. R., 1991, Structurally controlled gold trends imply large gold resources in Nevada,, *in* Raines, G. L., Lisle, R. E., Schafer, R. W., and Wilkinson, W. H., Eds., Geology and ore deposits of the Great Basin – Symposium Proceedings: Geological Society of Nevada, v. 1, p. 199-212

Sillitoe, R. H., 1988, Gold and silver deposits in porphyry systems, *in* Schafer, R. W., Cooper, J. J., and Vikre, P. G., Eds., Bulk mineable precious metal deposits of the western United States, Symposium Proceedings: Geological Society of Nevada, p. 233-257.

Simon, G., Kesler, S. E., Peltonen, D. R., Chryssoulis, S. L., Huang, H., and Penner-Hahn, J. E., 1997, Relation between pyrite and gold at the Twin Creeks SHMG Deposit, Nevada, *in* Thompson, T. B., ED., Carlin-Type gold deposits, field conference: Society of Economic Geologist, p. 137-138.

Taylor, R.S., 1990, Airborne EM resistivity applied to exploration for precious metal deposits, The Leading Edge: Society of Exploration Geophysicists, Feb 1990, p. 34-41

Teal, L., and Branham, A., 1997, Geology of the Mike Gold-Copper Deposit, Eureka County, Nevada, *in* Thompson, T. B., ED., Carlin-Type gold deposits, field conference: Society of Economic Geologist, p. 257-276.

Teal, L., and Jackson, M., 1997, Geologic overview of the Carlin Trend gold deposits and descriptions of recent deep discoveries, *in* Thompson, T. B., Ed., Carlin-Type gold deposits, field conference: Society of Economic Geologists, p. 3-37.

Thorson, R. F., 1991, Geology and gold deposits of the Rain subdistrict, Elko County, Nevada, *in* Raines, G. L., Lisle, R. E., Schafer, R. W., and Wilkinson, W. H., Eds., Geology and ore deposits of the Great Basin – Symposium Proceedings: Geological Society of Nevada, v. 2, p. 635-643.

Van Nieuwenhuyse, Geology and ore controls of gold silver mineralization in the Talapoosa mining district, Lyon County, Nevada, *in* Raines, G.L., Lisle, R.E., Schafer, R.W., and Wilkinson W.H., Eds., Geology and ore deposits of the Great Basin-Symposium Proceedings: Geological Society of Nevada, v.2, p.979-992

Wieduwilt, W.G., 1987, Induced polarization and resistivity survey on the McCoy project, Mining Geophysical Surveys Inc. report 1712, Unpublished report to Echo Bay Exploration.

Wotruba, P. R., Benson, R. G., and Schmidt, K. W., 1988, Geology of the Fortitude gold-silver skarn deposit, Copper Canyon, Lander County, Nevada, *in* Schafer, R. W., Cooper, J. J., and Vikre, P. G., Eds., Bulk mineable precious metal deposits of the western United States, Symposium Proceedings: Geological Society of Nevada, p. 159-171.

Wright, J. L., 1996, North area data review, *in* Wright, J. L., Freeman, K., and Phillips, N., Eds., Geophysical field trip guide, Carlin Trend, Nevada: Society of Exploration Geophysicists, section VIII.

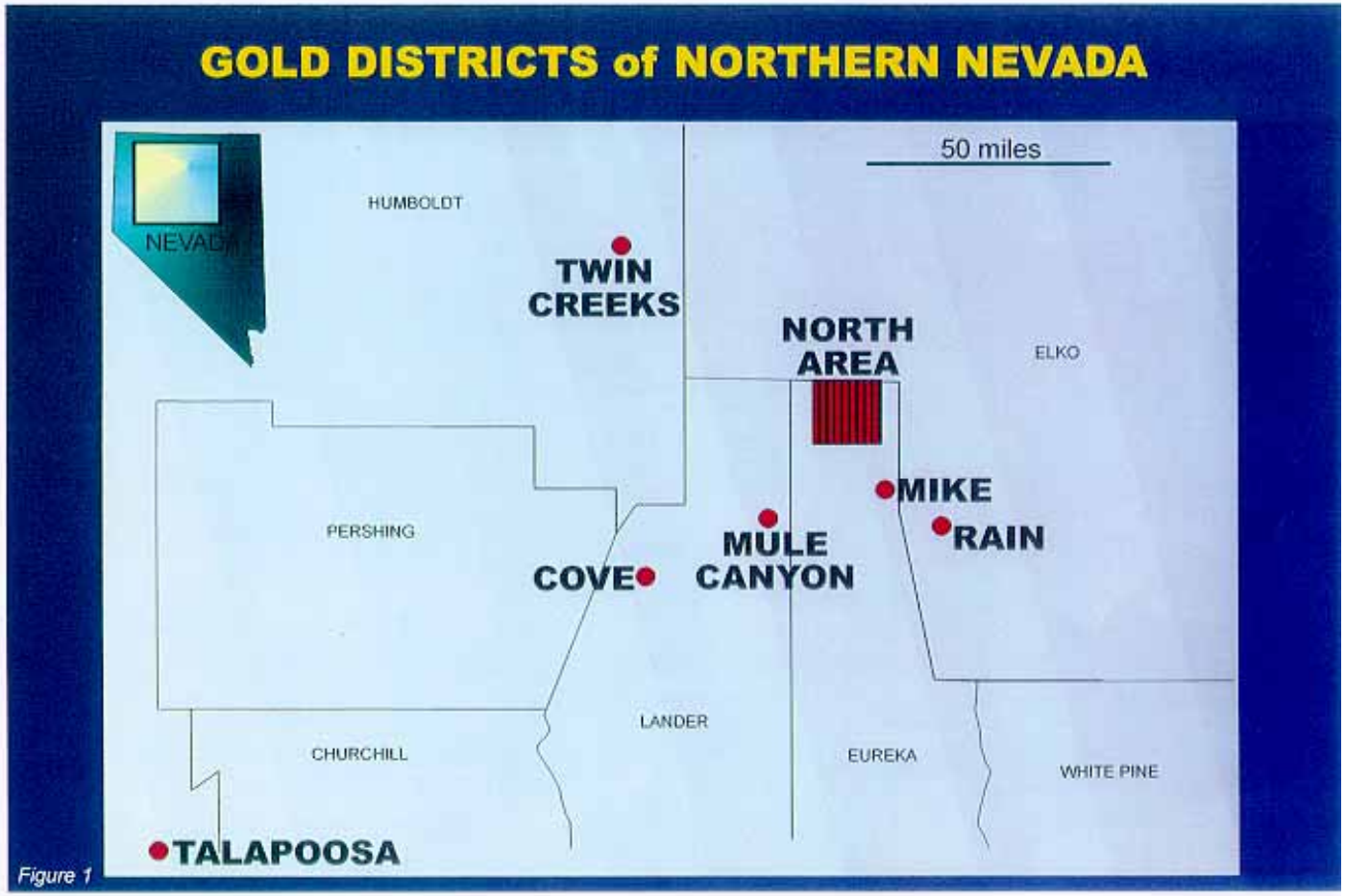
GOLD DISTRICTS of NORTHERN NEVADA
50 miles
NEVADA
HUMBOLDT
TWIN CREEKS
NORTH AREA
ELKO
MIKE
RAIN
PERSHING
MULE CANYON
COVE
LANDER
CHURCHILL
EUREKA
WHITE PINE
TALAPOOSA

Figure 1

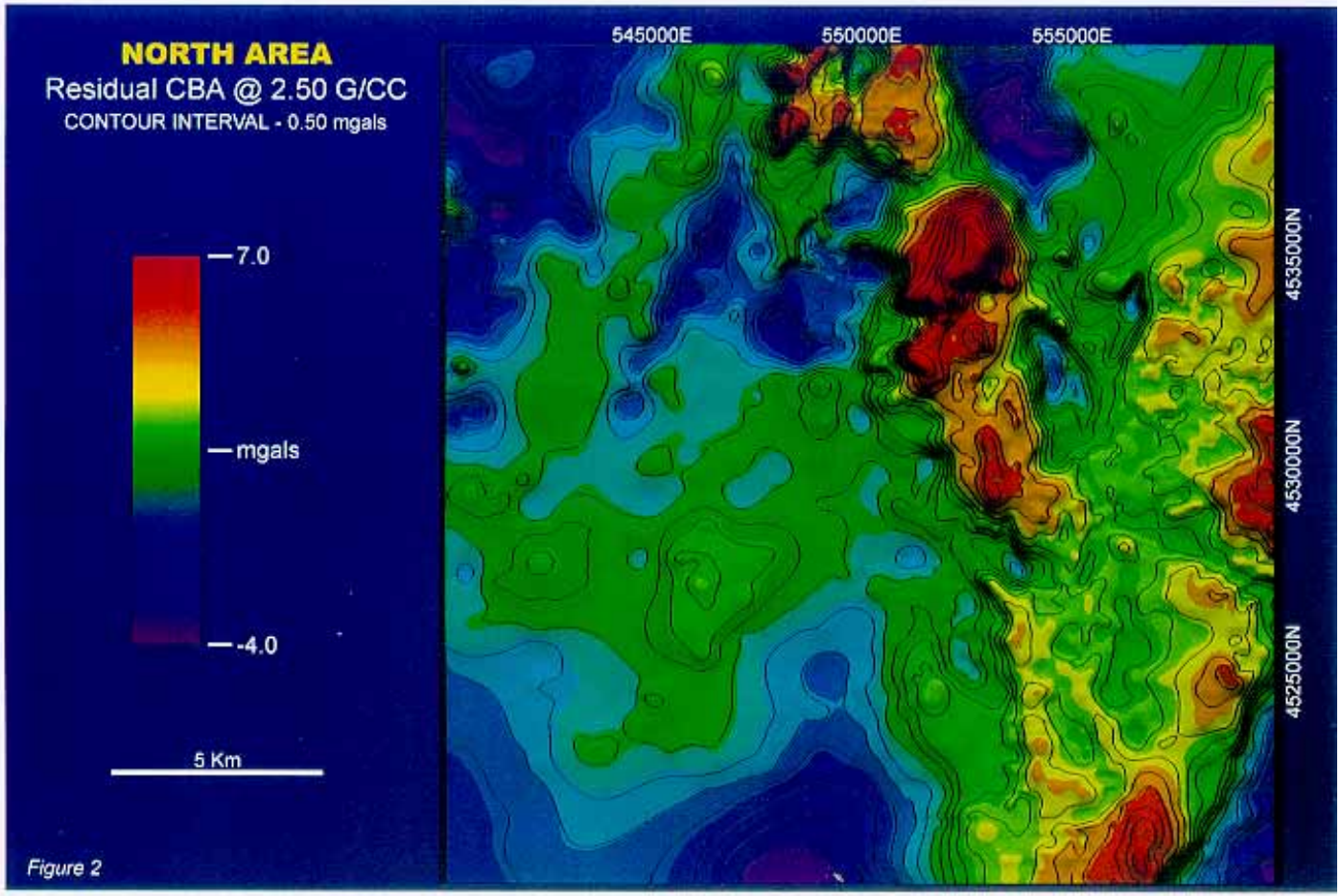
NORTH AREA
Residual CBA @ 2.50 G/CC
CONTOUR INTERVAL - 0.50 mgals
7.0
mgals
-4.0
5 Km
545000E
550000E
555000E
4535000N
4530000N
4525000N

Figure 2

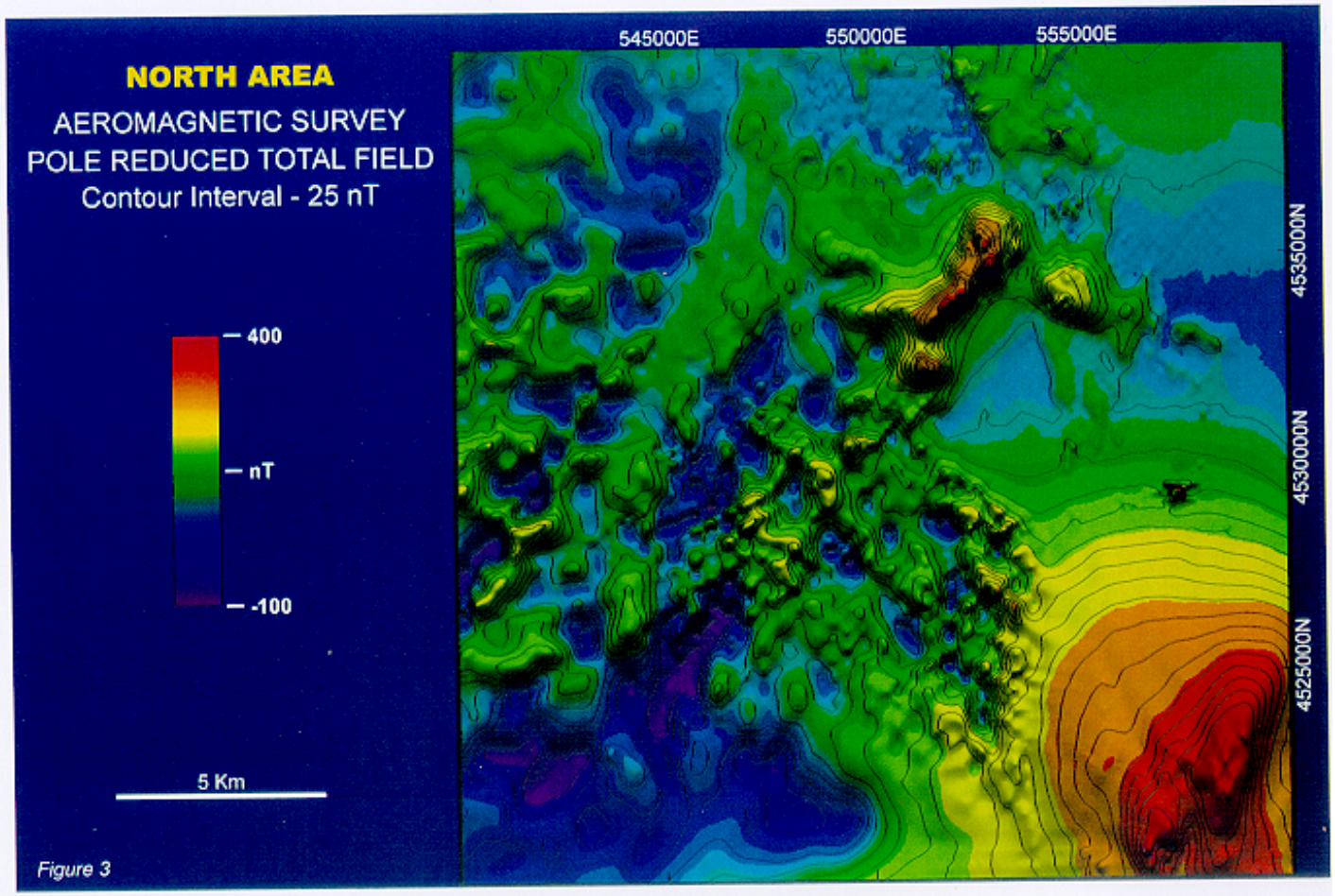
NORTH AREA
AEROMAGNETIC SURVEY
POLE REDUCED TOTAL FIELD
Contour Interval - 25 nT
400
nT
-100
5 Km
545000E
550000E
555000E
4535000N
4530000N
4525000N

Figure 3

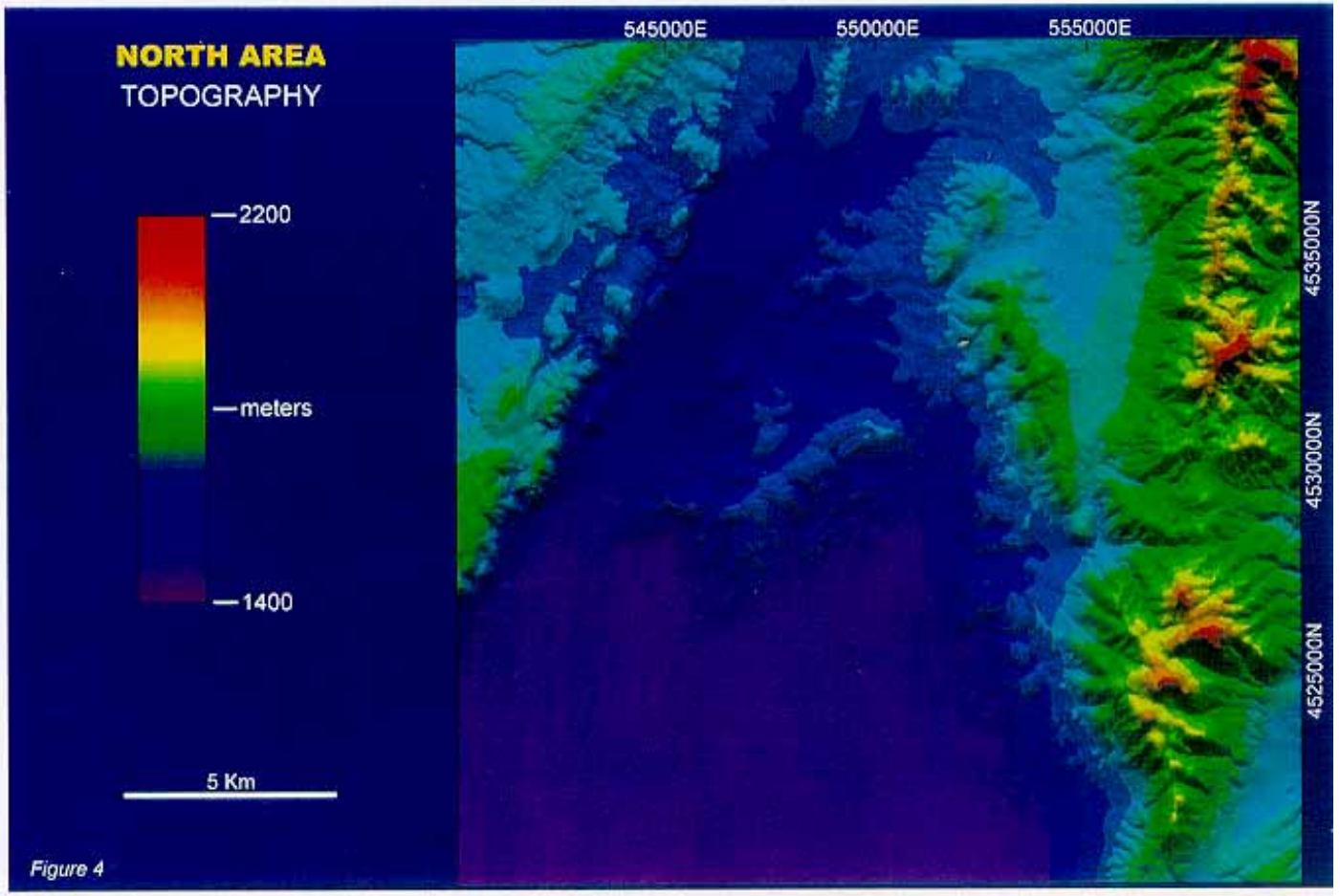
NORTH AREA
TOPOGRAPHY
2200
meters
1400
5 Km
545000E
550000E
555000E
4535000N
4530000N
4525000N

Figure 4

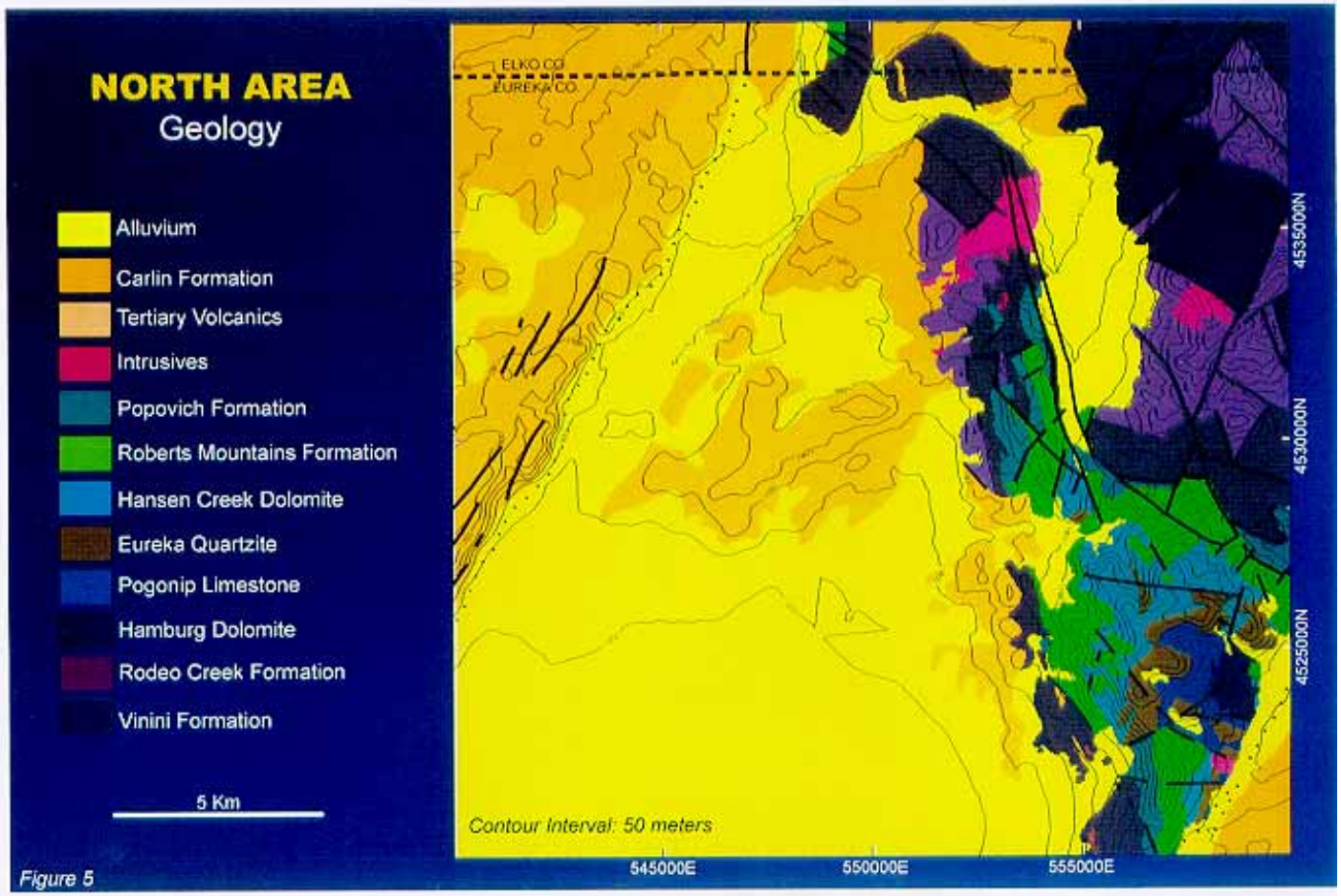
NORTH AREA
Geology
Alluvium
Carlin Formation
Tertiary Volcanics
Intrusives
Popovich Formation
Roberts Mountains Formation
Hansen Creek Dolomite
Eureka Quartzite
Pogonip Limestone
Hamburg Dolomite
Rodeo Creek Formation
Vinini Formation
5 Km
ELKO CO
EUREKA CO
Contour Interval: 50 meters
545000E
550000E
555000E
4535000N
4530000N
4525000N

Figure 5

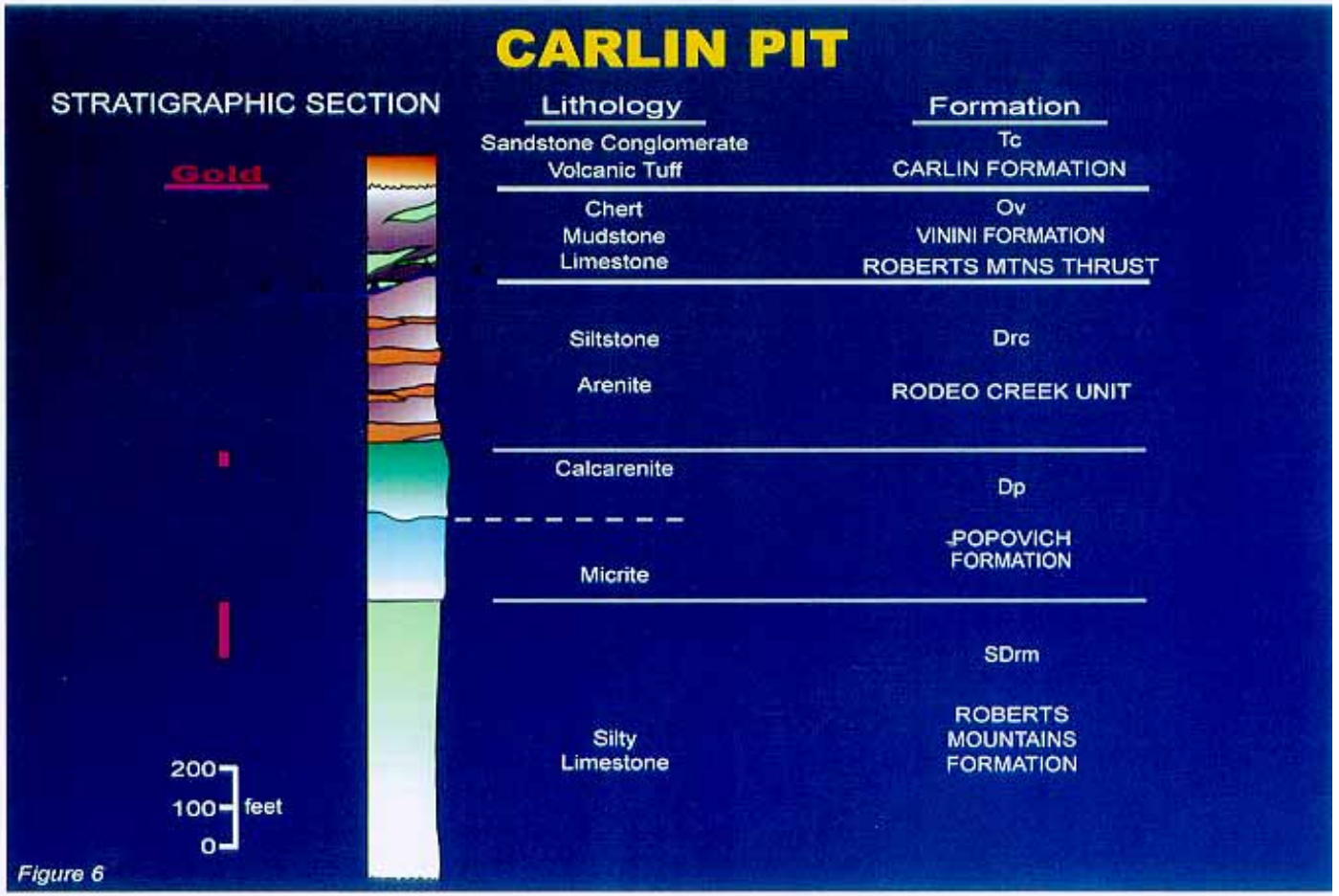
CARLIN PIT
STRATIGRAPHIC SECTION
Gold
Lithology
Formation
Sandstone Conglomerate
Volcanic Tuff
Tc
CARLIN FORMATION
Chert
Mudstone
Limestone
Ov
VININI FORMATION
ROBERTS MTNS THRUST
Siltstone
Arenite
Drc
RODEO CREEK UNIT
Calcarenite
Micrite
Dp
POPOVICH FORMATION
SDrm
Silty Limestone
ROBERTS MOUNTAINS FORMATION
200
100
0
feet

Figure 6

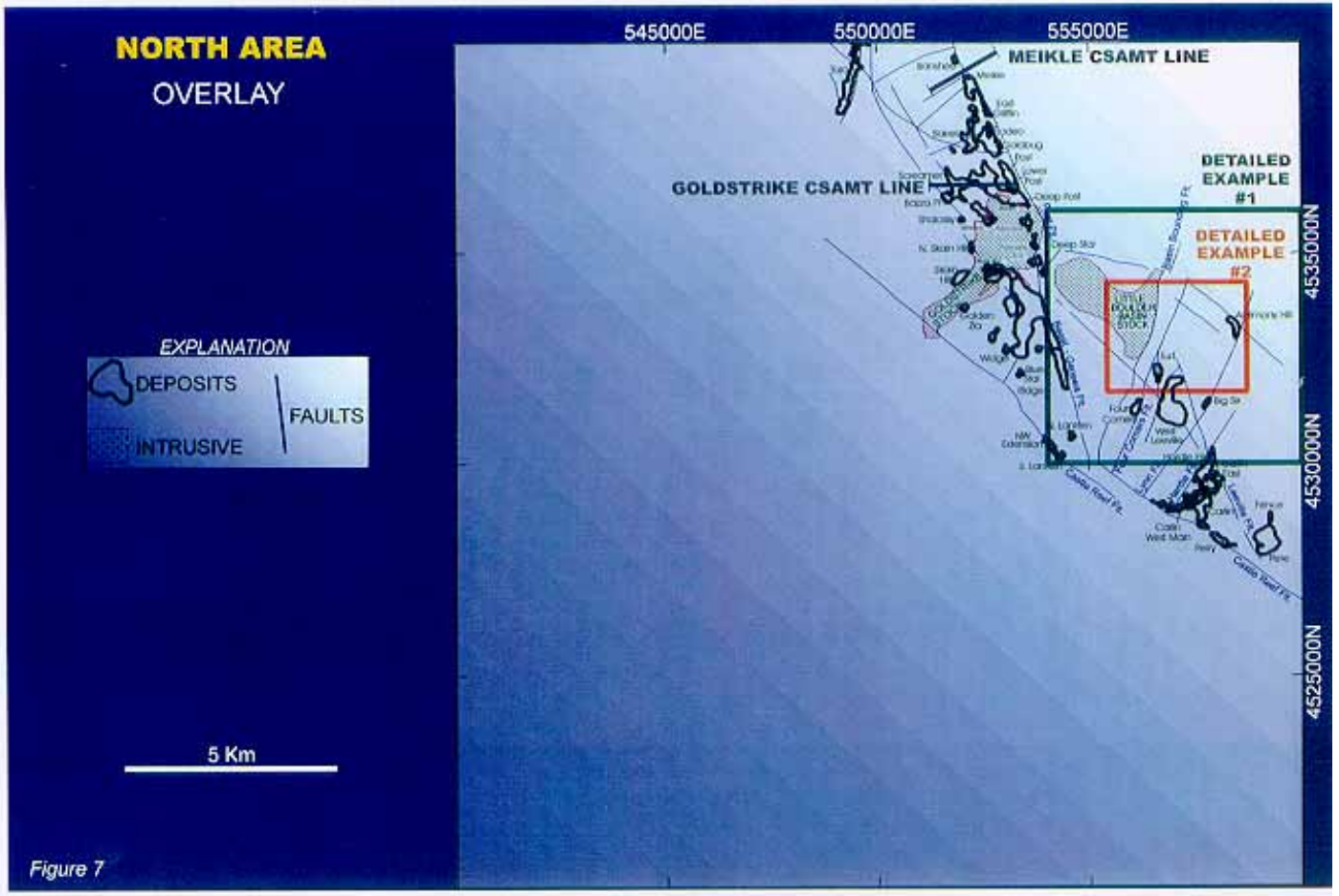
NORTH AREA
OVERLAY
EXPLANATION
DEPOSITS
FAULTS
INTRUSIVE
5 Km
545000E
550000E
555000E
MEIKLE CSAMT LINE
GOLDSTRIKE CSAMT LINE
DETAILED EXAMPLE #1
DETAILED EXAMPLE #2
4535000N
4530000N
4525000N

Figure 7

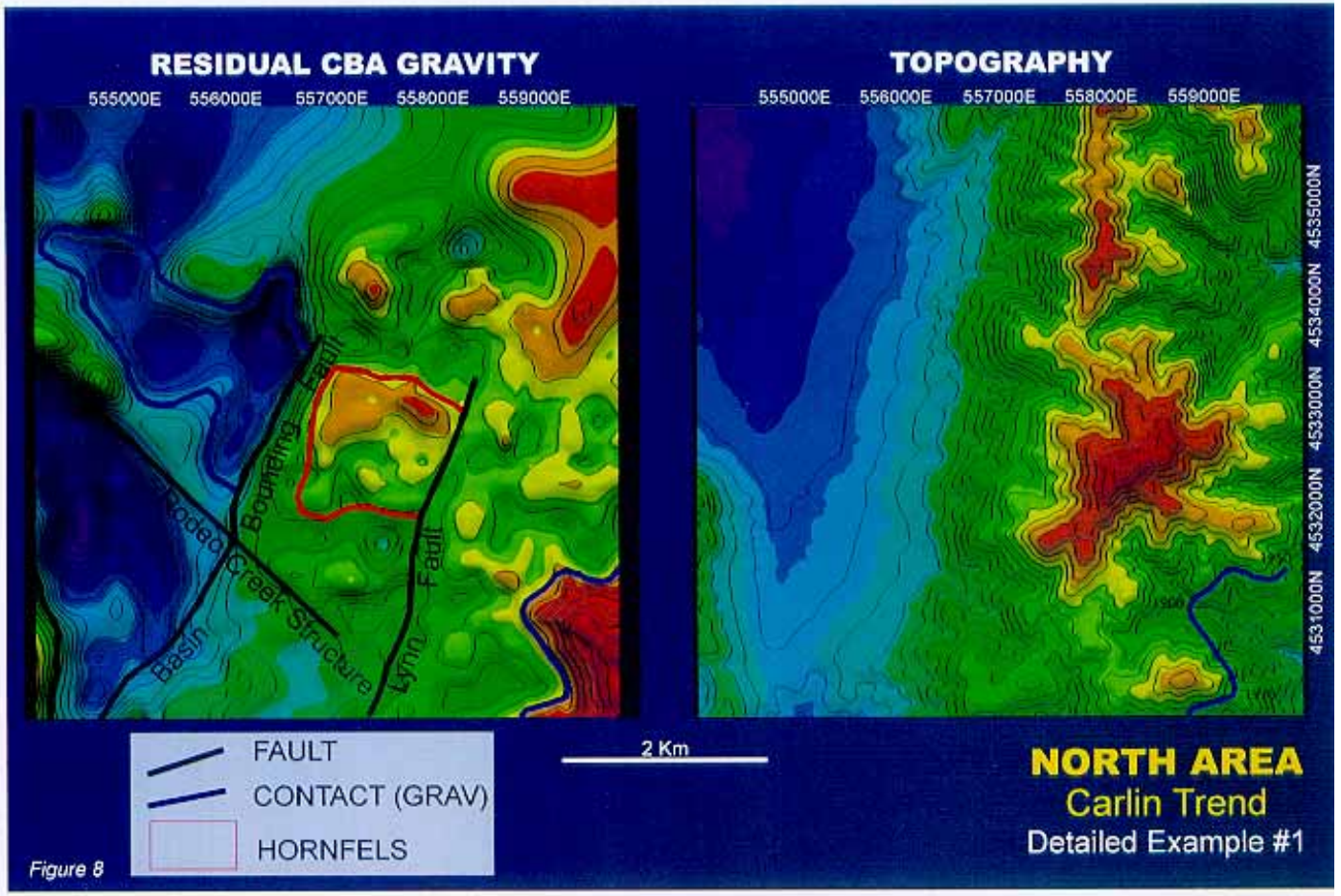
RESIDUAL CBA GRAVITY
555000E
556000E
557000E
558000E
559000E
Bounding Fault
Rodeo Creek Structure
Basin
Lynn Fault
TOPOGRAPHY
555000E
556000E
557000E
558000E
559000E
4535000N
4534000N
4533000N
4532000N
4531000N
FAULT
CONTACT (GRAV)
HORNFELS
2 Km
NORTH AREA
Carlin Trend
Detailed Example #1

Figure 8

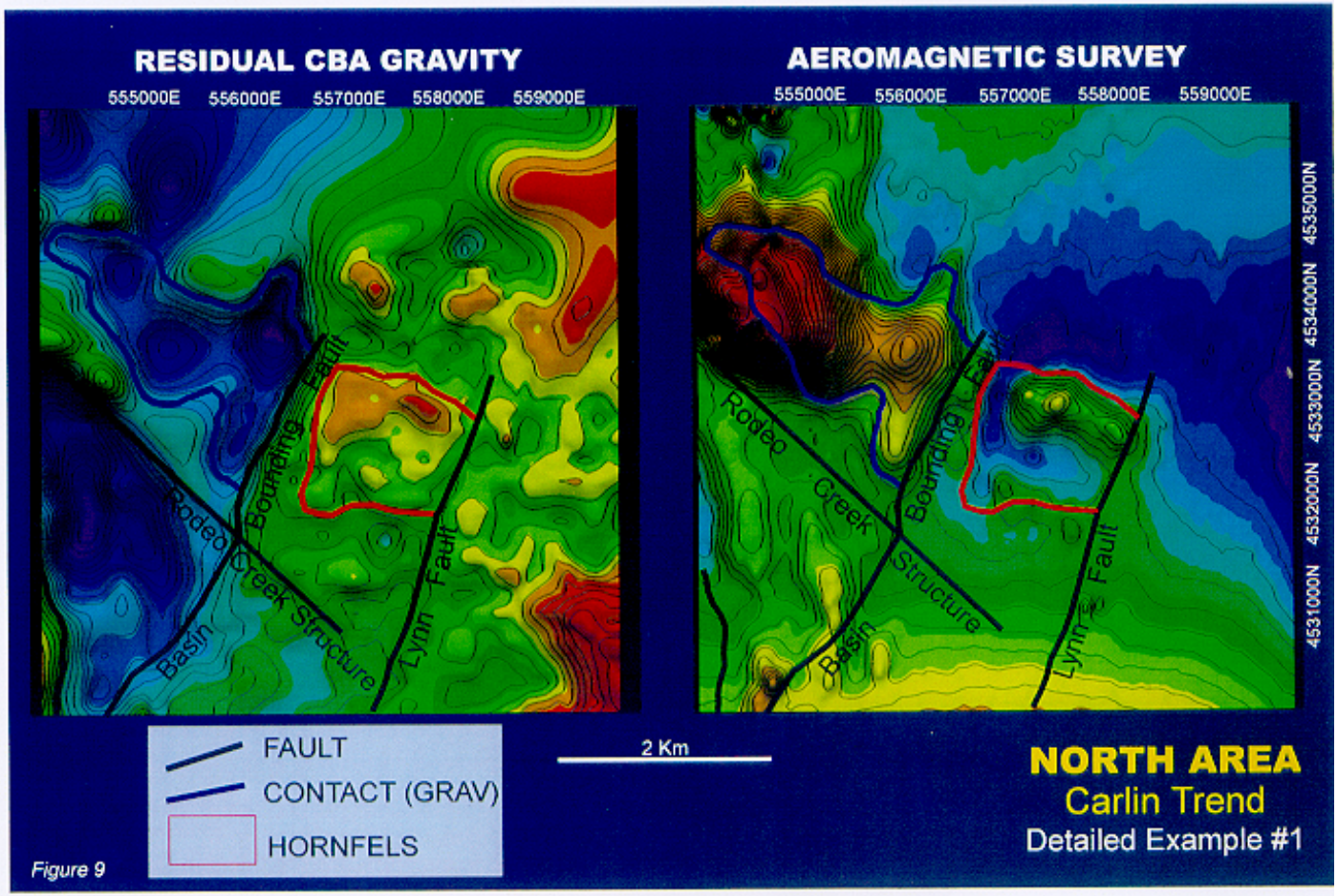
RESIDUAL CBA GRAVITY
555000E
556000E
557000E
558000E
559000E
AEROMAGNETIC SURVEY
555000E
556000E
557000E
558000E
559000E
4535000N
4534000N
4533000N
4532000N
4531000N
Rodeo Creek Basin
Bounding Fault
Rodeo Creek Structure
Lynn Fault
FAULT
CONTACT (GRAV)
HORNFELS
2 Km
NORTH AREA
Carlin Trend
Detailed Example #1

Figure 9

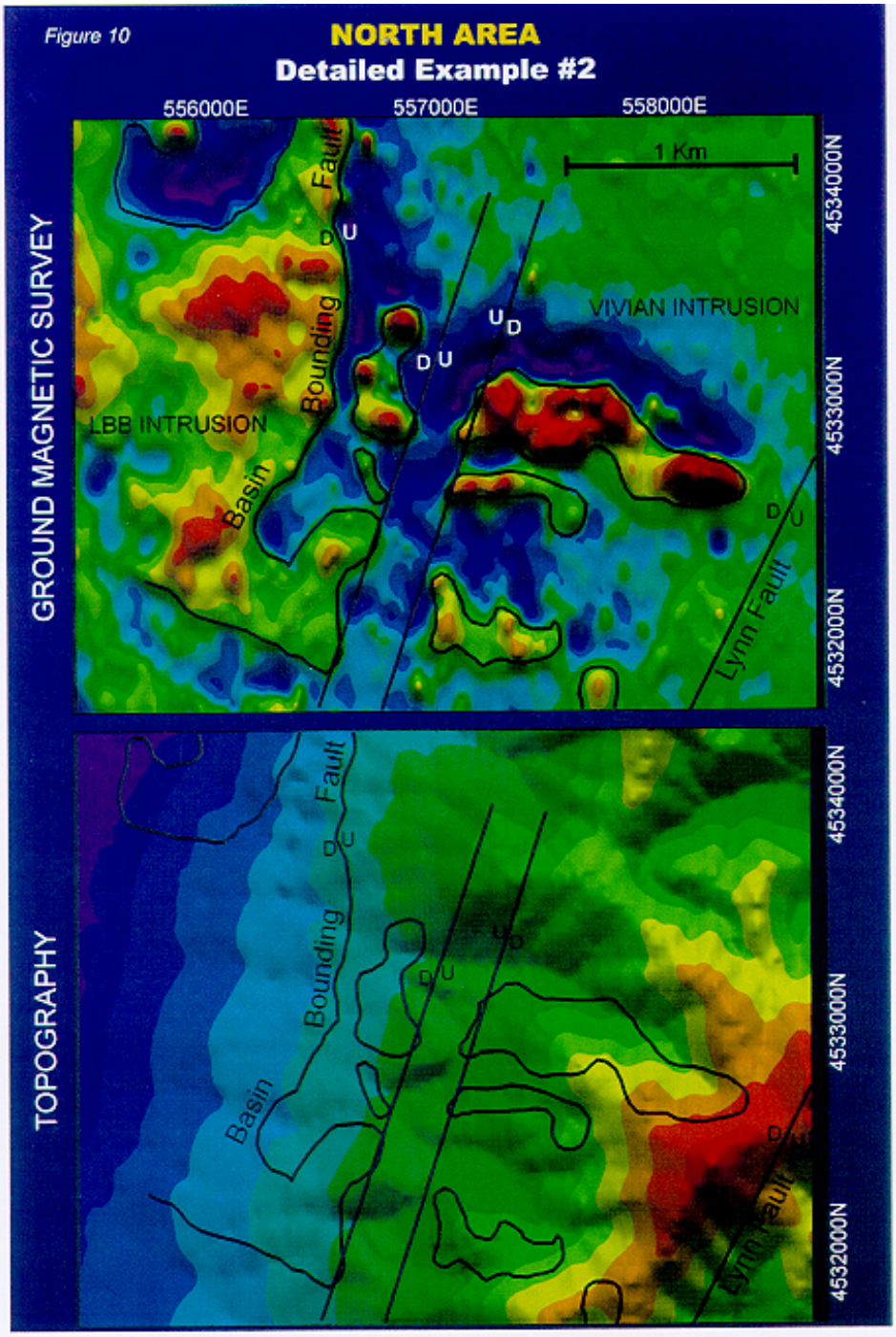
Figure 10
NORTH AREA
Detailed Example #2
556000E
557000E
558000E
1 Km
4534000N
4533000N
4532000N
GROUND MAGNETIC SURVEY
TOPOGRAPHY
Basin Bounding Fault
LBB INTRUSION
VIVIAN INTRUSION
Lynn Fault
U
D
C

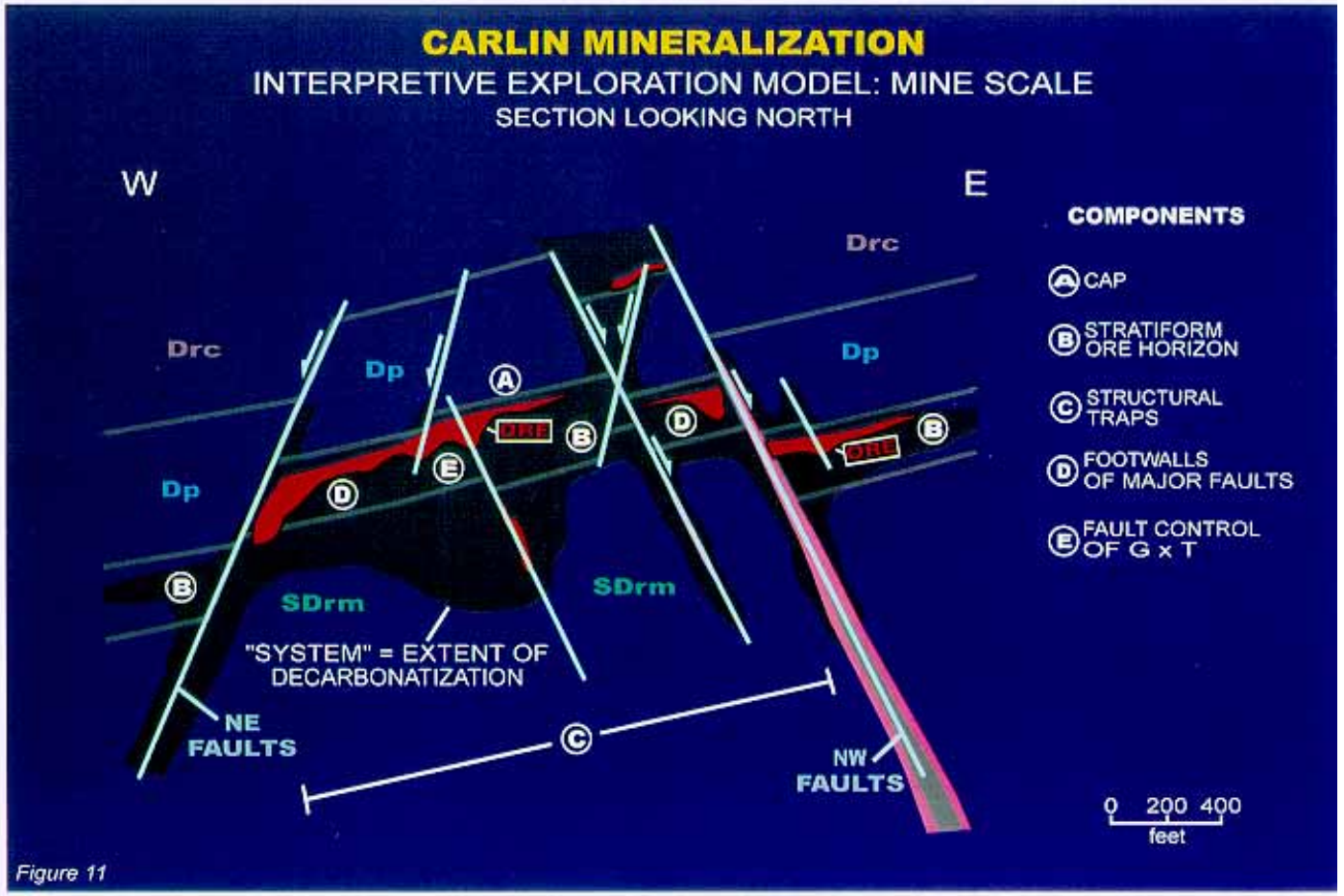
CARLIN MINERALIZATION
INTERPRETIVE EXPLORATION MODEL: MINE SCALE
SECTION LOOKING NORTH
W
E
Drc
Dp
Drc
Dp
Dp
ORE
ORE
SDrm
SDrm
"SYSTEM" = EXTENT OF DECARBONATIZATION
NE FAULTS
NW FAULTS
A
B
C
D
E
COMPONENTS
A CAP
B STRATIFORM ORE HORIZON
C STRUCTURAL TRAPS
D FOOTWALLS OF MAJOR FAULTS
E FAULT CONTROL OF G x T
0 200 400
feet

Figure 11

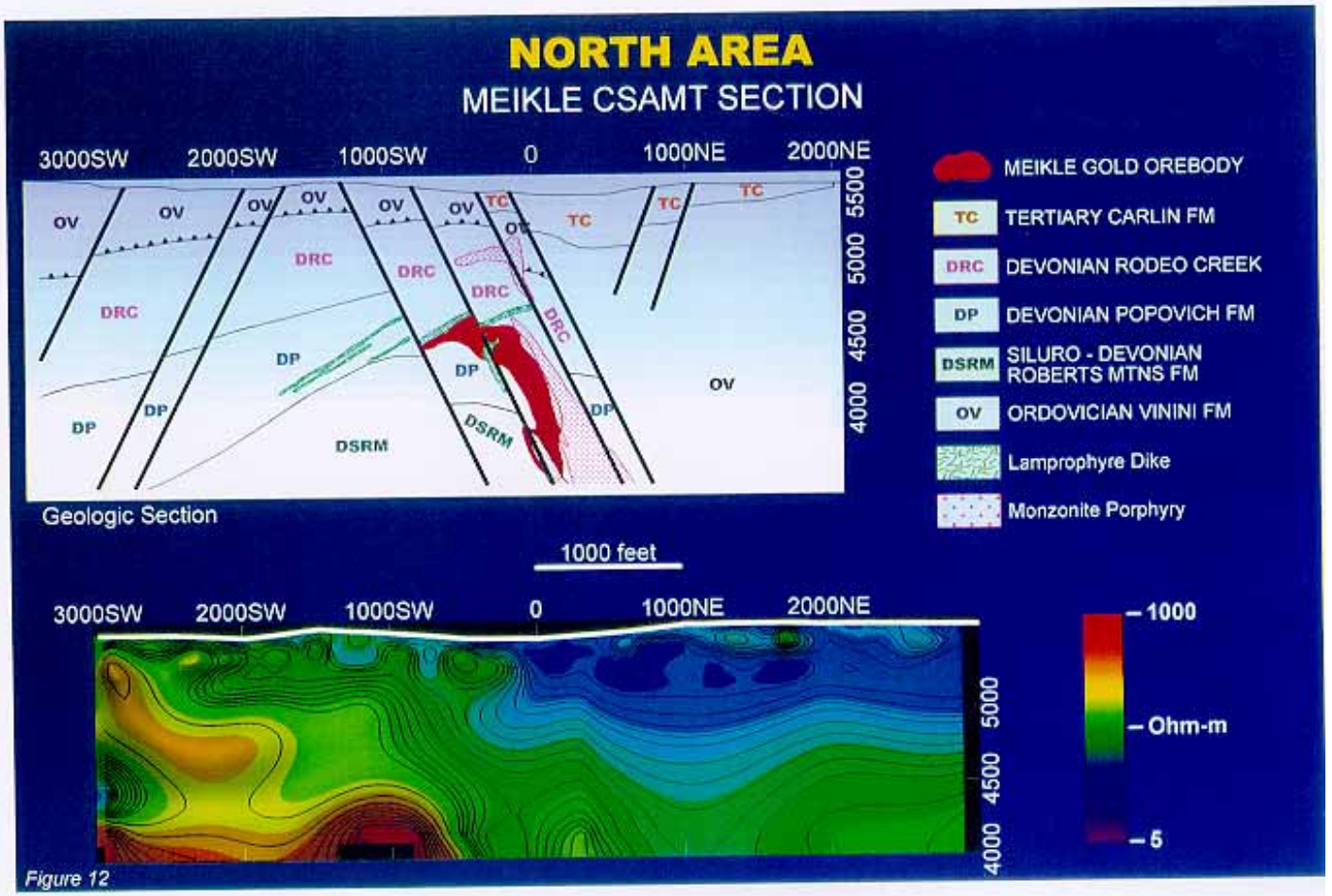
NORTH AREA
MEIKLE CSAMT SECTION
3000SW
2000SW
1000SW
0
1000NE
2000NE
5500
5000
4500
4000
OV
DRC
DP
DSRM
TC
Geologic Section
1000 feet
MEIKLE GOLD OREBODY
TERTIARY CARLIN FM
DEVONIAN RODEO CREEK
DEVONIAN POPOVICH FM
SILURO - DEVONIAN ROBERTS MTNS FM
ORDOVICIAN VININI FM
Lamprophyre Dike
Monzonite Porphyry
1000
Ohm-m
5

Figure 12

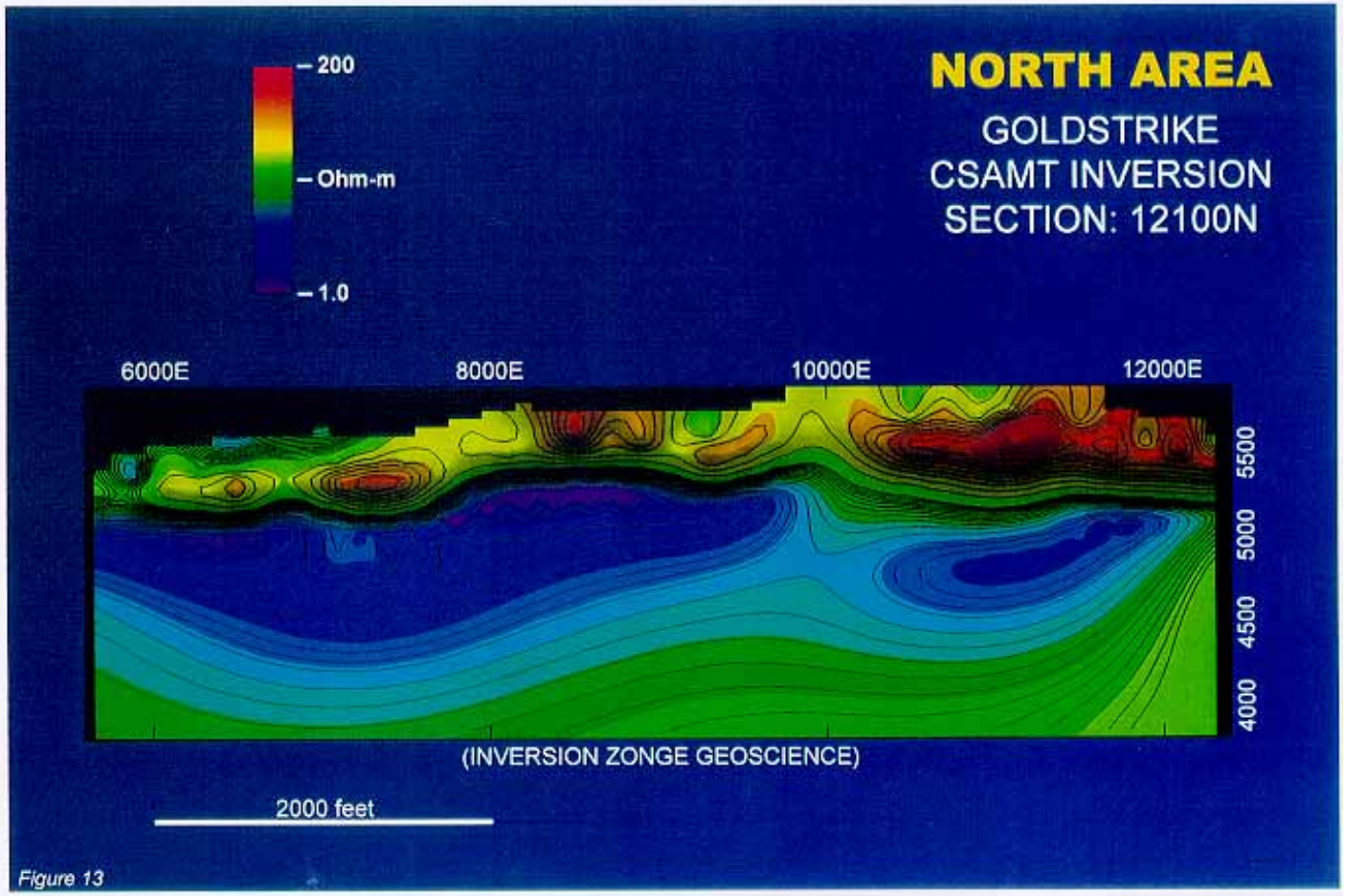
200
Ohm-m
1.0
NORTH AREA
GOLDSTRIKE
CSAMT INVERSION
SECTION: 12100N
6000E
8000E
10000E
12000E
5500
5000
4500
4000
(INVERSION ZONGE GEOSCIENCE)
2000 feet

Figure 13

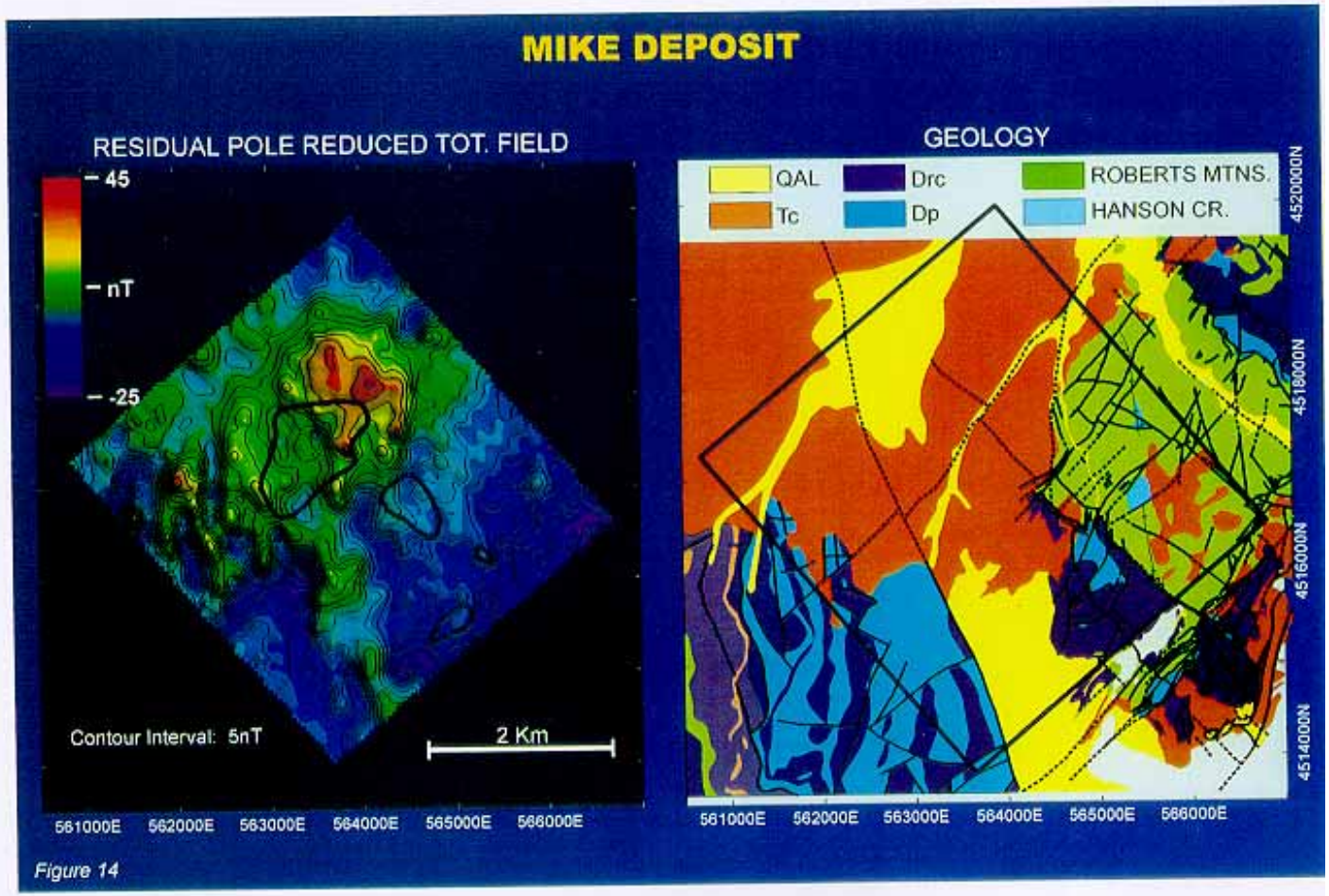
MIKE DEPOSIT
RESIDUAL POLE REDUCED TOT. FIELD
45
nT
-25
Contour Interval: 5nT
2 Km
561000E
562000E
563000E
564000E
565000E
566000E
GEOLOGY
QAL
Drc
ROBERTS MTNS.
Tc
Dp
HANSON CR.
4520000N
4518000N
4516000N
4514000N
561000E
562000E
563000E
564000E
565000E
566000E

Figure 14

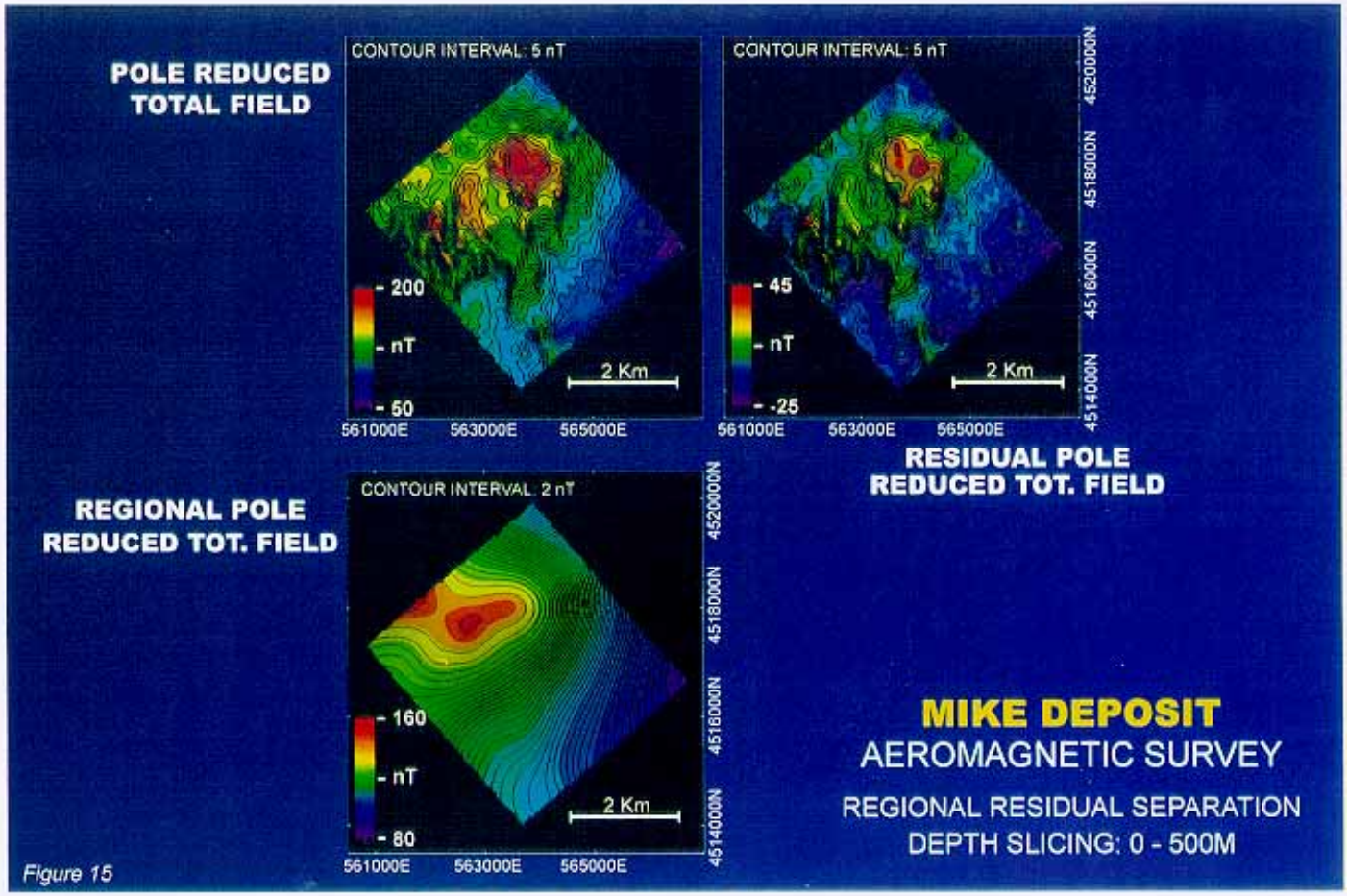
POLE REDUCED
TOTAL FIELD
CONTOUR INTERVAL: 5 nT
200
nT
50
2 Km
561000E
563000E
565000E
CONTOUR INTERVAL: 5 nT
45
nT
-25
2 Km
561000E
563000E
565000E
4520000N
4518000N
4516000N
4514000N
RESIDUAL POLE
REDUCED TOT. FIELD
REGIONAL POLE
REDUCED TOT. FIELD
CONTOUR INTERVAL: 2 nT
160
nT
80
2 Km
561000E
563000E
565000E
4520000N
4518000N
4516000N
4514000N
MIKE DEPOSIT
AEROMAGNETIC SURVEY
REGIONAL RESIDUAL SEPARATION
DEPTH SLICING: 0 - 500M

Figure 15

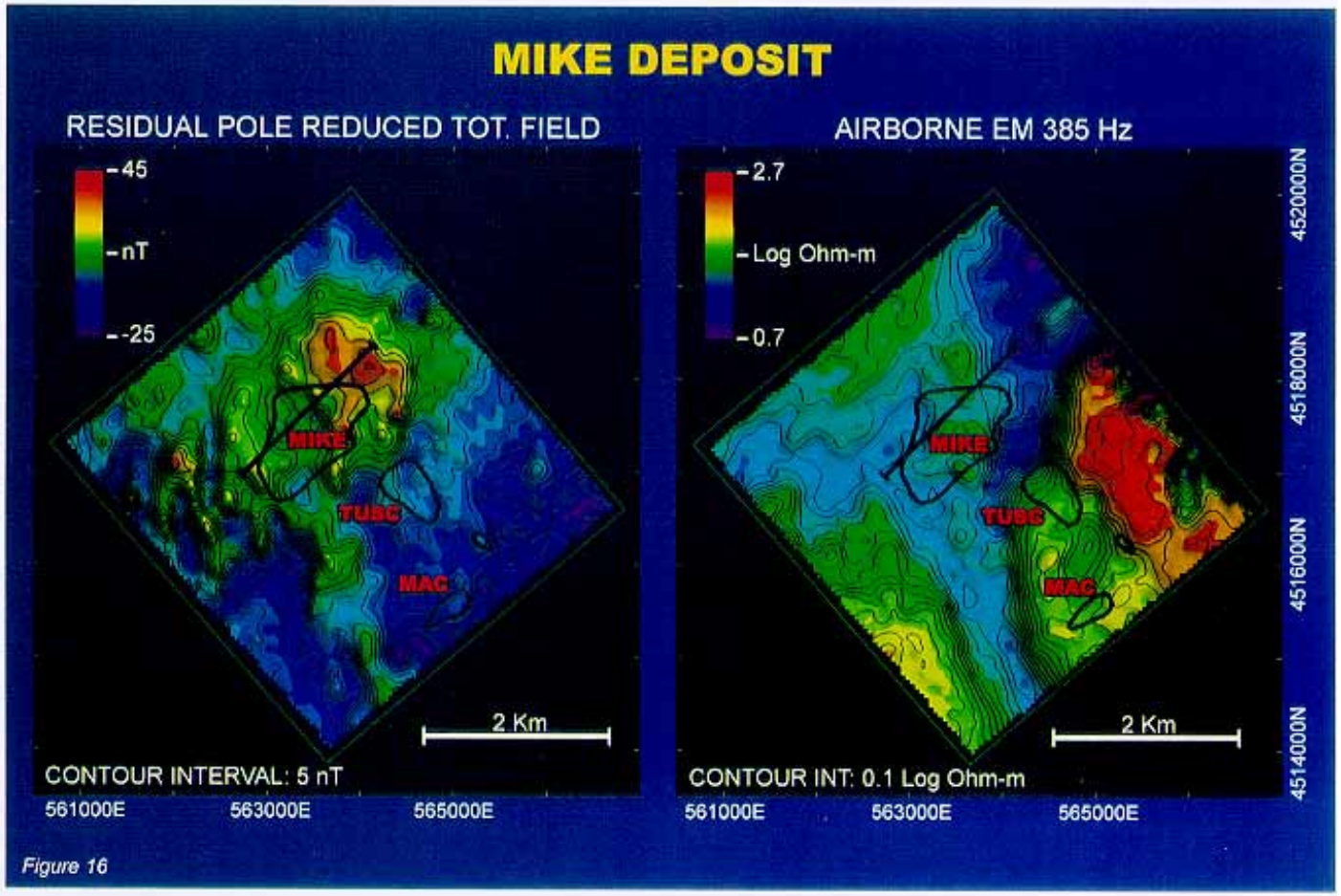
MIKE DEPOSIT
RESIDUAL POLE REDUCED TOT. FIELD
-45
-nT
--25
MIKE
TUBC
MAC
2 Km
CONTOUR INTERVAL: 5 nT
561000E
563000E
565000E
AIRBORNE EM 385 Hz
-2.7
-Log Ohm-m
-0.7
MIKE
TUBC
MAC
2 Km
CONTOUR INT: 0.1 Log Ohm-m
561000E
563000E
565000E
4520000N
4518000N
4516000N
4514000N

Figure 16

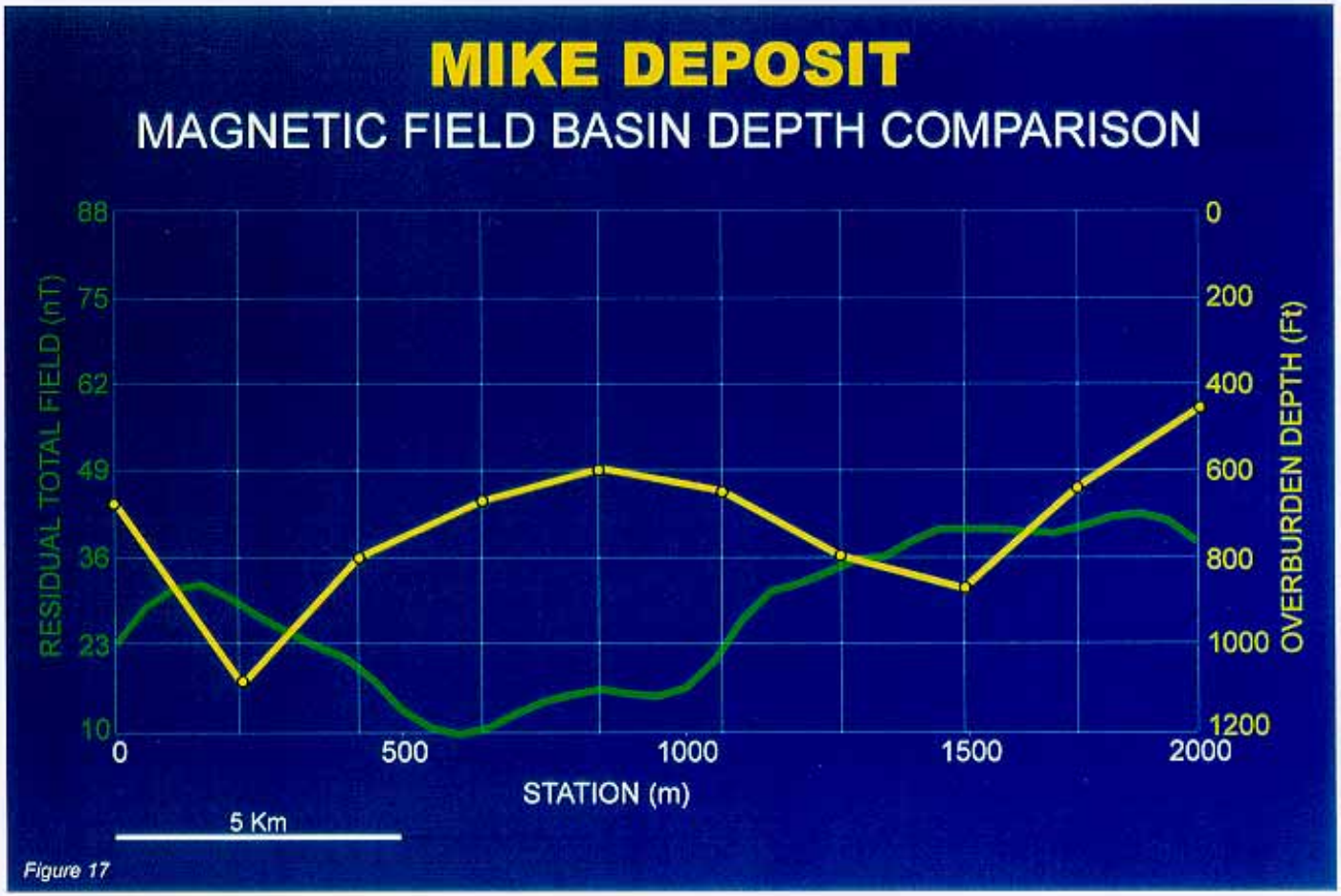
MIKE DEPOSIT
MAGNETIC FIELD BASIN DEPTH COMPARISON
RESIDUAL TOTAL FIELD (nT)
88
75
62
49
36
23
10
0
500
1000
1500
2000
STATION (m)
OVERBURDEN DEPTH (Ft)
0
200
400
600
800
1000
1200
5 Km
Figure 17

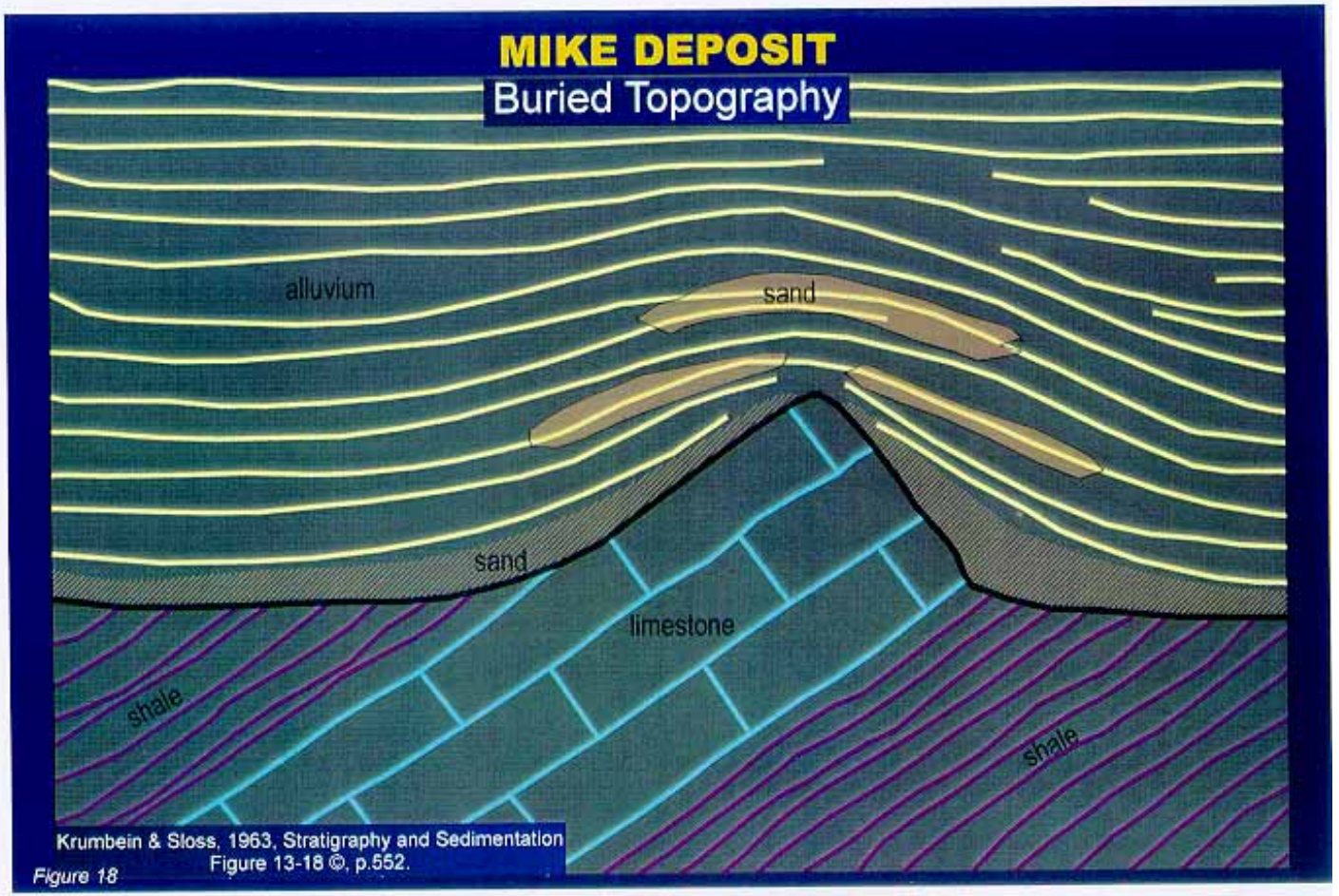
MIKE DEPOSIT
Buried Topography
alluvium
sand
sand
limestone
shale
shale
Krumbein & Sloss, 1963, Stratigraphy and Sedimentation
Figure 13-18 ©, p.552.

Figure 18

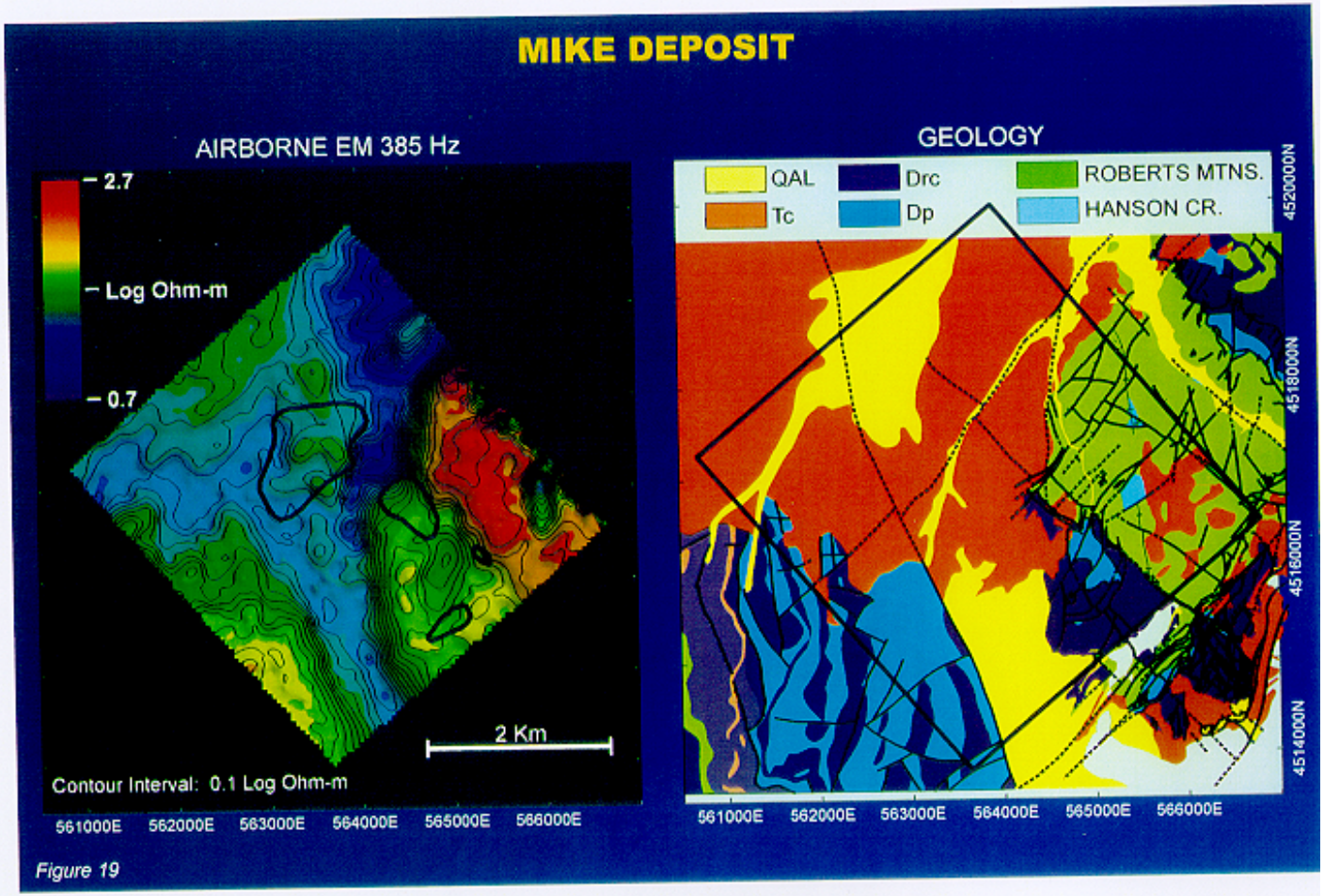
MIKE DEPOSIT
AIRBORNE EM 385 Hz
2.7
Log Ohm-m
0.7
2 Km
Contour Interval: 0.1 Log Ohm-m
561000E
562000E
563000E
564000E
565000E
566000E
GEOLOGY
QAL
Drc
ROBERTS MTNS.
Tc
Dp
HANSON CR.
4520000N
4518000N
4516000N
4514000N
561000E
562000E
563000E
564000E
565000E
566000E

Figure 19

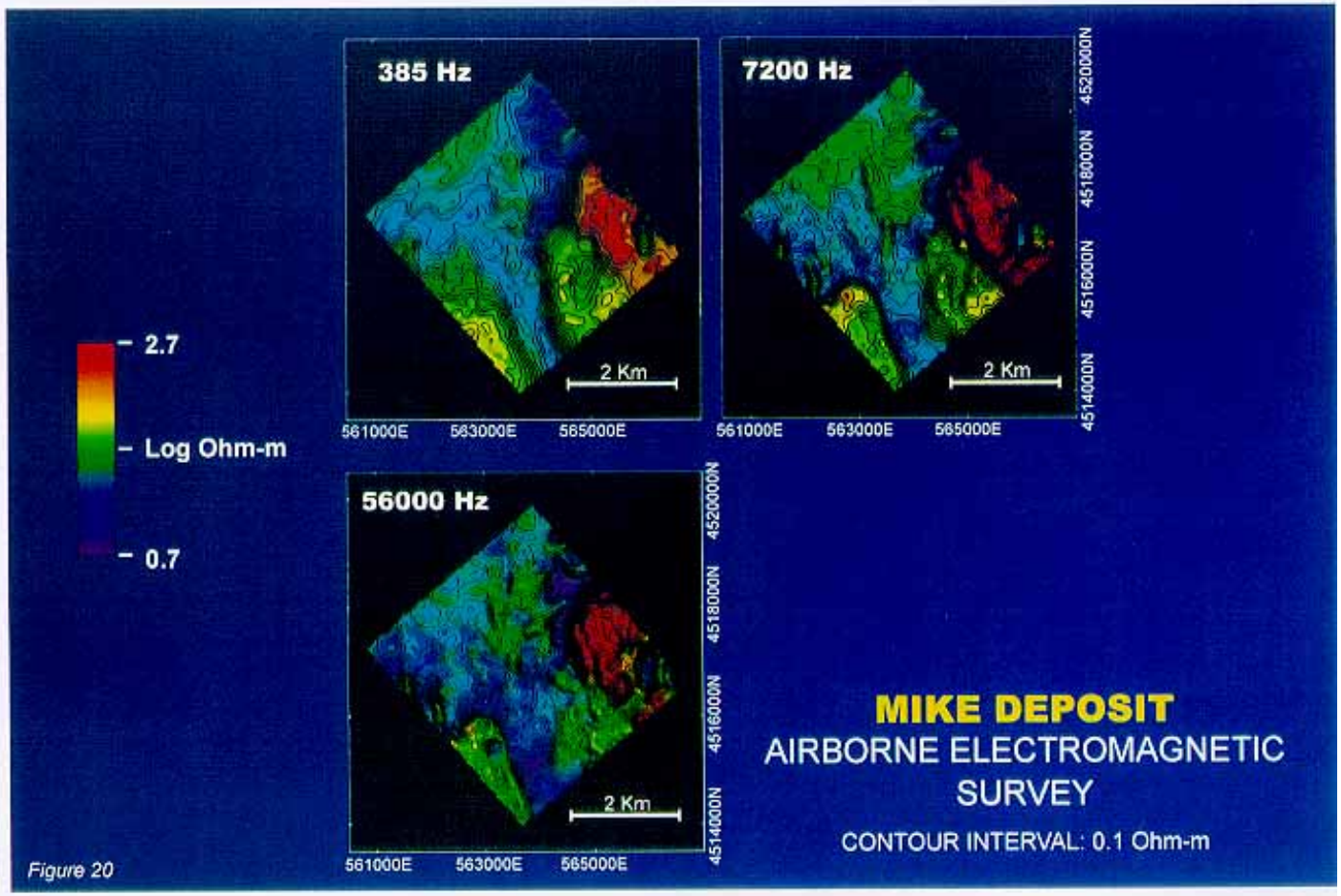
385 Hz
7200 Hz
56000 Hz
2 Km
2 Km
2 Km
2.7
Log Ohm-m
0.7
561000E
563000E
565000E
4520000N
4518000N
4516000N
4514000N
MIKE DEPOSIT
AIRBORNE ELECTROMAGNETIC SURVEY
CONTOUR INTERVAL: 0.1 Ohm-m

Figure 20

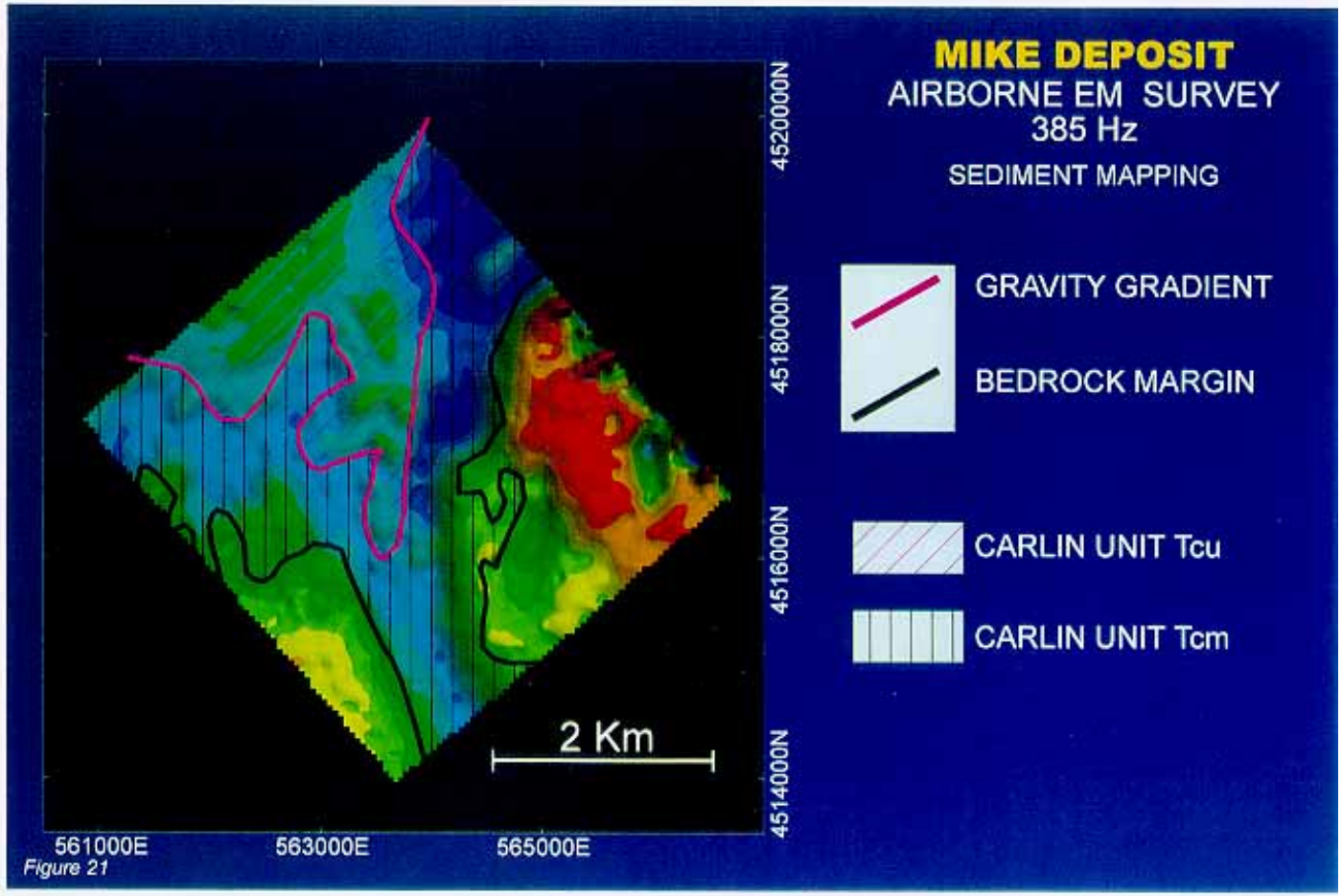
MIKE DEPOSIT
AIRBORNE EM SURVEY
385 Hz
SEDIMENT MAPPING
GRAVITY GRADIENT
BEDROCK MARGIN
CARLIN UNIT Tcu
CARLIN UNIT Tcm
2 Km
4520000N
4518000N
4516000N
4514000N
561000E
563000E
565000E

Figure 21

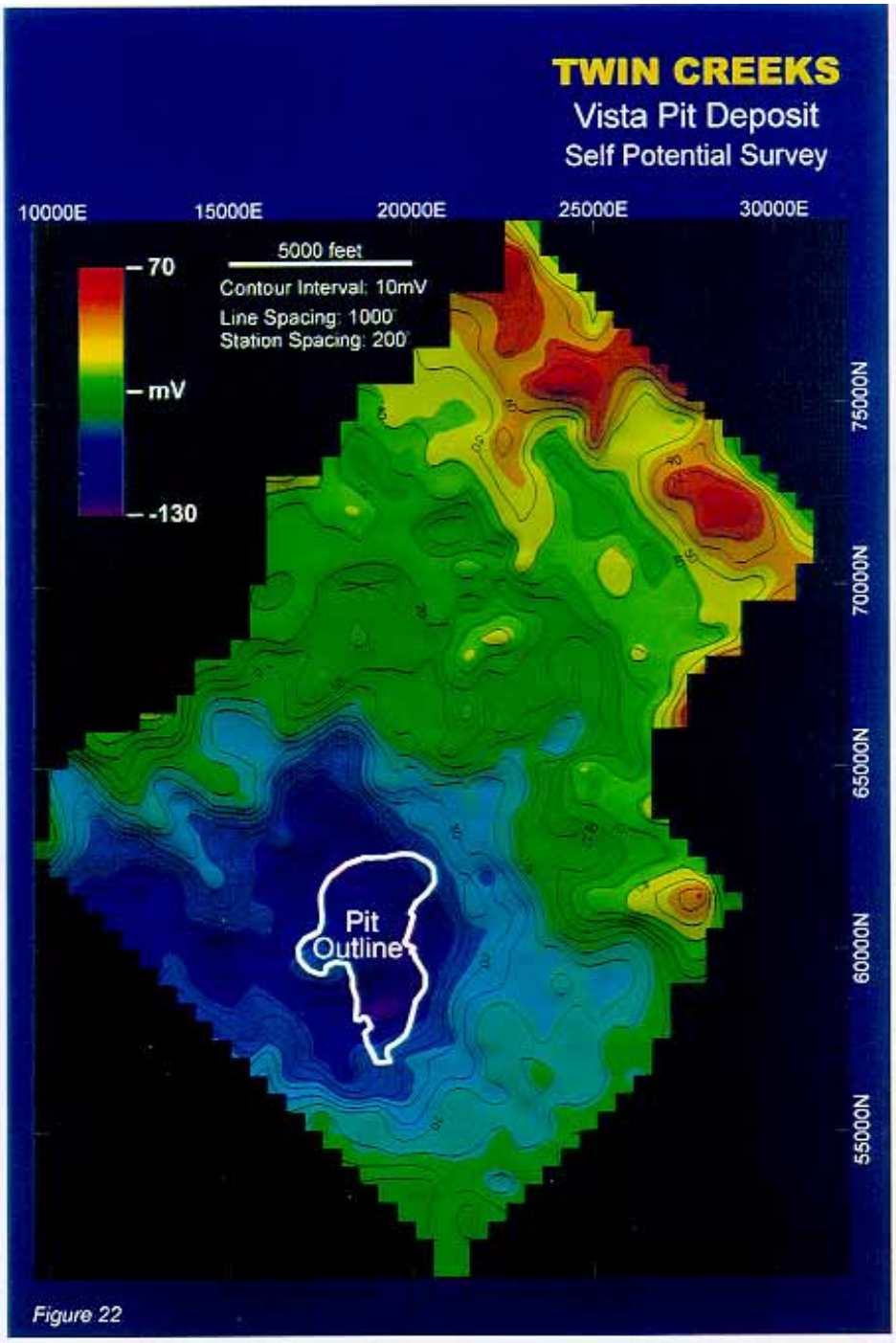
TWIN CREEKS
Vista Pit Deposit
Self Potential Survey
10000E
15000E
20000E
25000E
30000E
75000N
70000N
65000N
60000N
55000N
5000 feet
Contour Interval: 10mV
Line Spacing: 1000'
Station Spacing: 200'
70
mV
-130
Pit
Outline

Figure 22

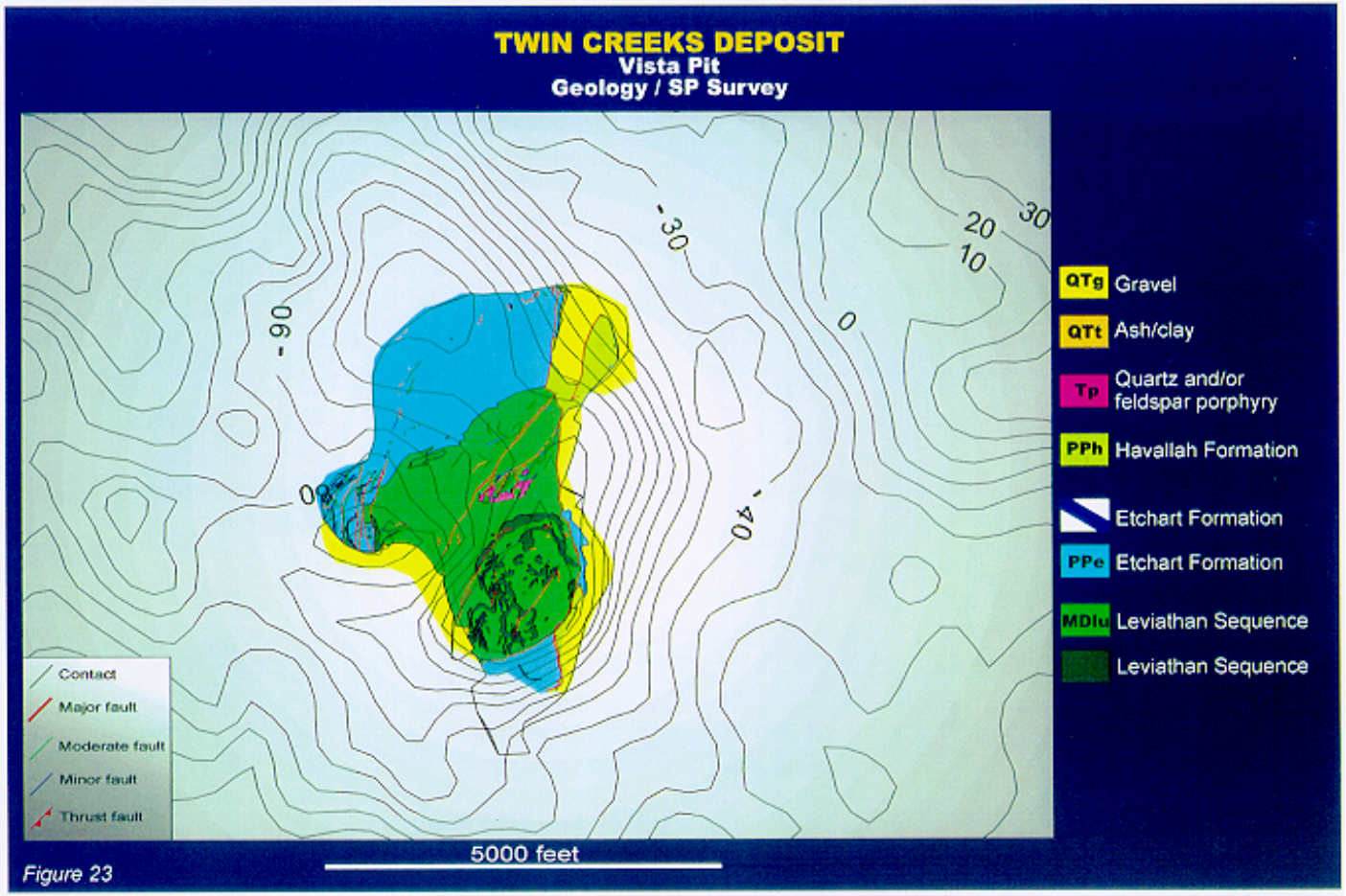
TWIN CREEKS DEPOSIT
Vista Pit
Geology / SP Survey
-90
-30
20
30
10
0
-40
0
Contact
Major fault
Moderate fault
Minor fault
Thrust fault
5000 feet
QTg Gravel
QTt Ash/clay
Tp Quartz and/or feldspar porphyry
PPh Havallah Formation
Etchart Formation
PPe Etchart Formation
MDlu Leviathan Sequence
Leviathan Sequence

Figure 23

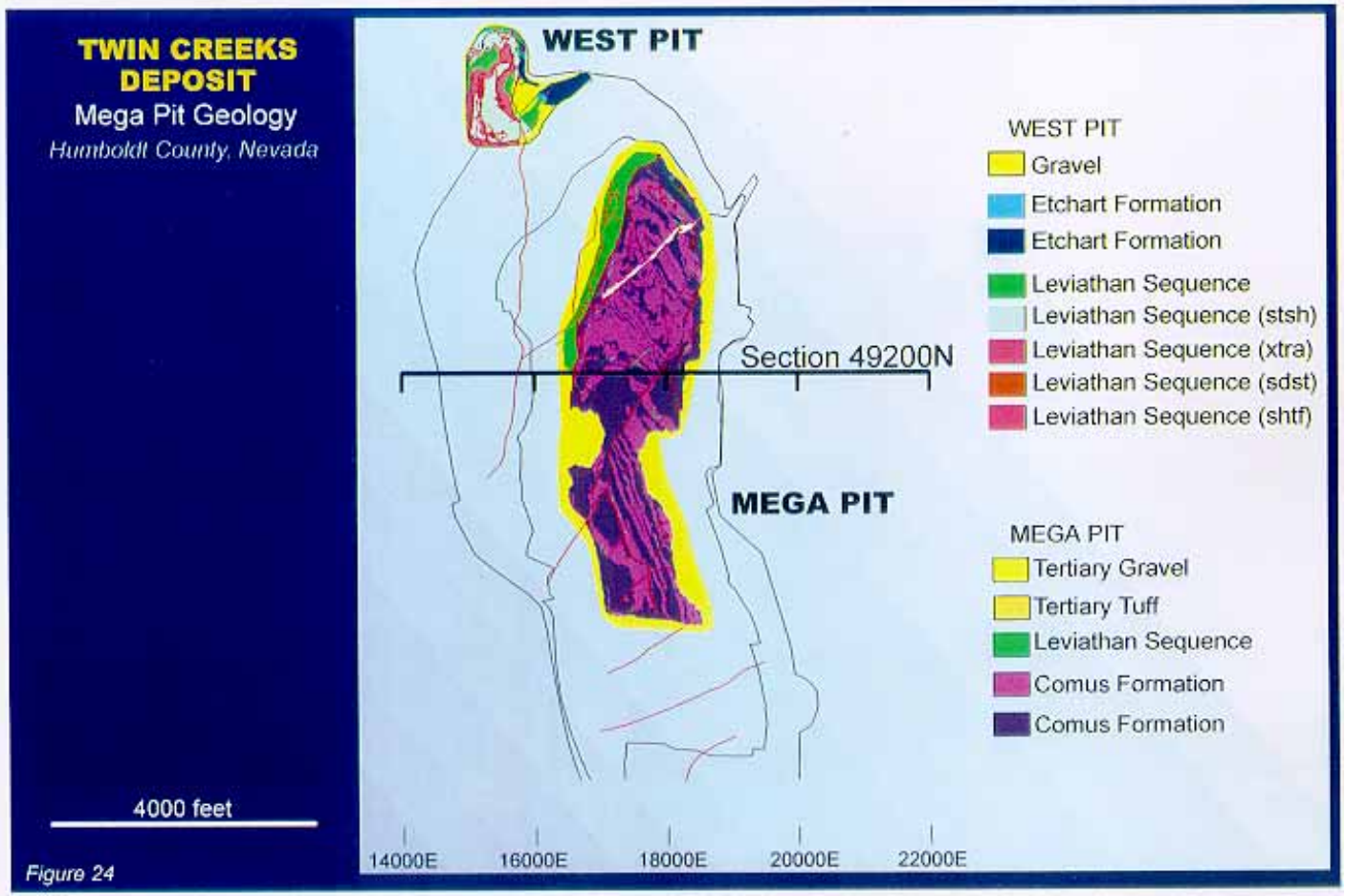
TWIN CREEKS DEPOSIT
Mega Pit Geology
Humboldt County, Nevada
WEST PIT
Section 49200N
MEGA PIT
WEST PIT
Gravel
Etchart Formation
Etchart Formation
Leviathan Sequence
Leviathan Sequence (stsh)
Leviathan Sequence (xtra)
Leviathan Sequence (sdst)
Leviathan Sequence (shtf)
MEGA PIT
Tertiary Gravel
Tertiary Tuff
Leviathan Sequence
Comus Formation
Comus Formation
4000 feet
14000E
16000E
18000E
20000E
22000E

Figure 24

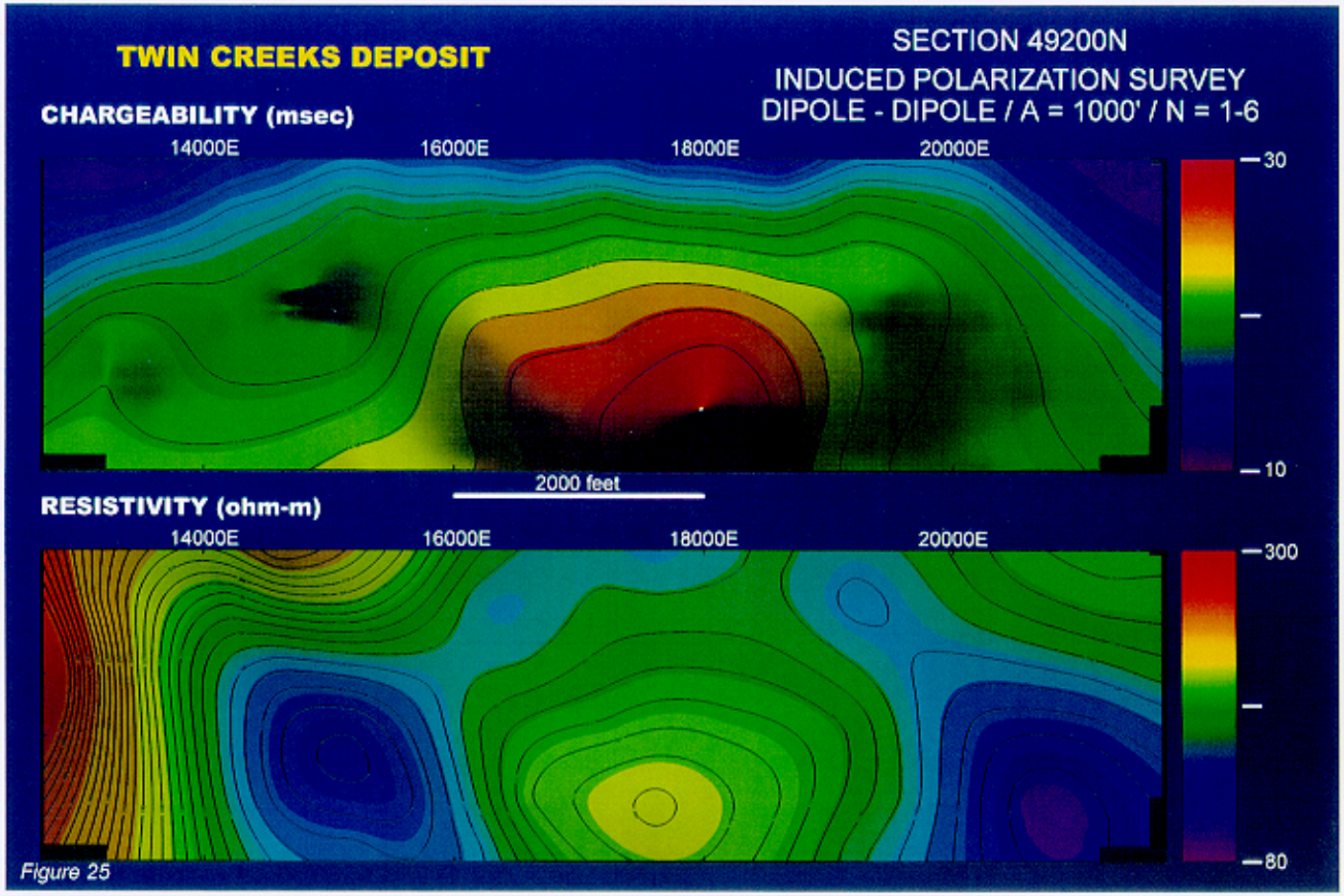
TWIN CREEKS DEPOSIT
SECTION 49200N
INDUCED POLARIZATION SURVEY
DIPOLE - DIPOLE / A = 1000' / N = 1-6
CHARGEABILITY (msec)
14000E
16000E
18000E
20000E
30
10
2000 feet
RESISTIVITY (ohm-m)
14000E
16000E
18000E
20000E
300
80

Figure 25

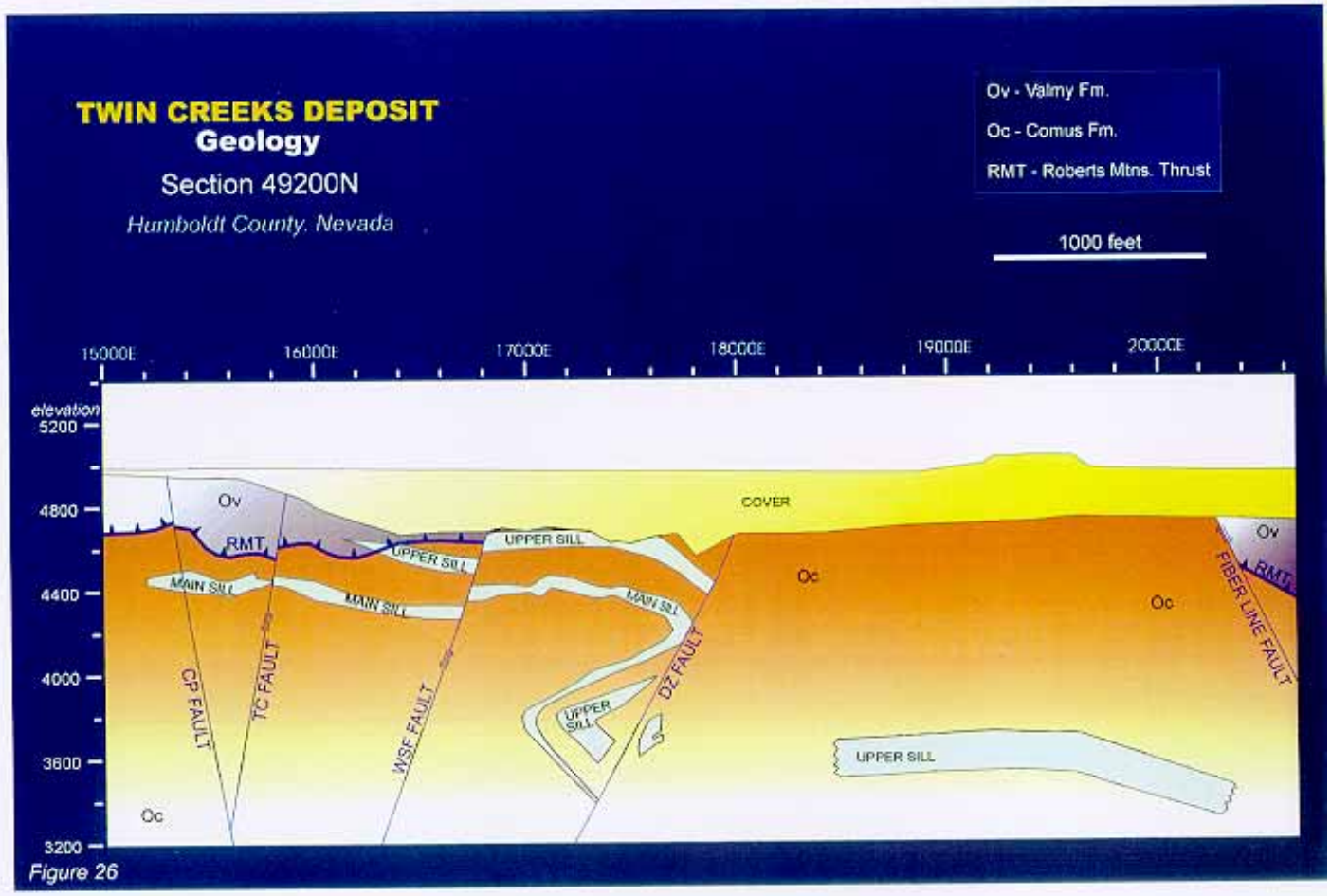
TWIN CREEKS DEPOSIT
Geology
Section 49200N
Humboldt County, Nevada
Ov - Valmy Fm.
Oc - Comus Fm.
RMT - Roberts Mtns. Thrust
1000 feet
15000E
16000E
17000E
18000E
19000E
20000E
elevation
5200
4800
4400
4000
3600
3200
Ov
RMT
COVER
UPPER SILL
MAIN SILL
Oc
CP FAULT
TC FAULT
WSE FAULT
DZ FAULT
FIBER LINE FAULT
Figure 26

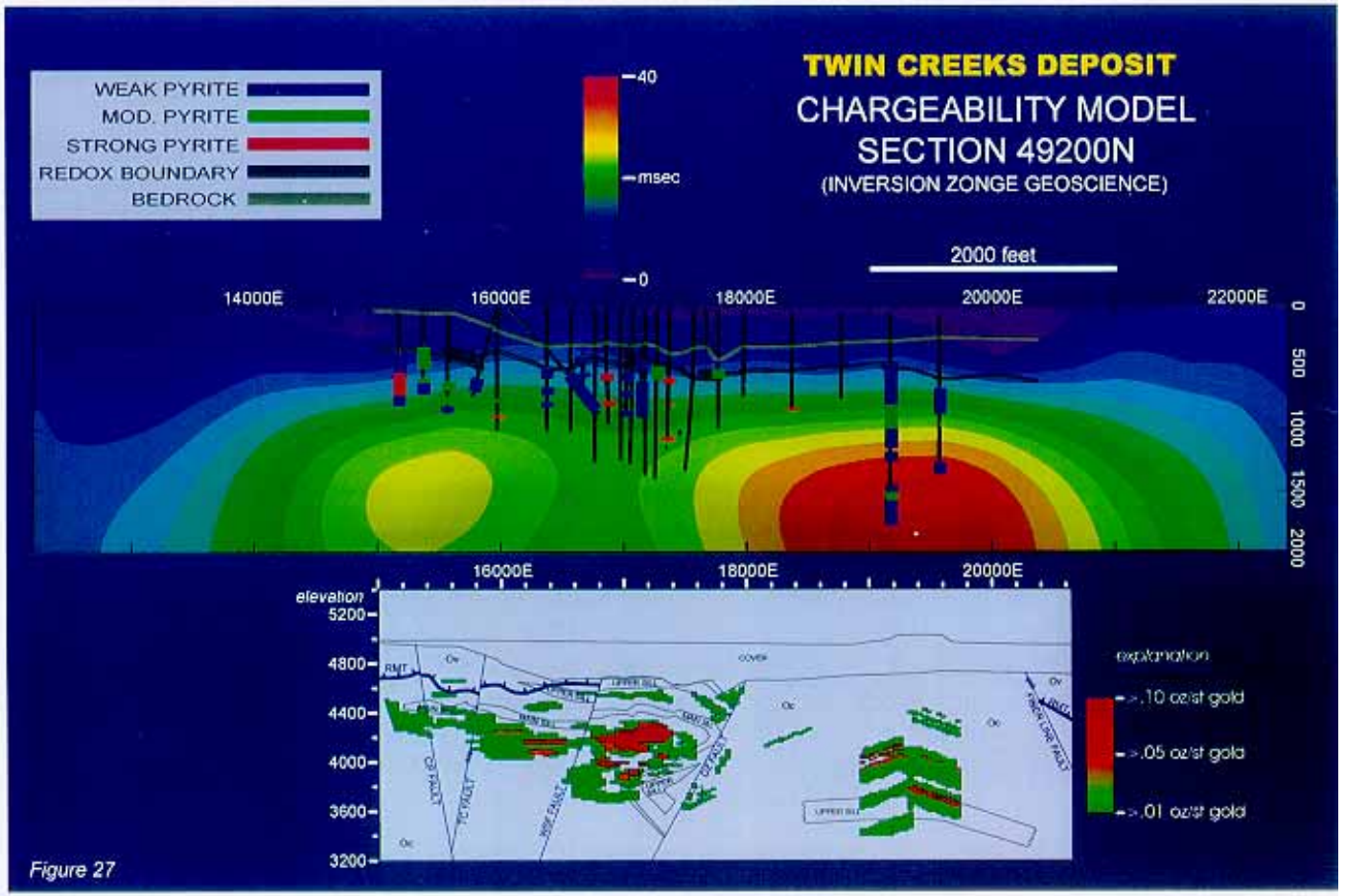
TWIN CREEKS DEPOSIT
CHARGEABILITY MODEL
SECTION 49200N
(INVERSION ZONGE GEOSCIENCE)
WEAK PYRITE
MOD. PYRITE
STRONG PYRITE
REDOX BOUNDARY
BEDROCK
40
msec
0
2000 feet
14000E
16000E
18000E
20000E
22000E
0
500
1000
1500
2000
16000E
18000E
20000E
elevation
5200
4800
4400
4000
3600
3200
explanation
>.10 oz/st gold
>.05 oz/st gold
>.01 oz/st gold

Figure 27

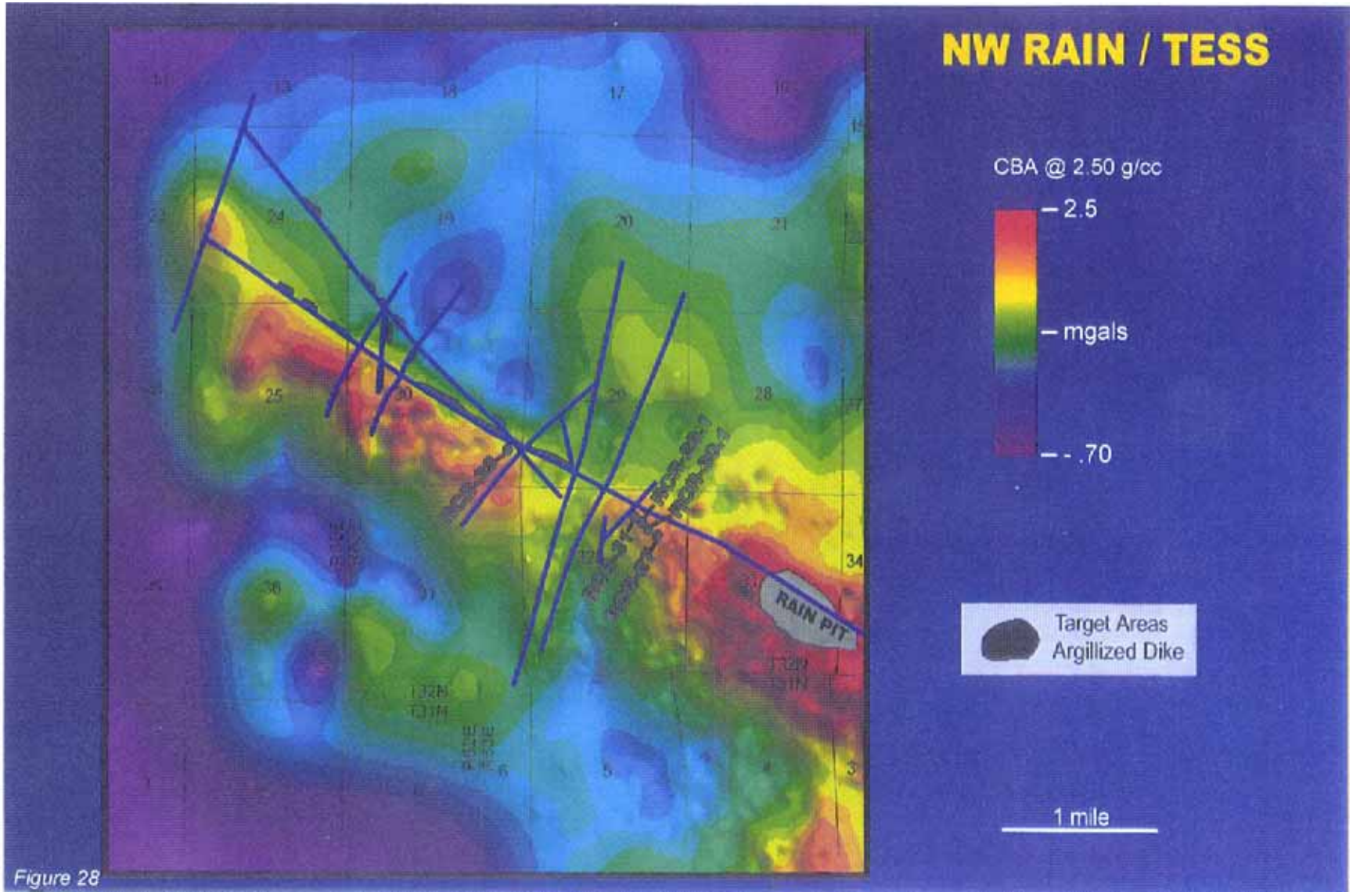
NW RAIN / TESS
CBA @ 2.50 g/cc
2.5
mgals
- .70
RAIN PIT
Target Areas
Argillized Dike
1 mile

Figure 28

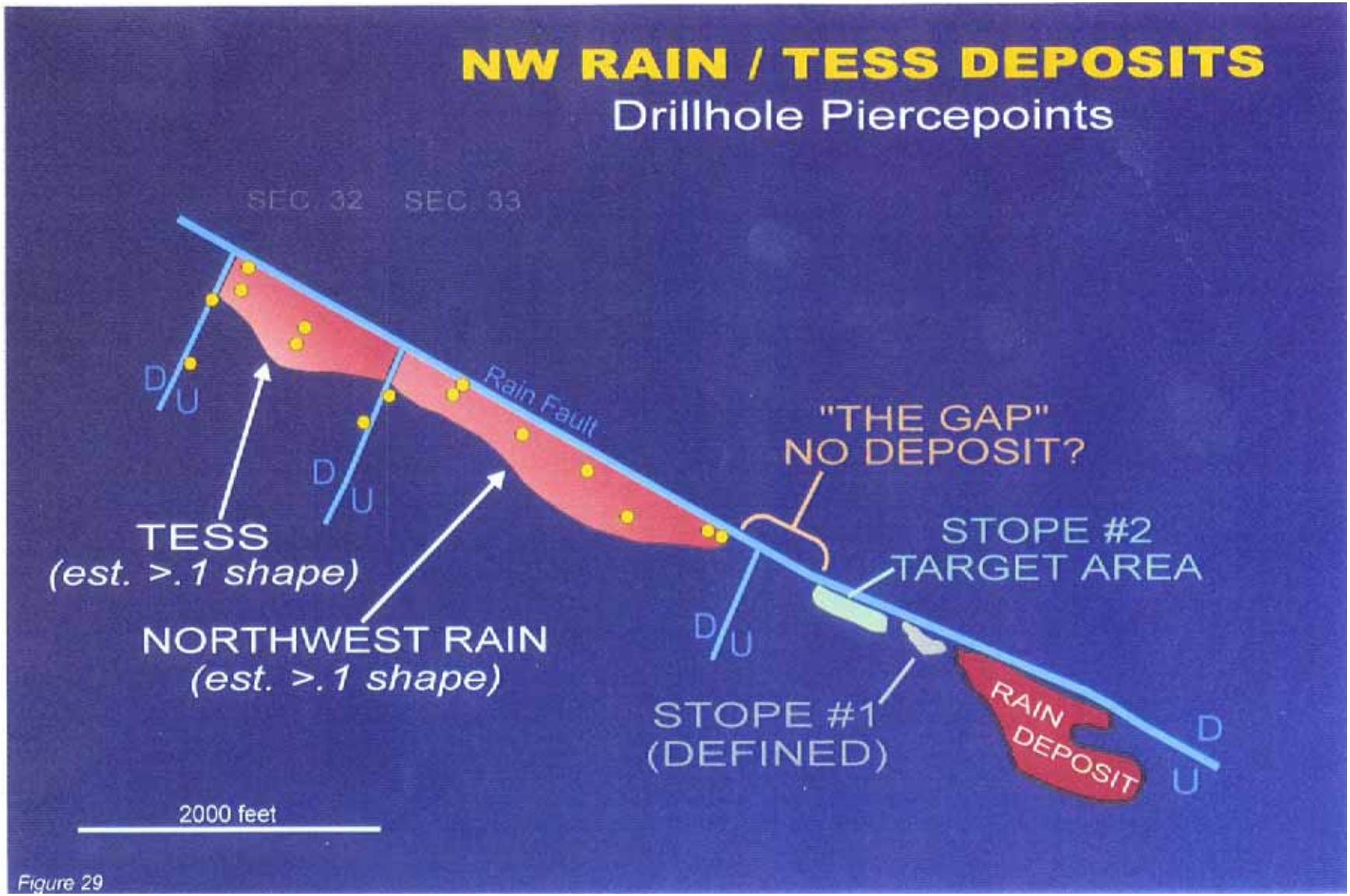
NW RAIN / TESS DEPOSITS
Drillhole Piercepoints
SEC 32
SEC 33
D
U
Rain Fault
"THE GAP"
NO DEPOSIT?
STOPE #2
TARGET AREA
TESS
(est. >.1 shape)
NORTHWEST RAIN
(est. >.1 shape)
STOPE #1
(DEFINED)
RAIN
DEPOSIT
2000 feet

Figure 29

TESS DEPOSIT

-2800 S E Cross-Section
Looking Northwest

MISSISSIPIAN

Chainman Sandstone

Webb Mudstone

DEVONIAN

Devils Gate Limestone

Woodruff Chert/Shale
(Allochthonous)

200 feet

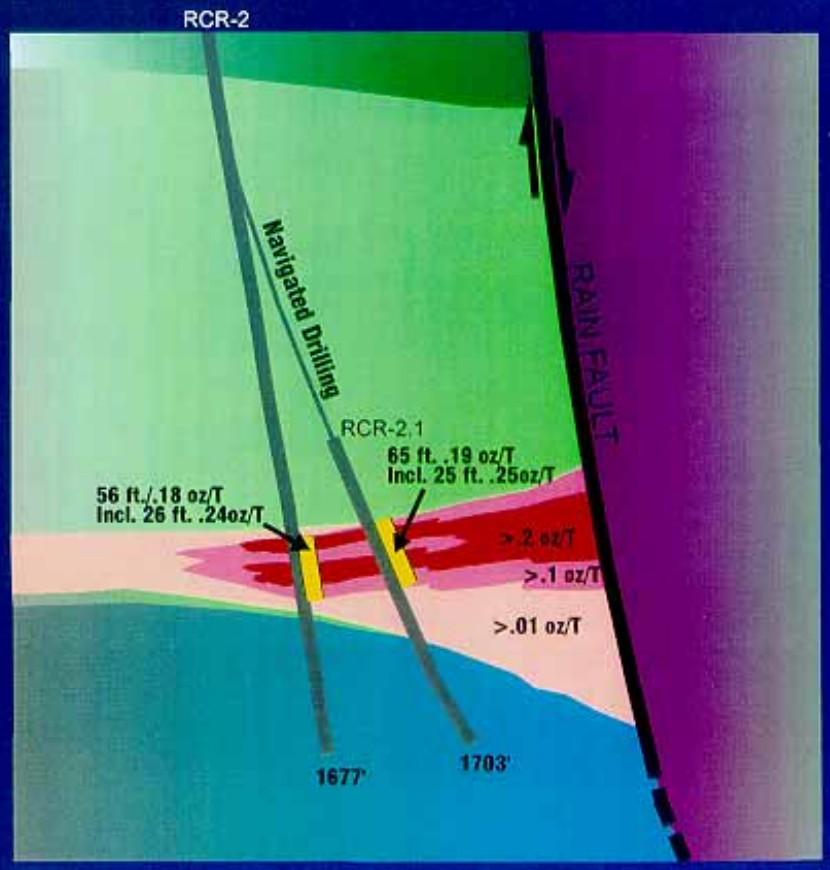

Figure 30

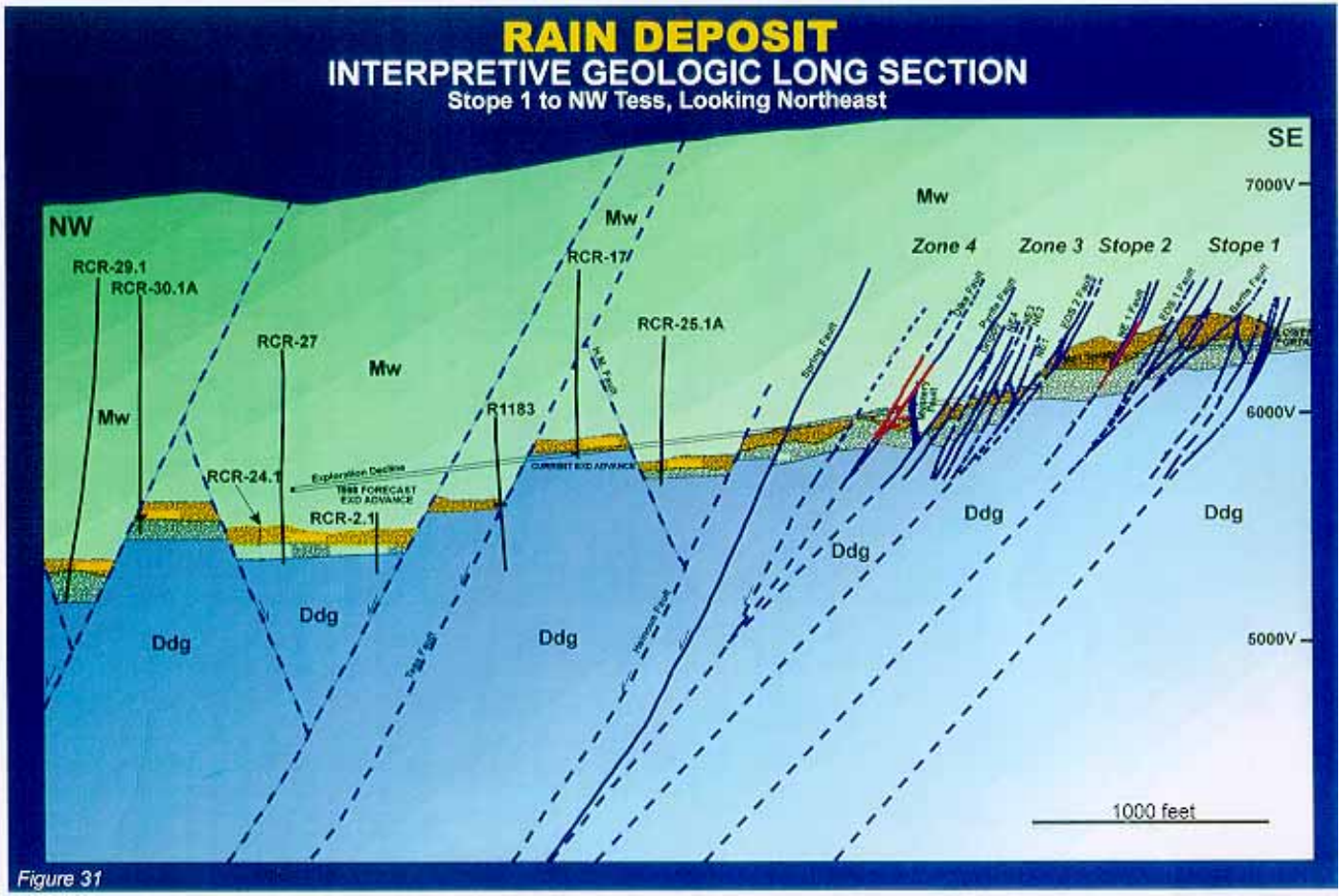
RAIN DEPOSIT
INTERPRETIVE GEOLOGIC LONG SECTION
Stope 1 to NW Tess, Looking Northeast
NW
SE
7000V
6000V
5000V
Mw
Zone 4
Zone 3
Stope 2
Stope 1
RCR-29.1
RCR-30.1A
RCR-27
RCR-17
RCR-25.1A
R1183
RCR-24.1
RCR-2.1
Exploration Decline
1995 FORECAST EXD ADVANCE
CURRENT EXD ADVANCE
Ddg
1000 feet

Figure 31

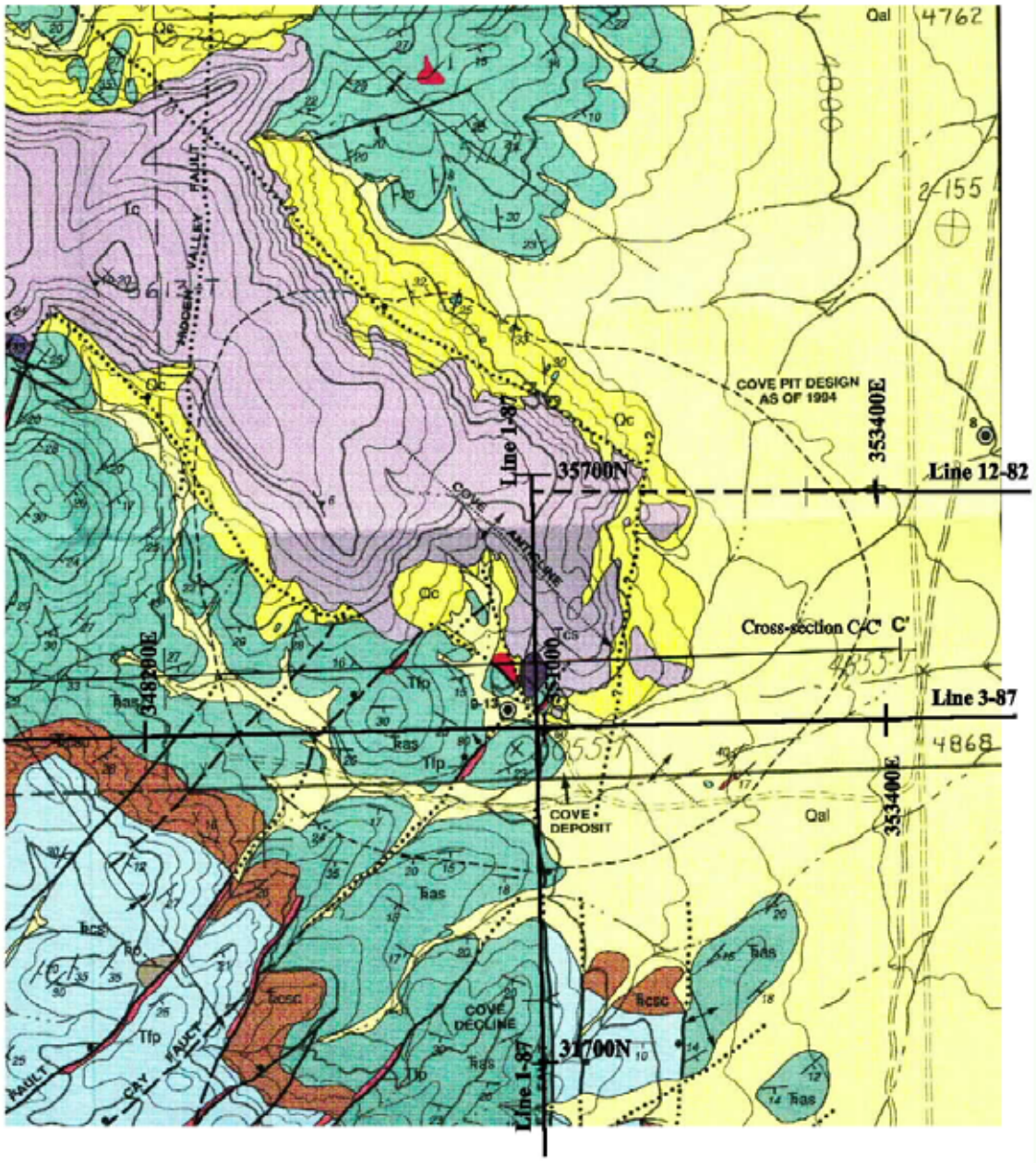

Map From Emmons and Eng, 1995
Nevada Bureau of Mines and Geology
Map Number 103

0 1000 feet

Scale 1:12000

Figure 32, Geologic Map
Showing Selected IP/Resistivity Lines over the Cove Deposit.

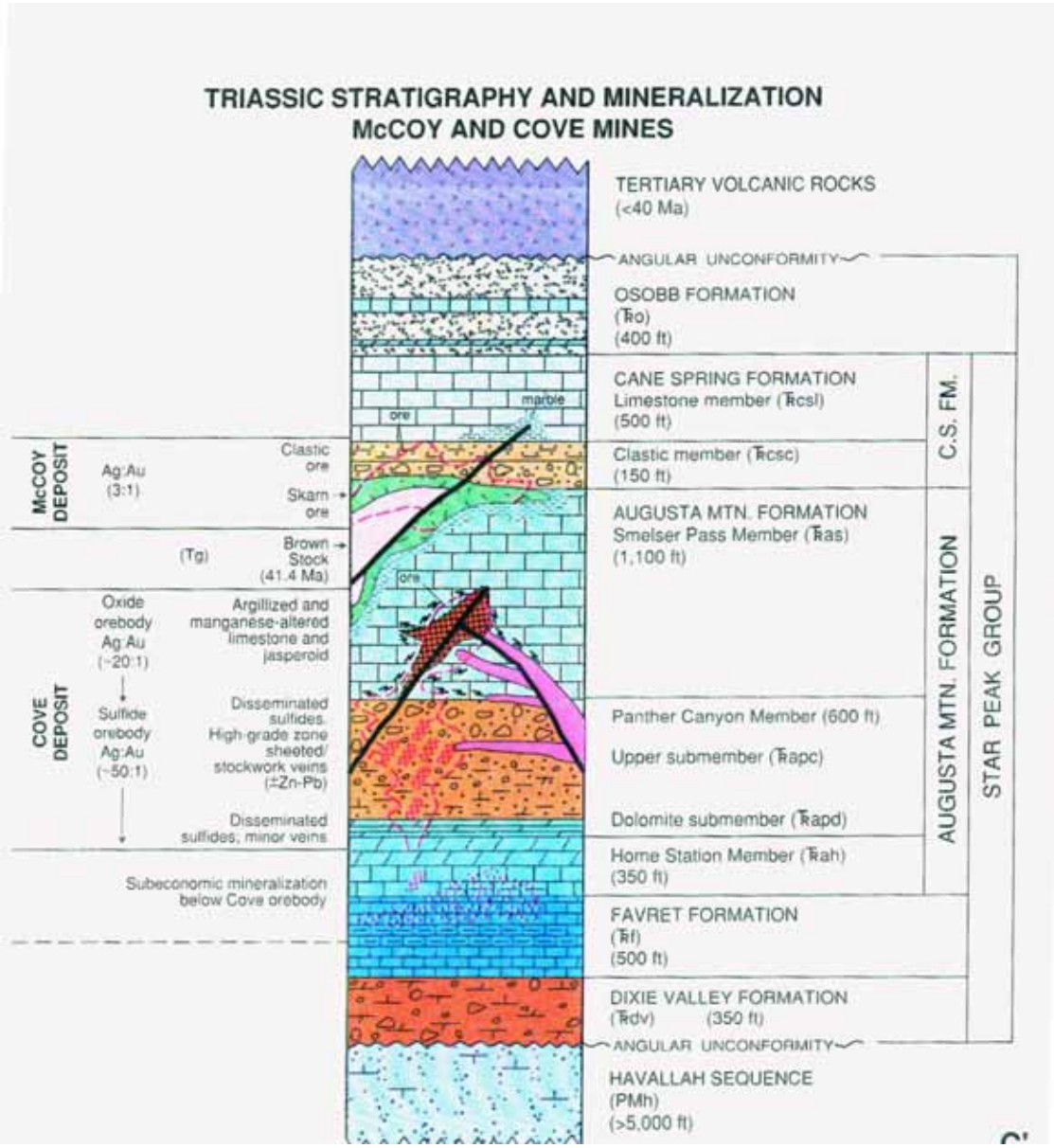

Figure 33
Generalized Stratigraphic Column of the McCoy District
Showing relationship of mineralization to stratigraphic units.
From Emmons and Eng, 1995
Nevada Bureau of MInes and Geology
Map 103

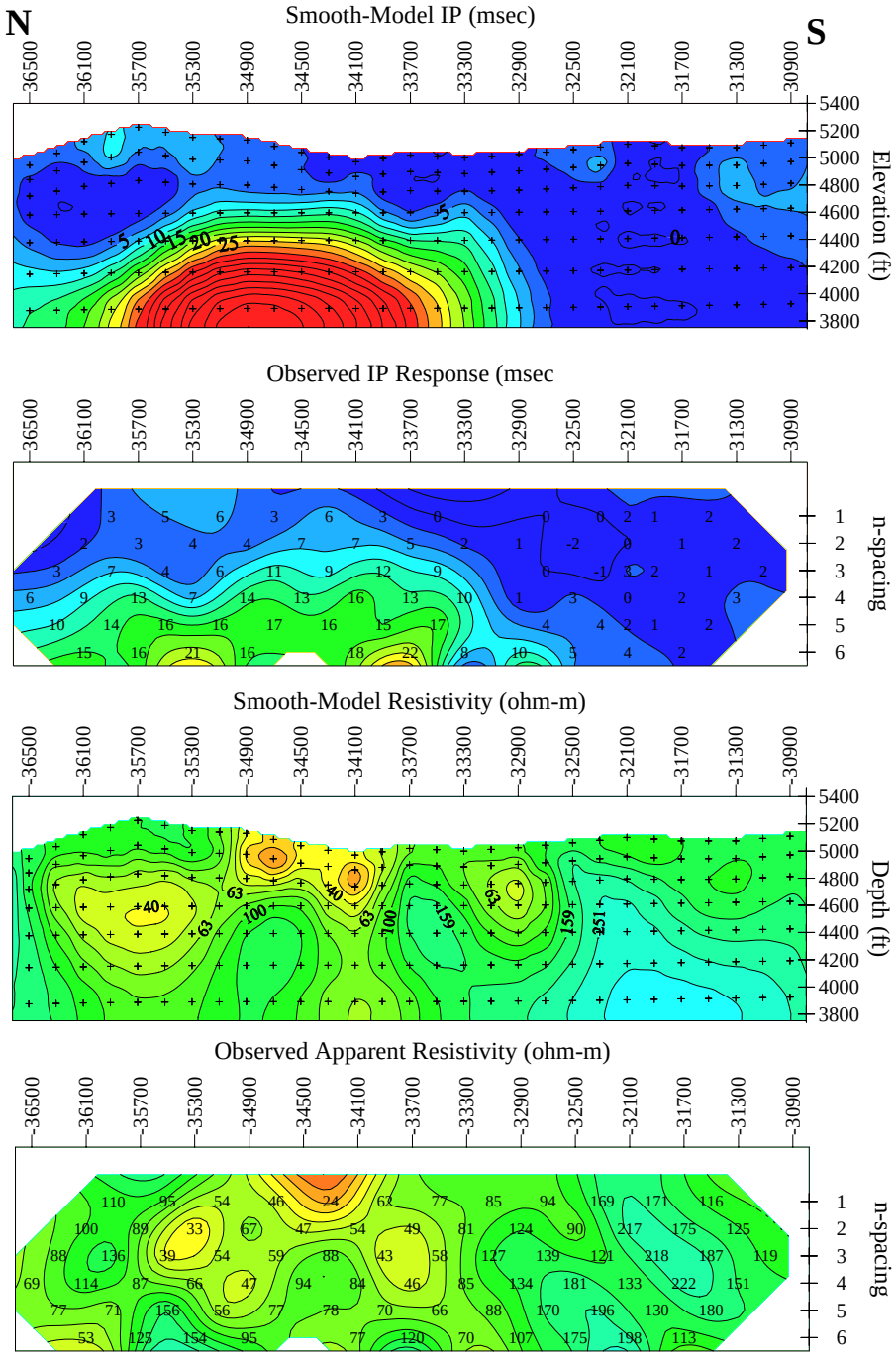

Figure 34
Cove Mine, Line 1-87
Two-dimensional smooth-model results
with raw data pseudosections.
400 Foot Dipole-Dipole Data

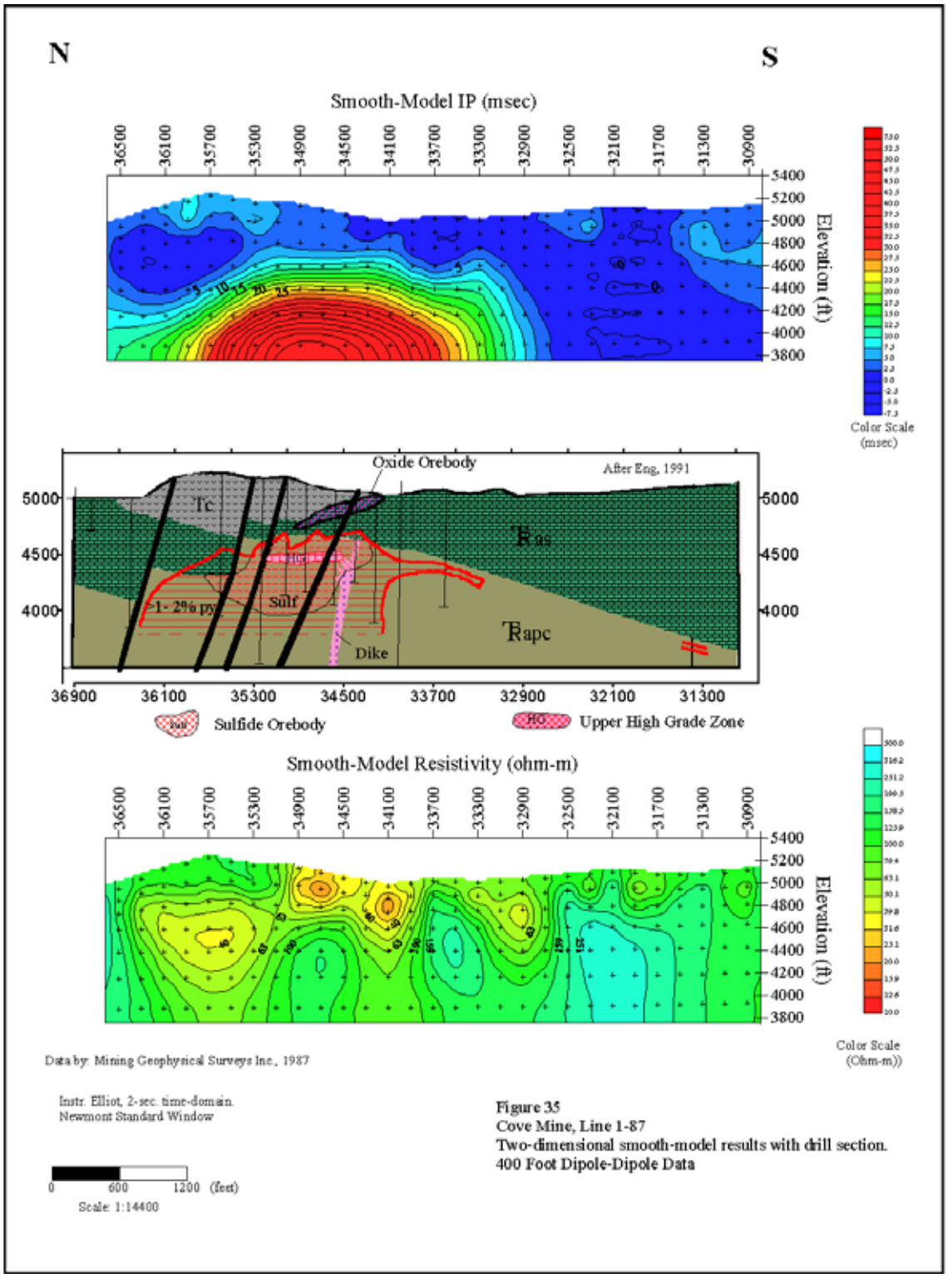

Figure 35
Cove Mine, Line 1-87
Two-dimensional smooth-model results with drill section.
400 Foot Dipole-Dipole Data

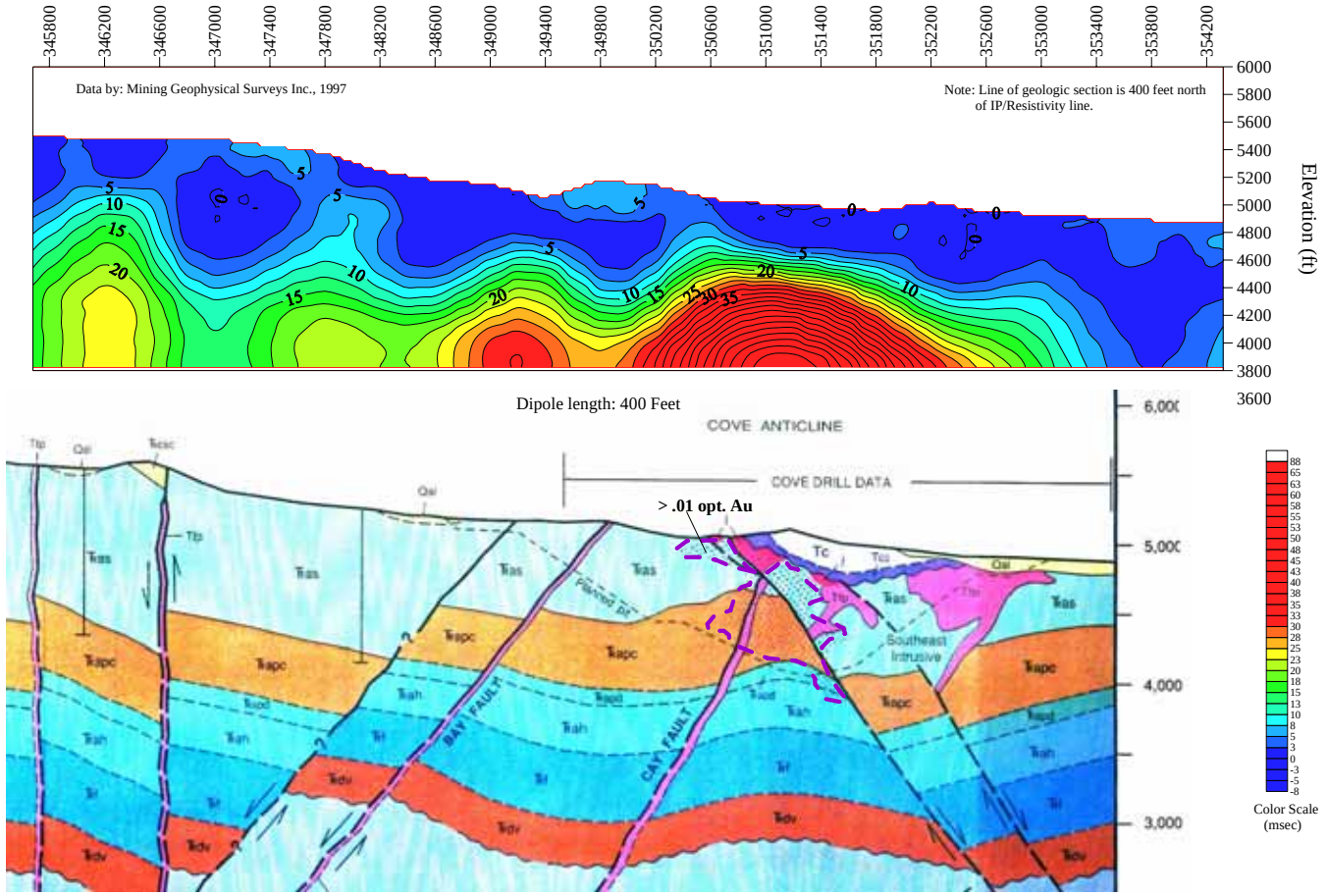

Geologic section from Emmons and Eng, 1995
Nevada Bureau of Mines and Geology
Map 103

Figure 36
Cove Mine, Line 3-87
Results of two-dimensional smooth model inversion of
dipole-dipole IP data with geologic section from Emmons and Eng, 1995.

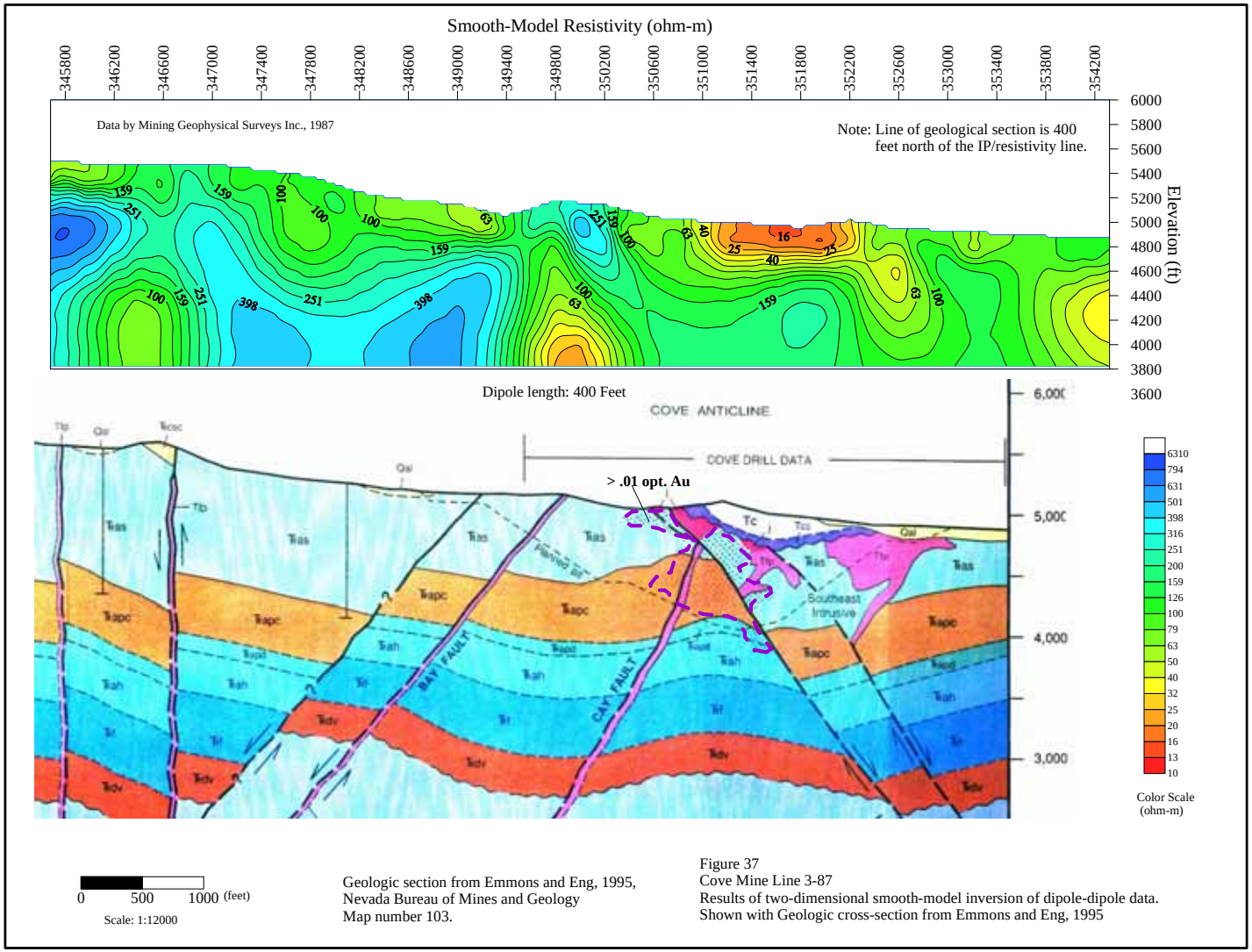

Geologic section from Emmons and Eng, 1995, Nevada Bureau of Mines and Geology Map number 103.

Figure 37
Cove Mine Line 3-87
Results of two-dimensional smooth-model inversion of dipole-dipole data.
Shown with Geologic cross-section from Emmons and Eng, 1995

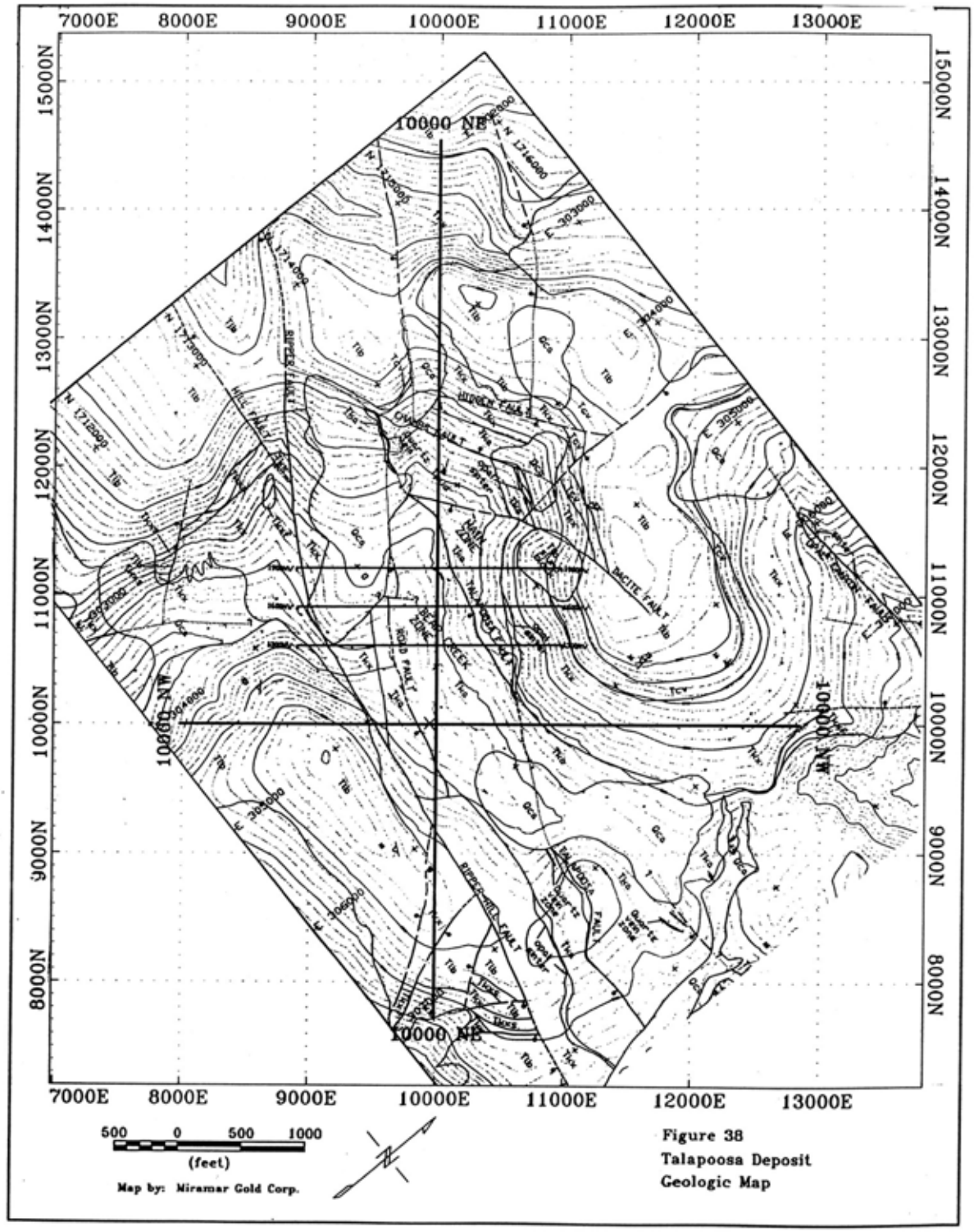

Figure 38
Talapoosa Deposit
Geologic Map

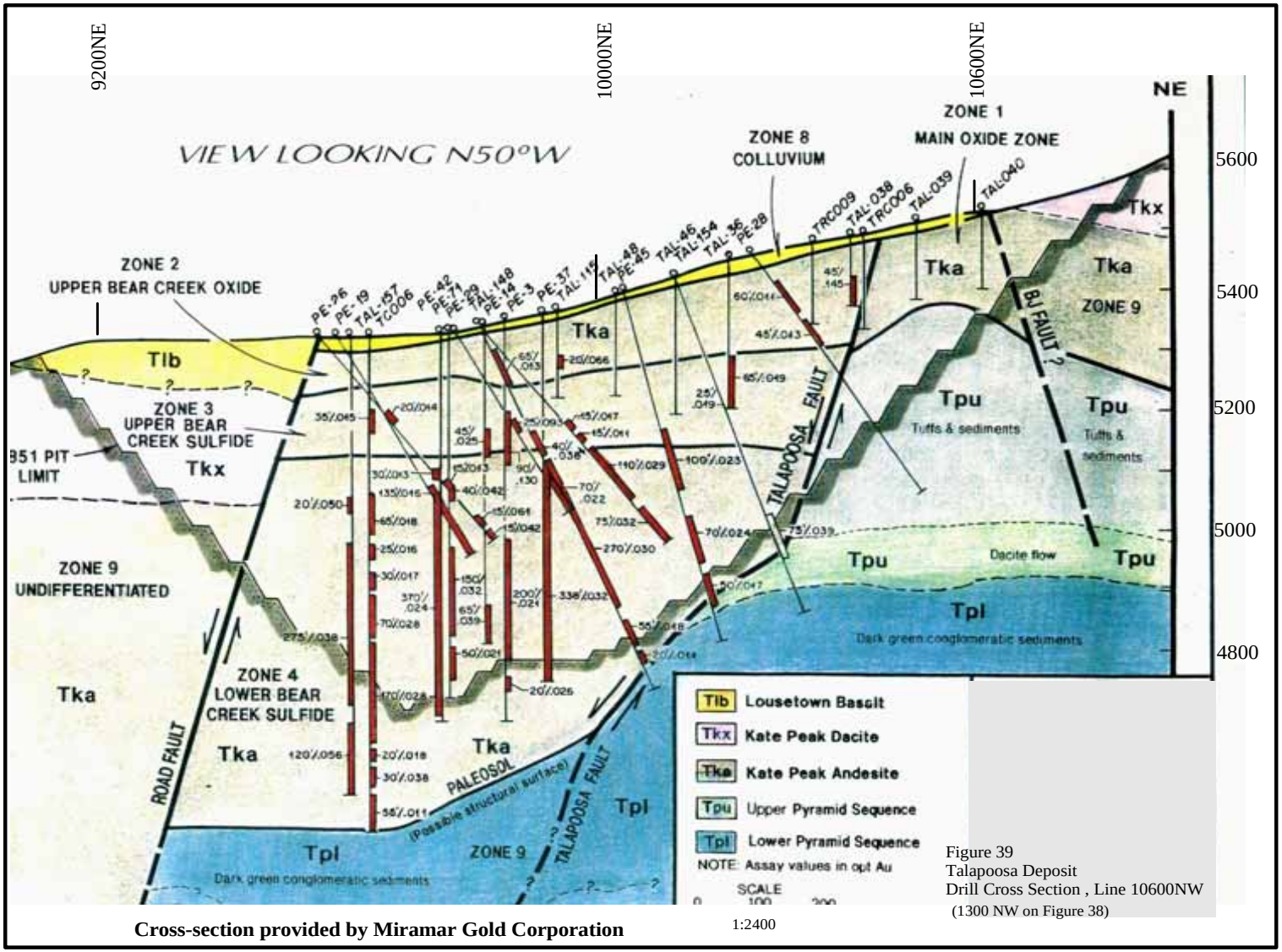

Cross-section provided by Miramar Gold Corporation

Figure 39
Talapoosa Deposit
Drill Cross Section , Line 10600NW
(1300 NW on Figure 38)

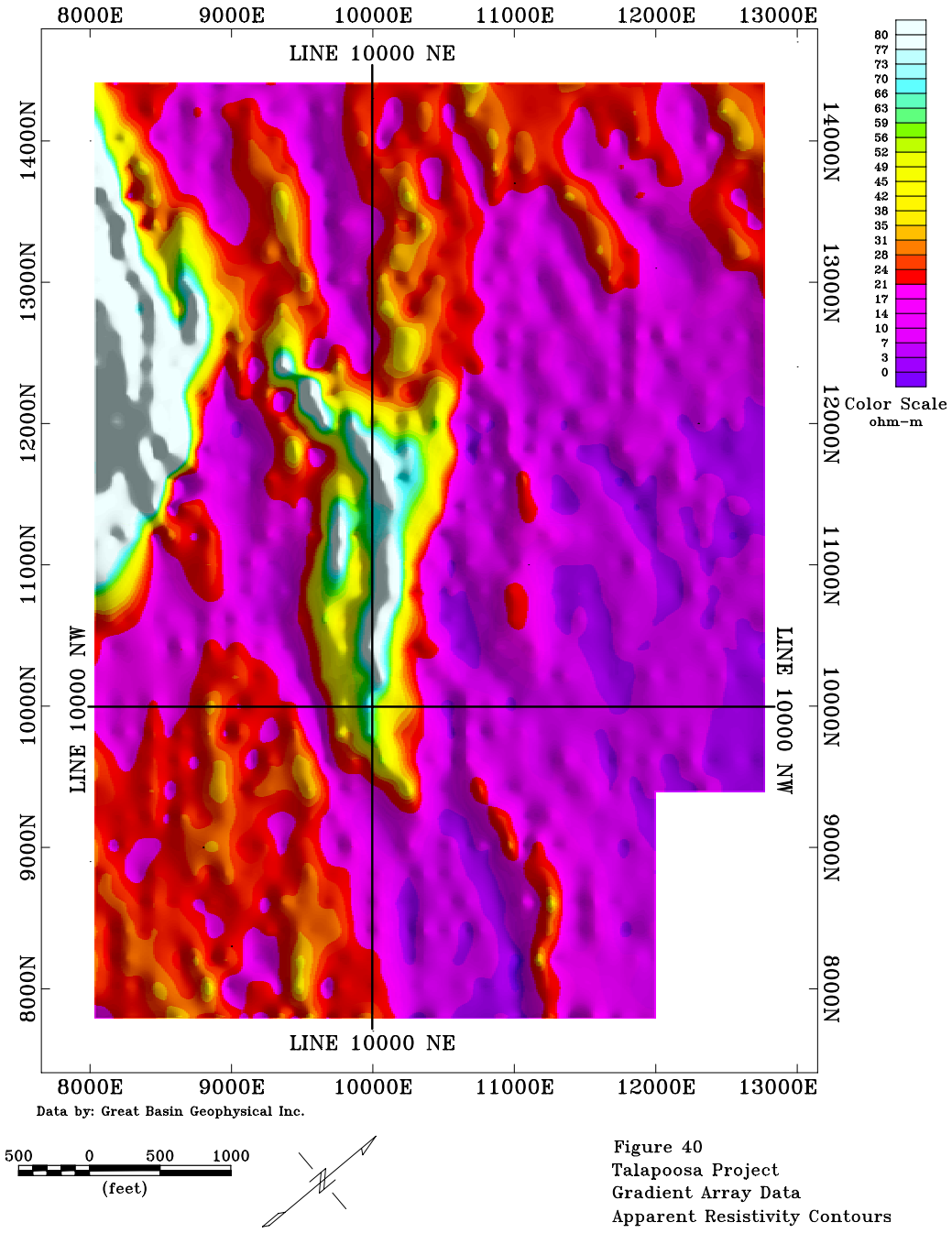

Figure 40
Talapoosa Project
Gradient Array Data
Apparent Resistivity Contours

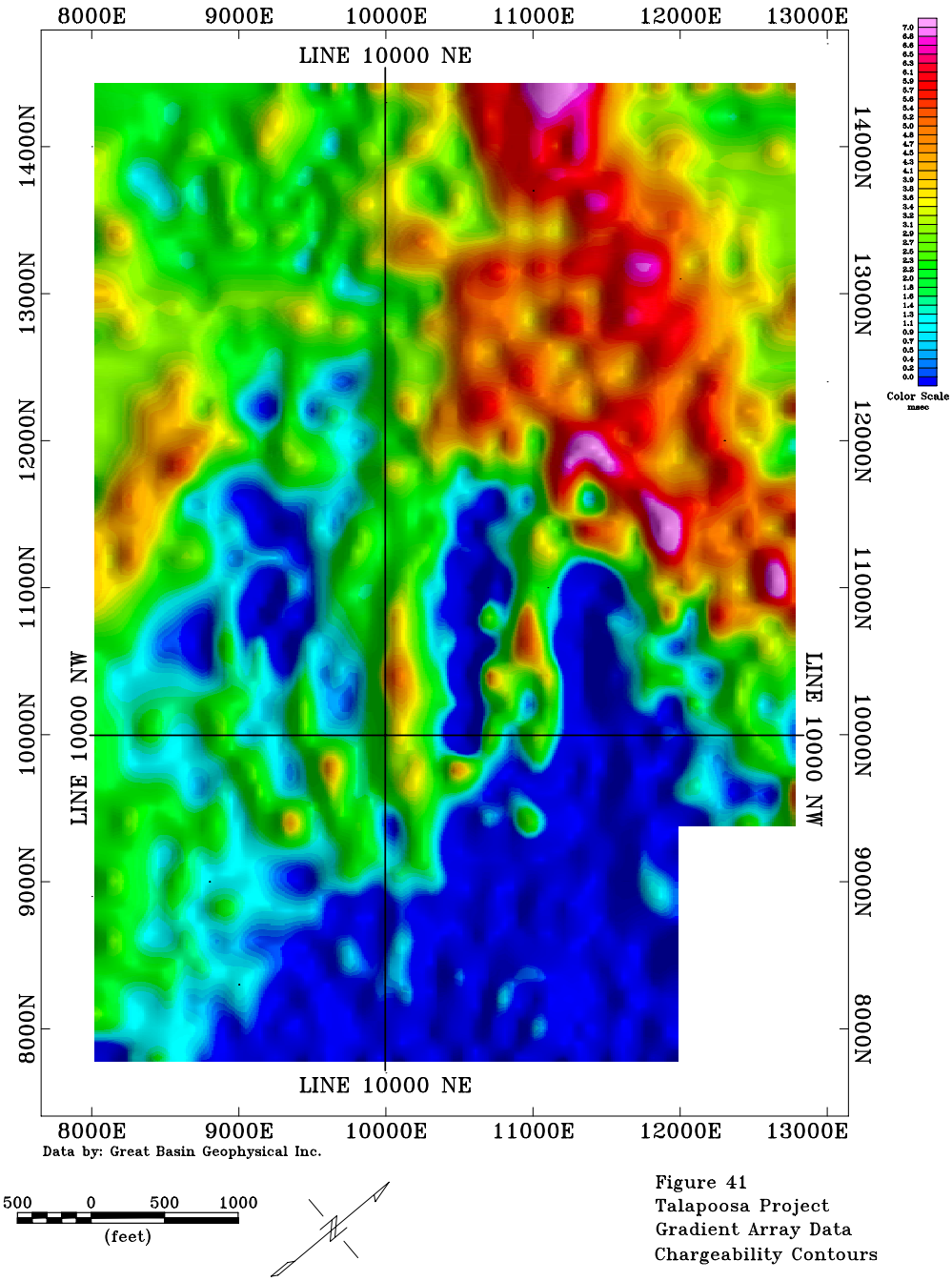

Figure 41
Talapoosa Project
Gradient Array Data
Chargeability Contours

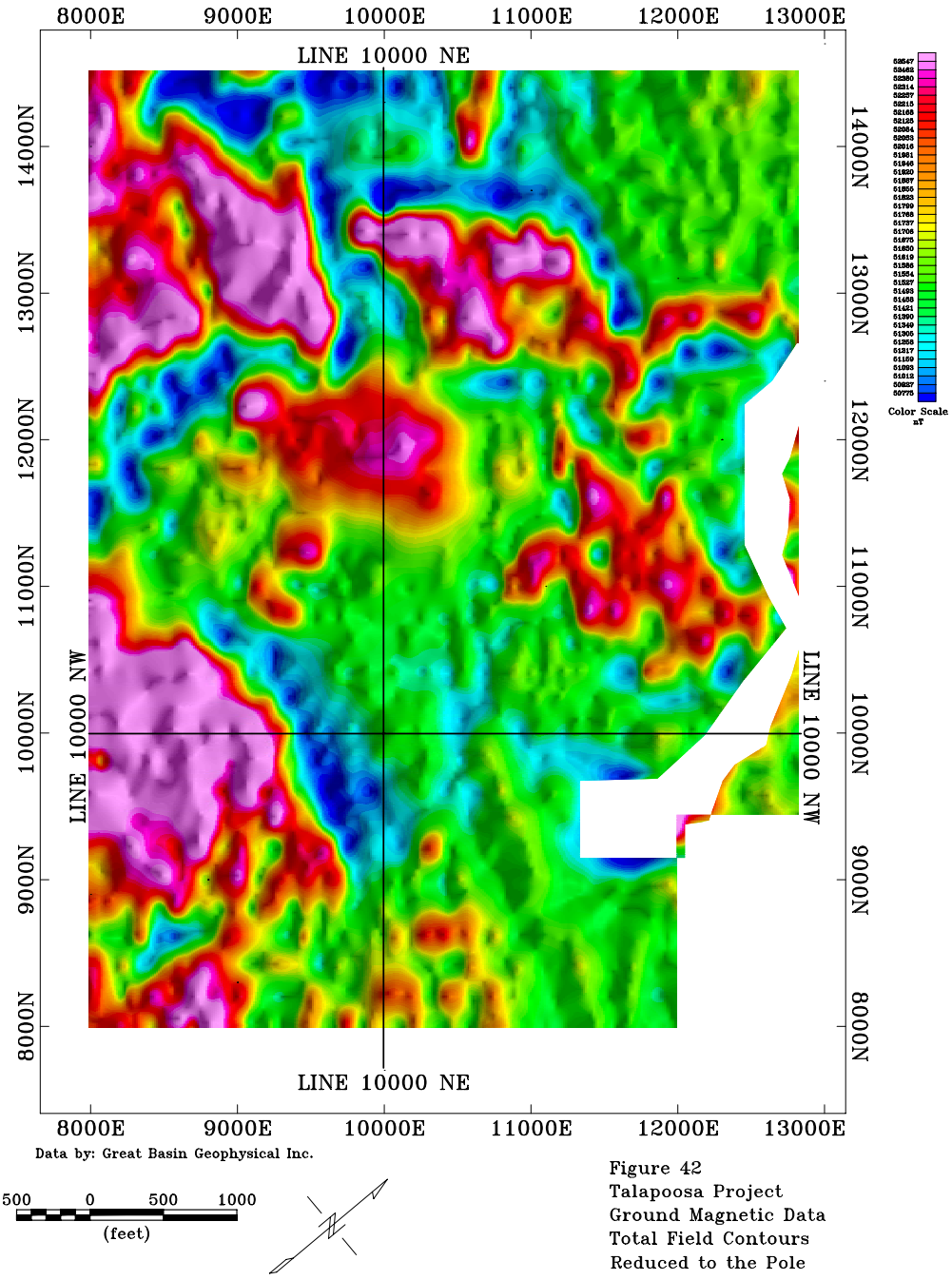

Figure 42
Talapoosa Project
Ground Magnetic Data
Total Field Contours
Reduced to the Pole

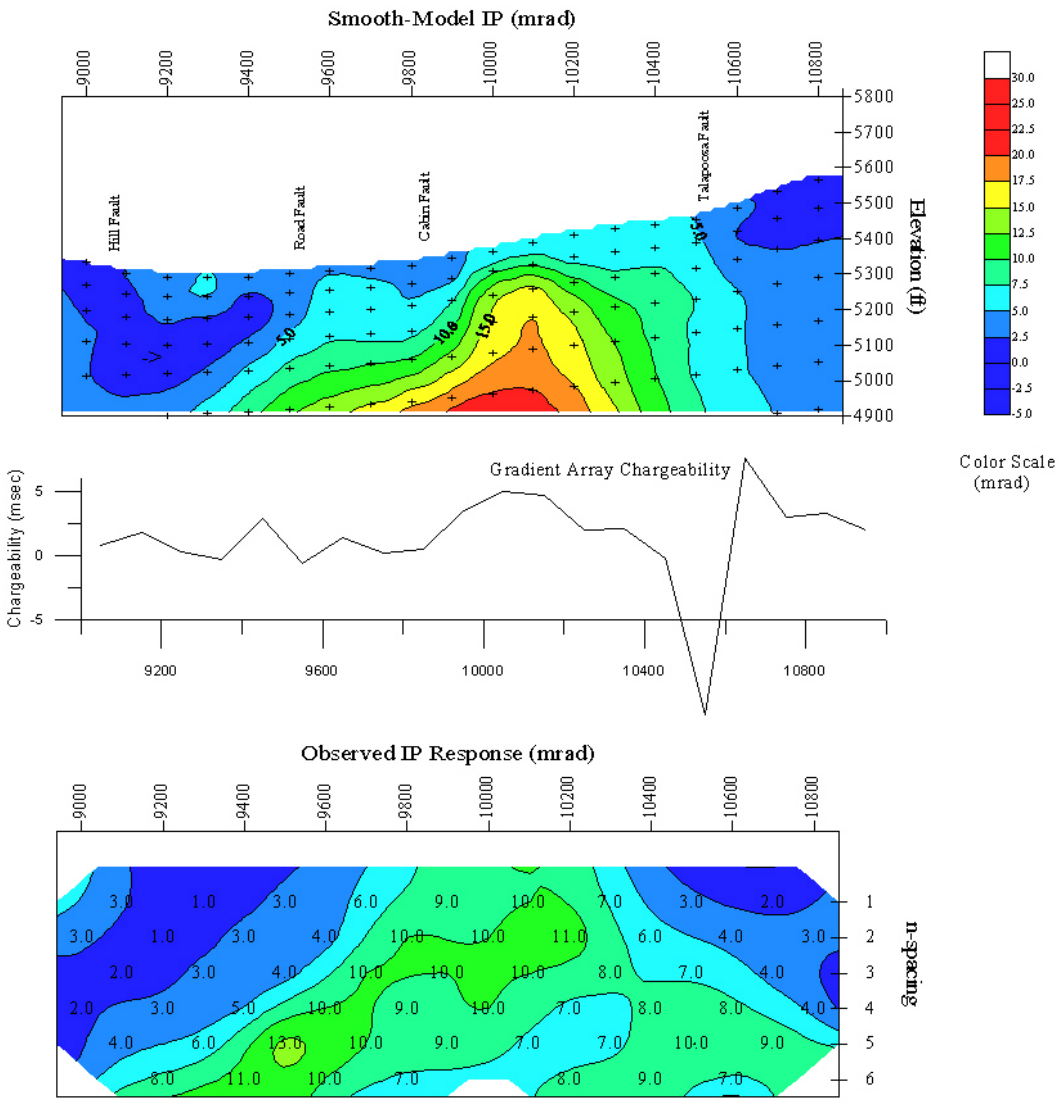

Figure 43
Talapoosa Project, Line 10400N
Dipole-dipole IP Data, 200 Foot Dipoles

Results of two-dimensional smooth-model inversion
shown with raw data pseudosections and gradient array profile.

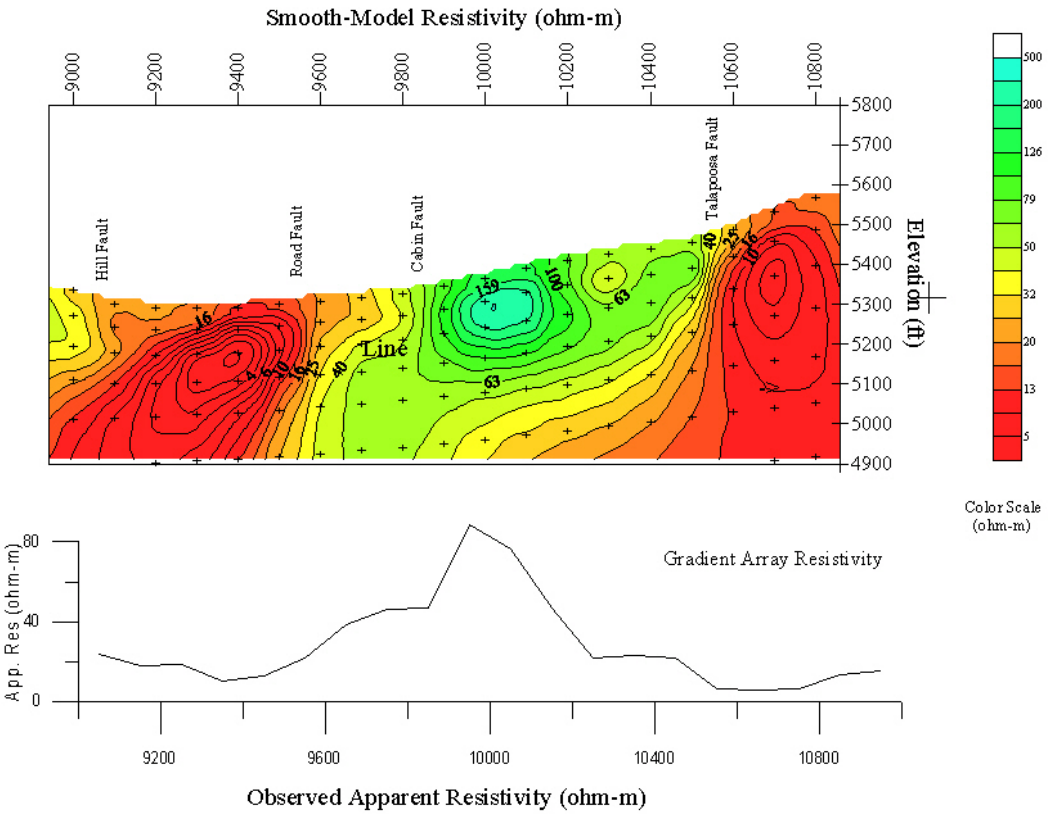

Data by: Great Basin Geophysical Inc., 1990

Figure 44
Talapoosa Deposit, Line 10400N
Dipole-dipole Resistivity Data, 200 foot Dipoles

Results of two-dimensional smooth-model inversion shown with raw data pseudosections and gradient array profile.

0 200 400 (feet)
Scale: 1:4800

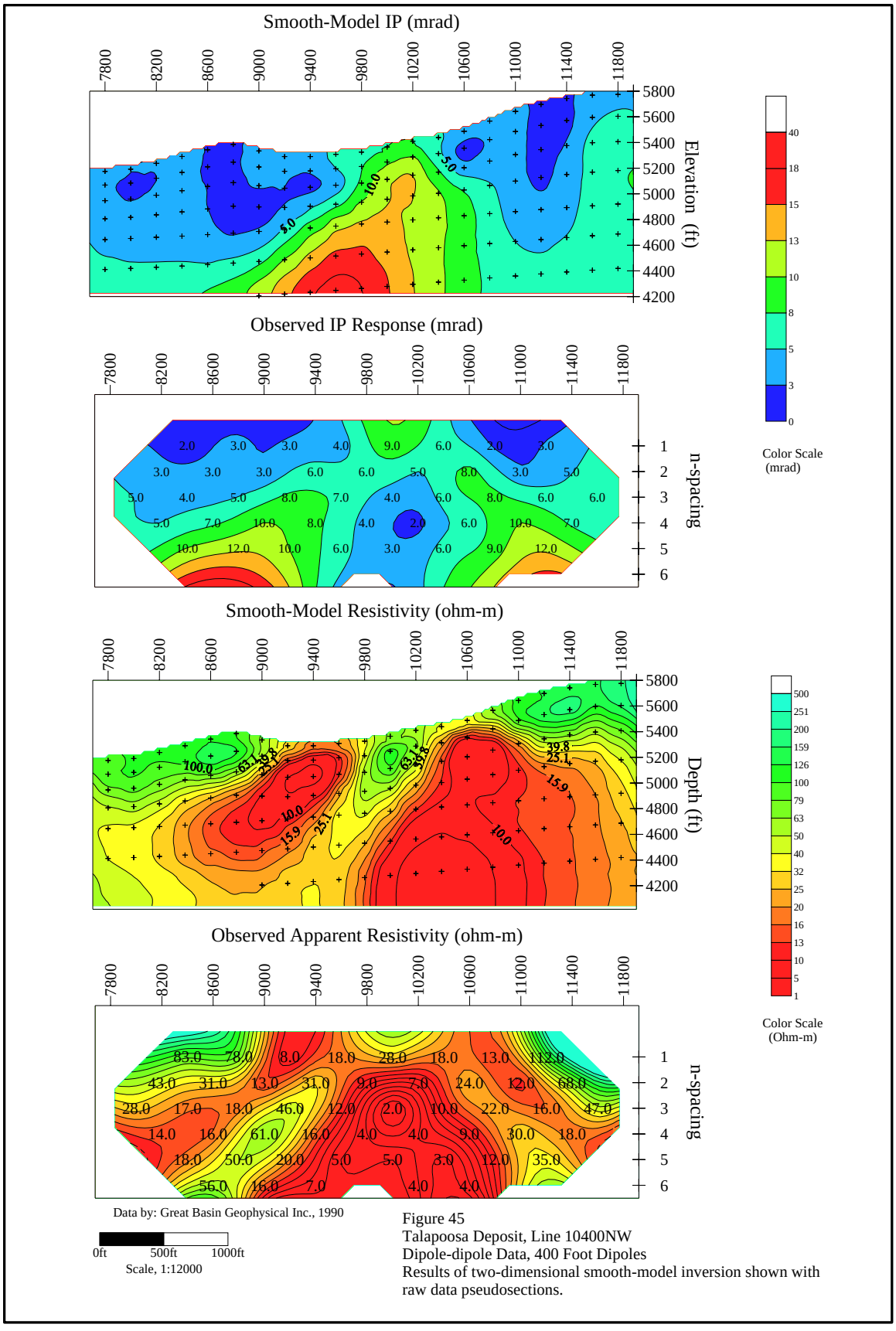

Figure 45
Talapoosa Deposit, Line 10400NW
Dipole-dipole Data, 400 Foot Dipoles
Results of two-dimensional smooth-model inversion shown with raw data pseudosections.

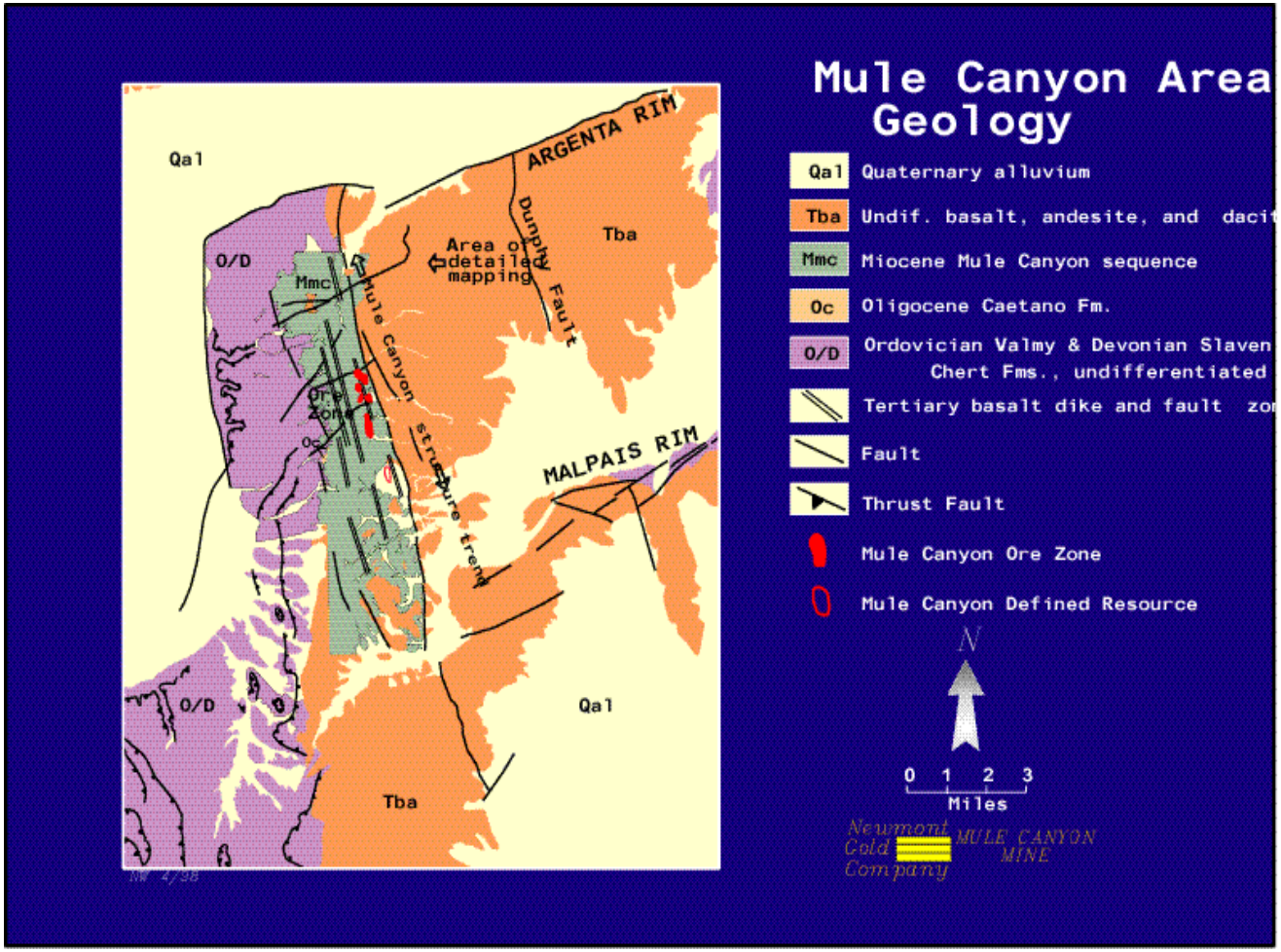

Figure 46
Mule Canyon Area Geology

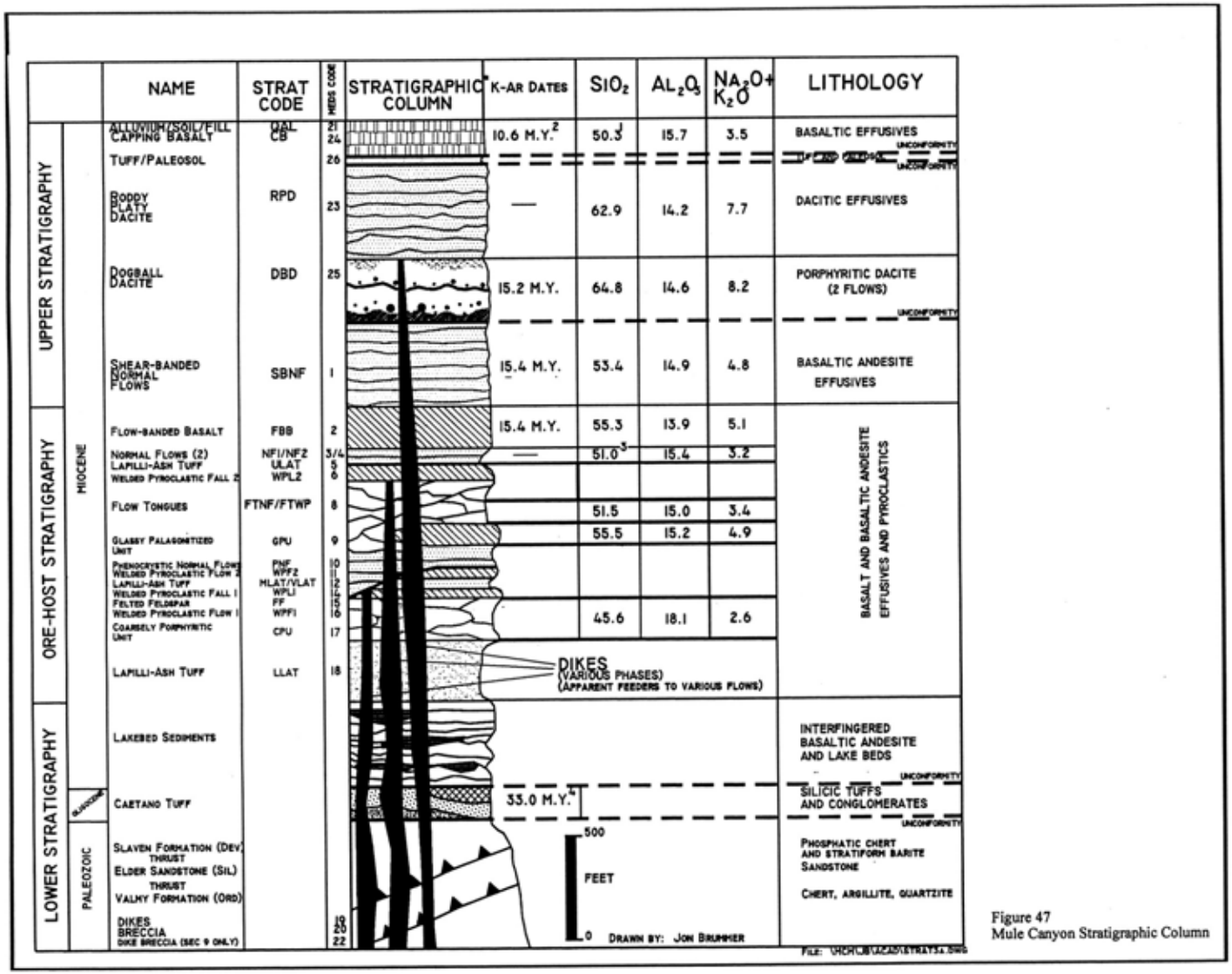

Figure 47
Mule Canyon Stratigraphic Column

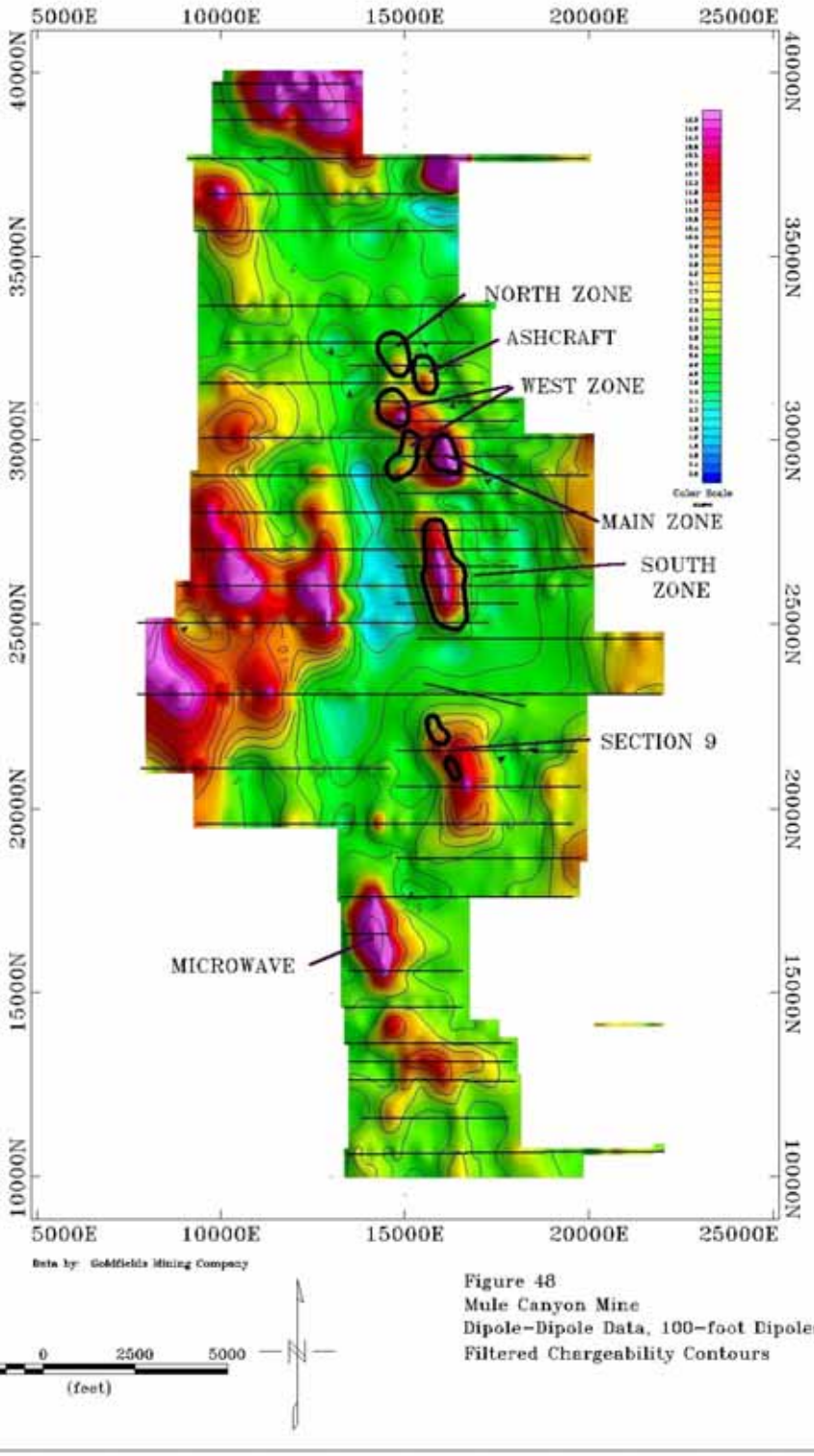

Figure 48
Mule Canyon Mine
Dipole-Dipole Data, 100-foot Dipoles
Filtered Chargeability Contours

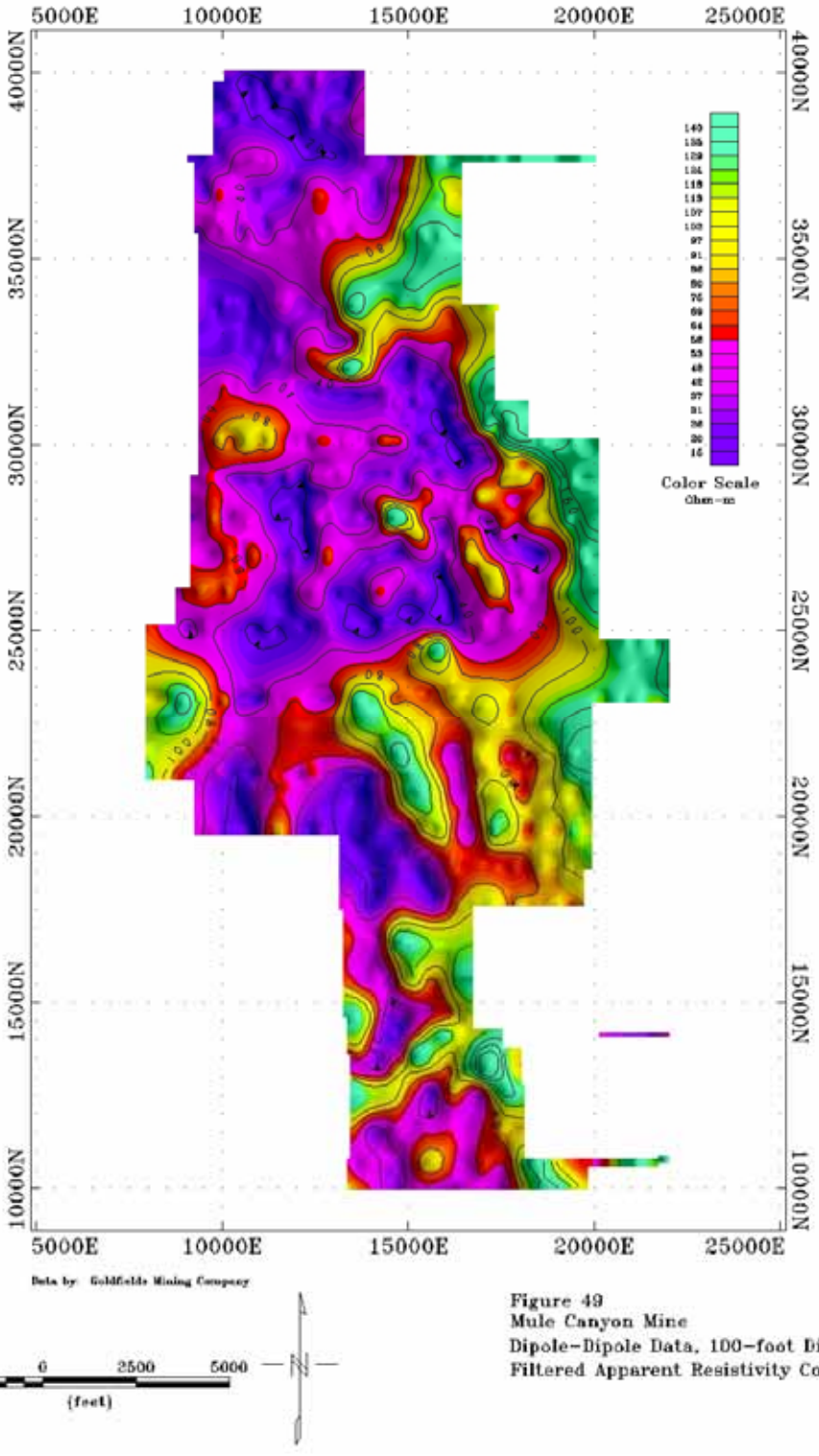

Figure 49
Mule Canyon Mine
Dipole-Dipole Data, 100-foot Dipoles
Filtered Apparent Resistivity Contours

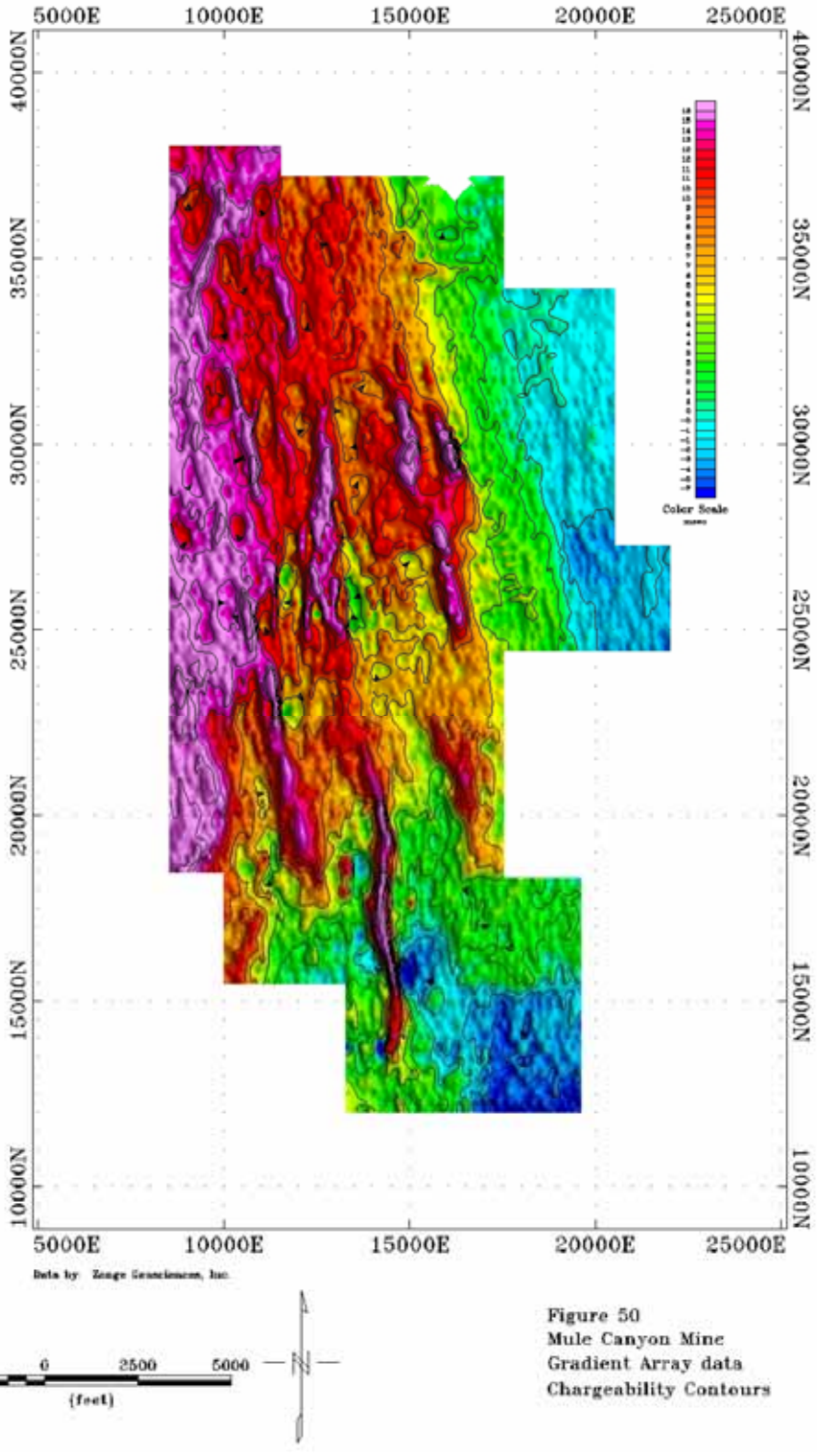

Figure 50
Mule Canyon Mine
Gradient Array data
Chargeability Contours

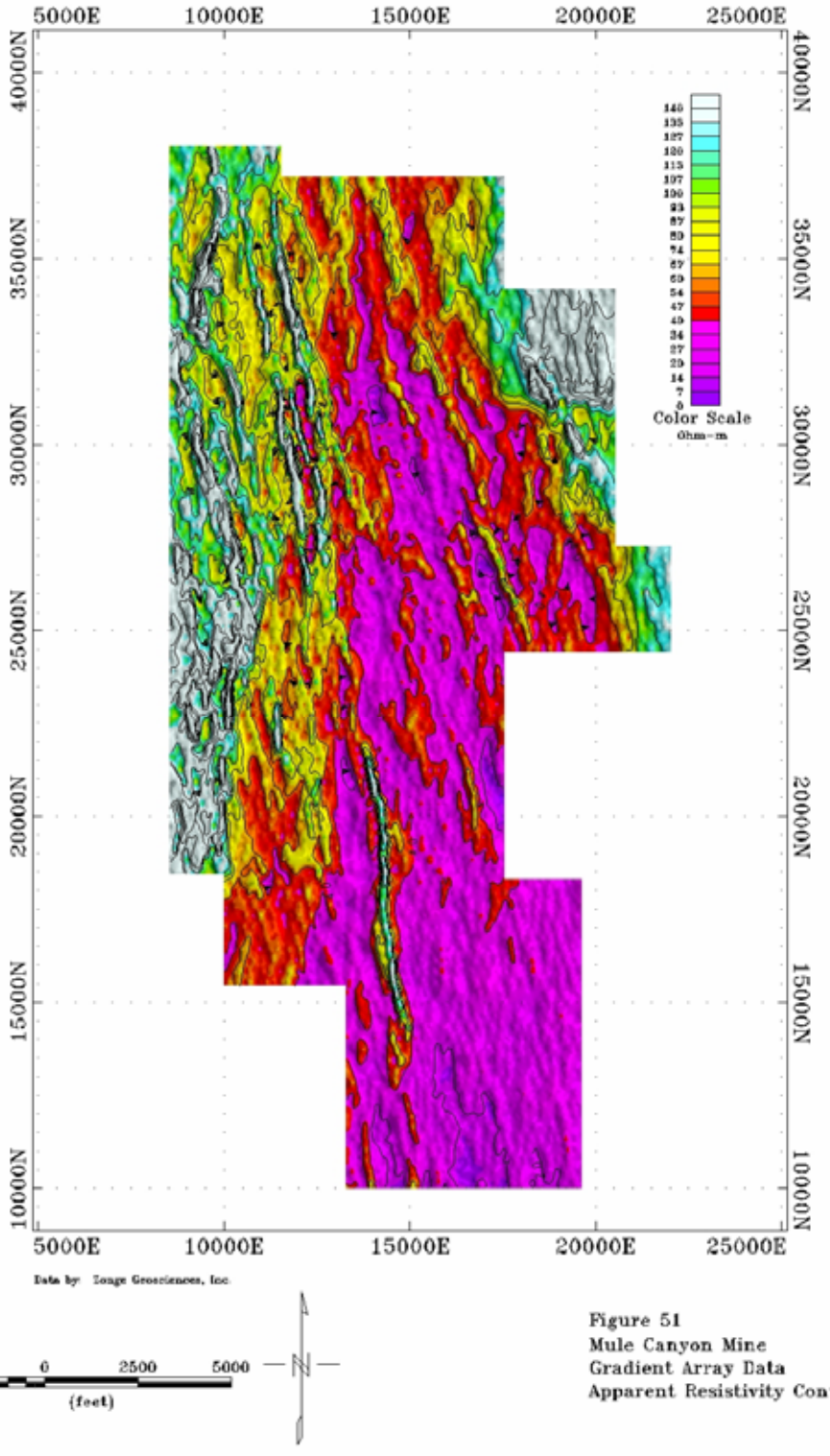

Figure 51
Mule Canyon Mine
Gradient Array Data
Apparent Resistivity Contours

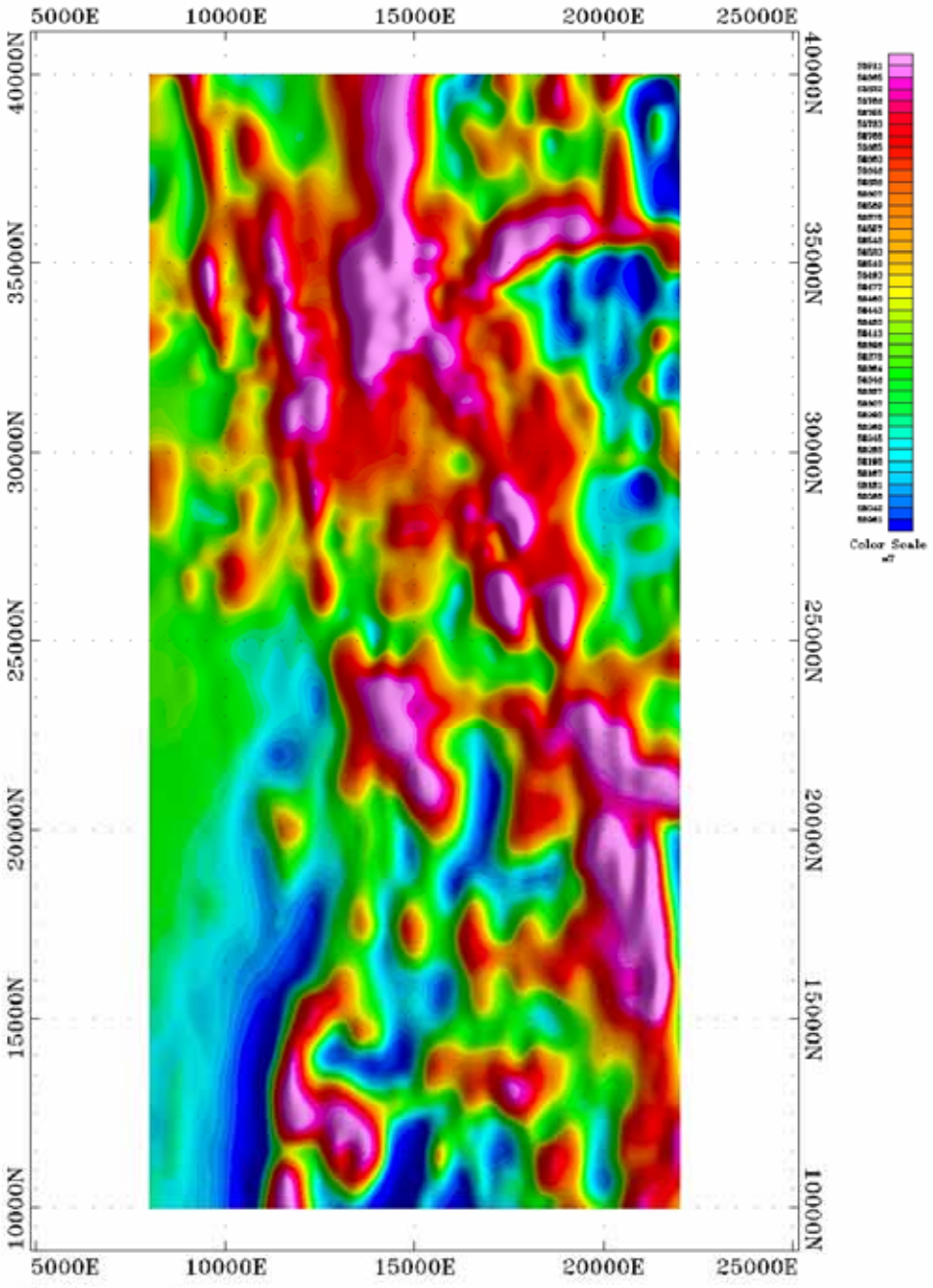

Figure 52
Mule Canyon Mine
Airborne Magnetic Survey
Total Field Intensity
Reduced to Pole

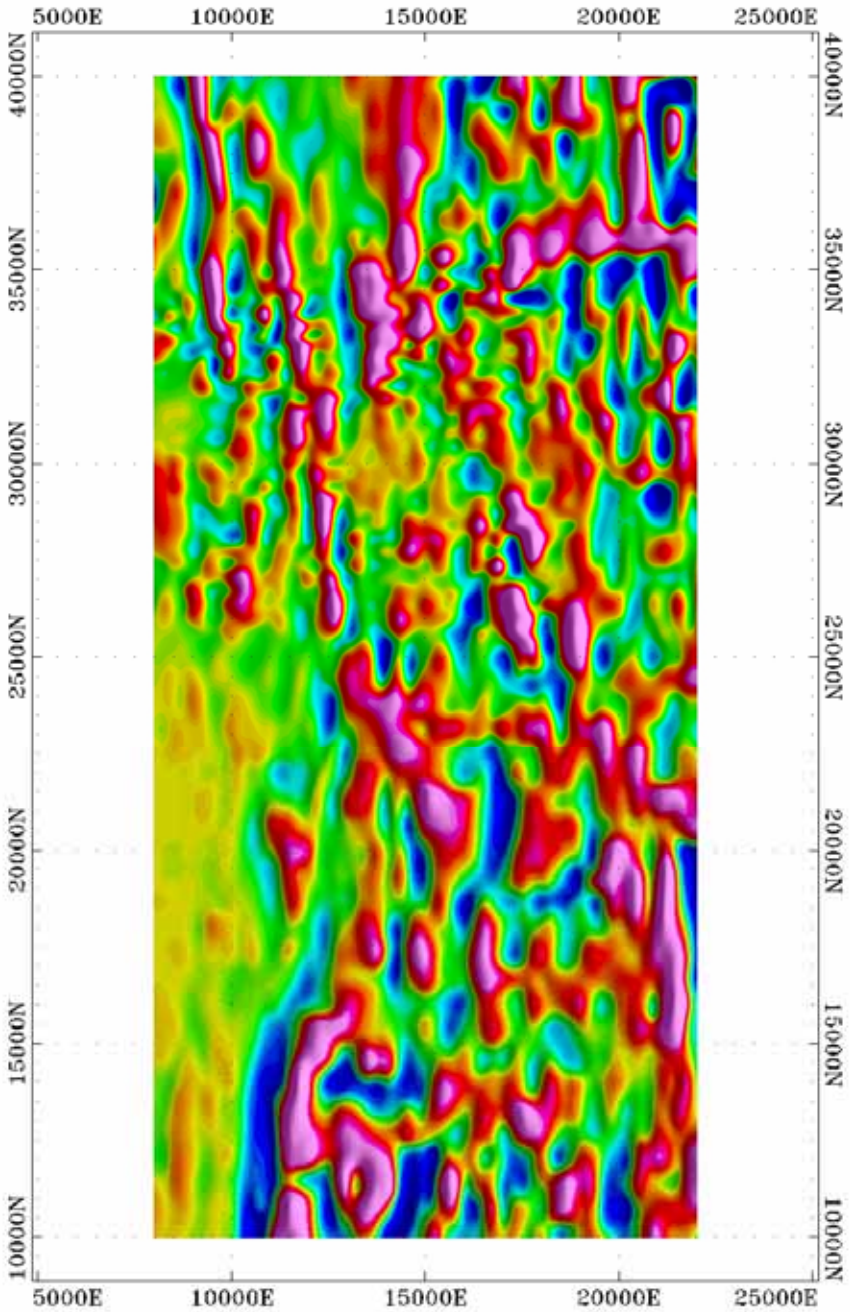

Figure 53
Mule Canyon Mine
Airborne Magnetic Survey
Calculated First Vertical Derivative of
Reduced to Pole Data

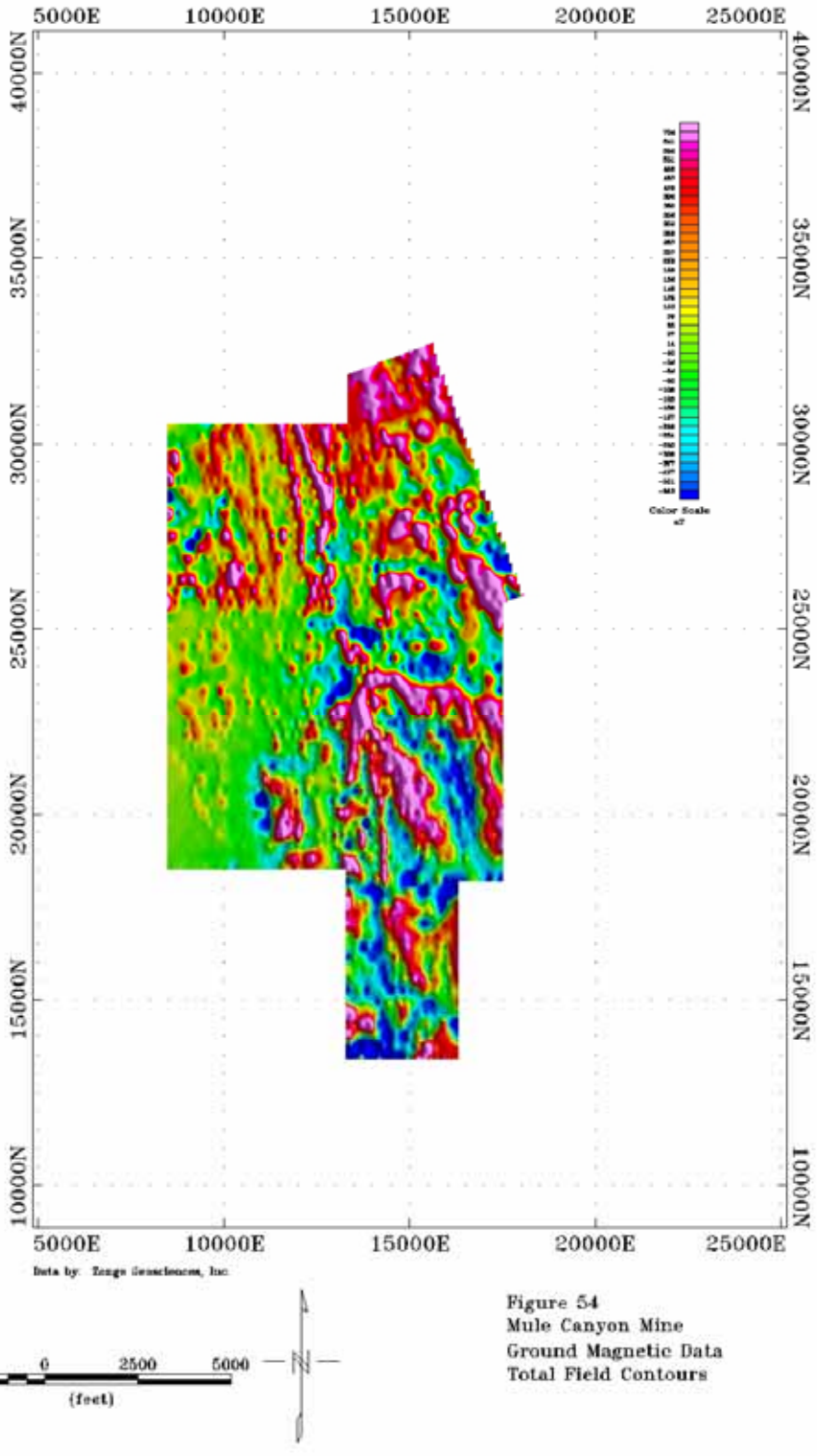

Figure 54
Mule Canyon Mine
Ground Magnetic Data
Total Field Contours

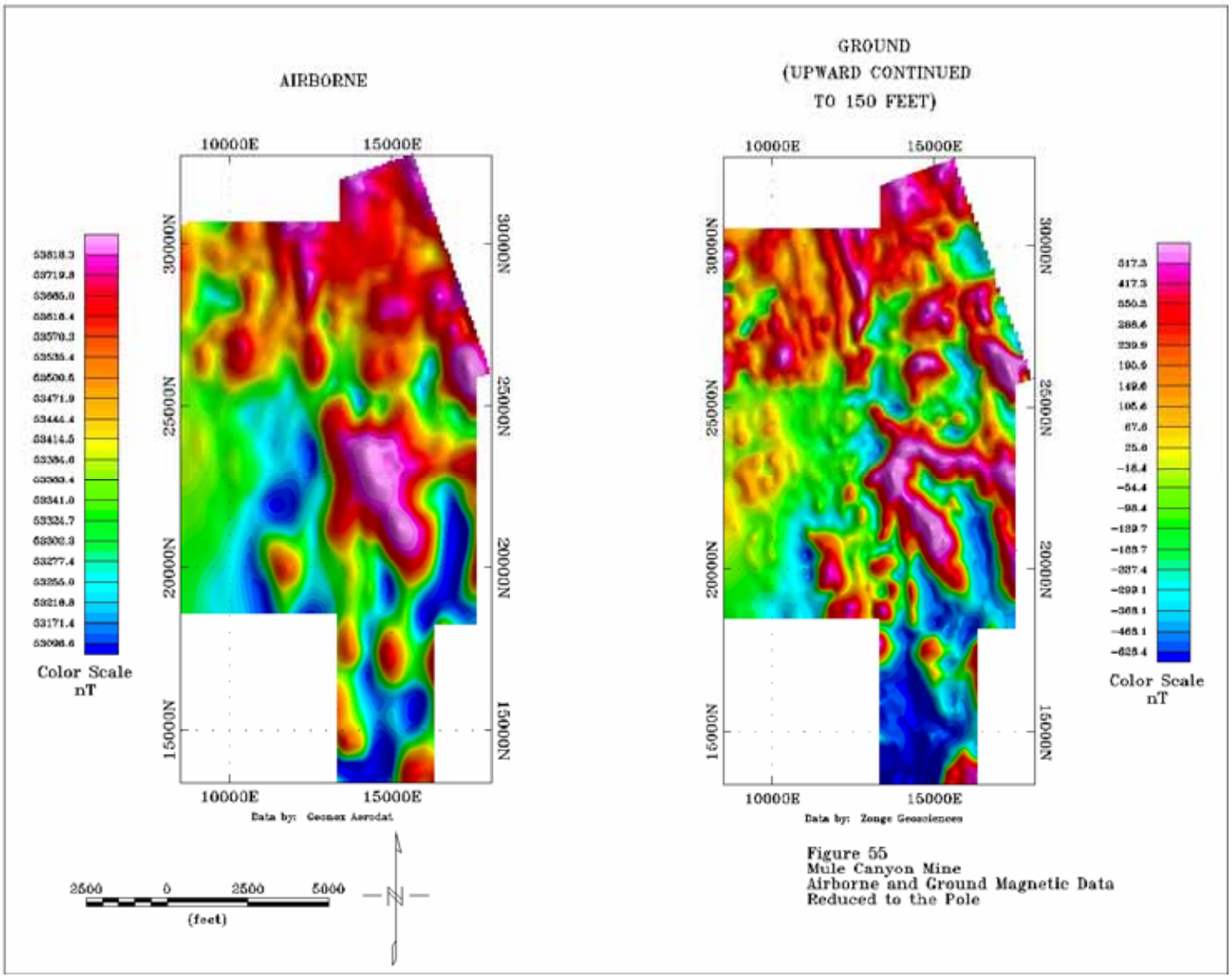

Figure 55
Mule Canyon Mine
Airborne and Ground Magnetic Data
Reduced to the Pole

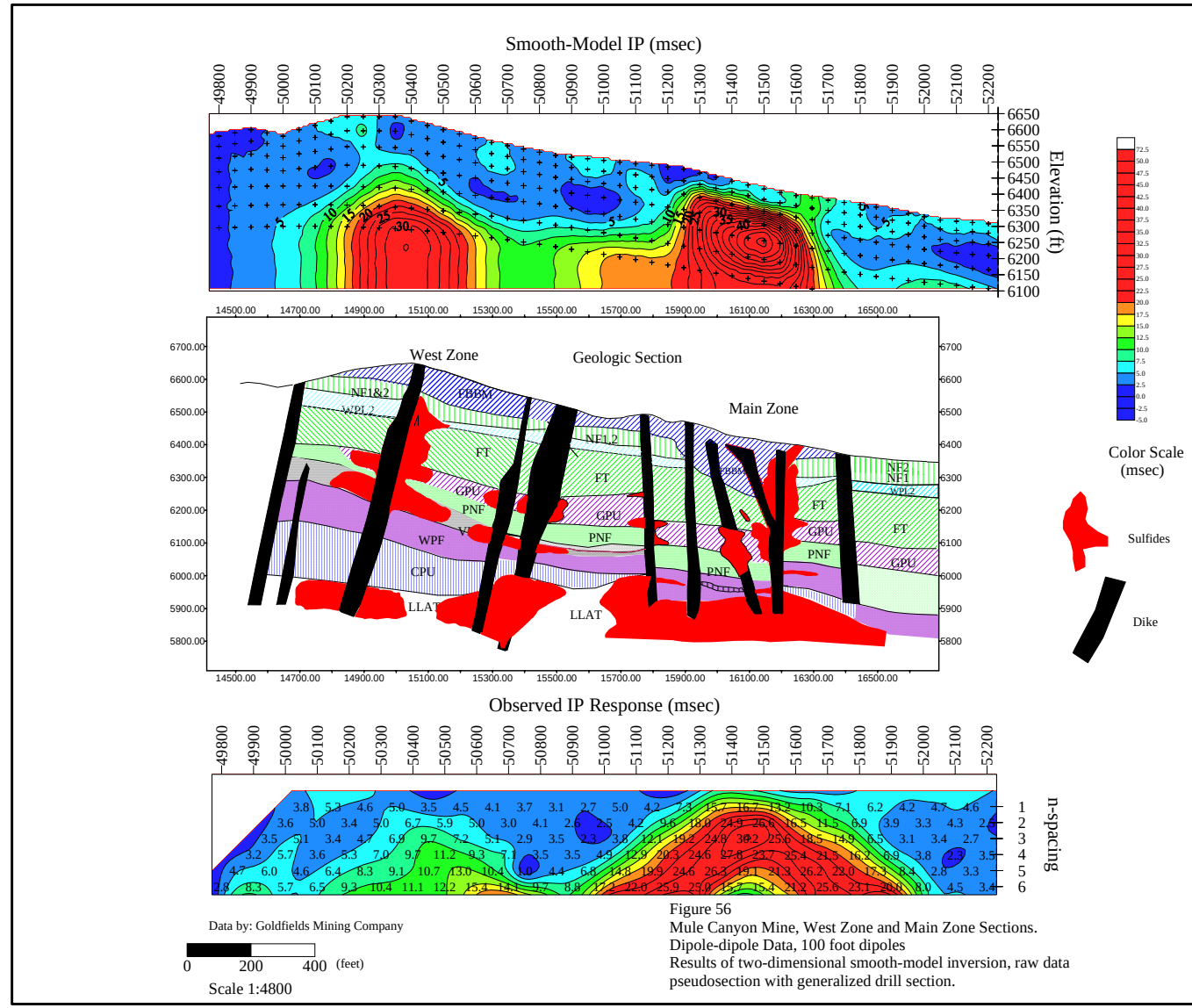

Data by: Goldfields Mining Company

0 200 400 (feet)

Scale 1:4800

Figure 56
Mule Canyon Mine, West Zone and Main Zone Sections.
Dipole-dipole Data, 100 foot dipoles
Results of two-dimensional smooth-model inversion, raw data pseudosection with generalized drill section.

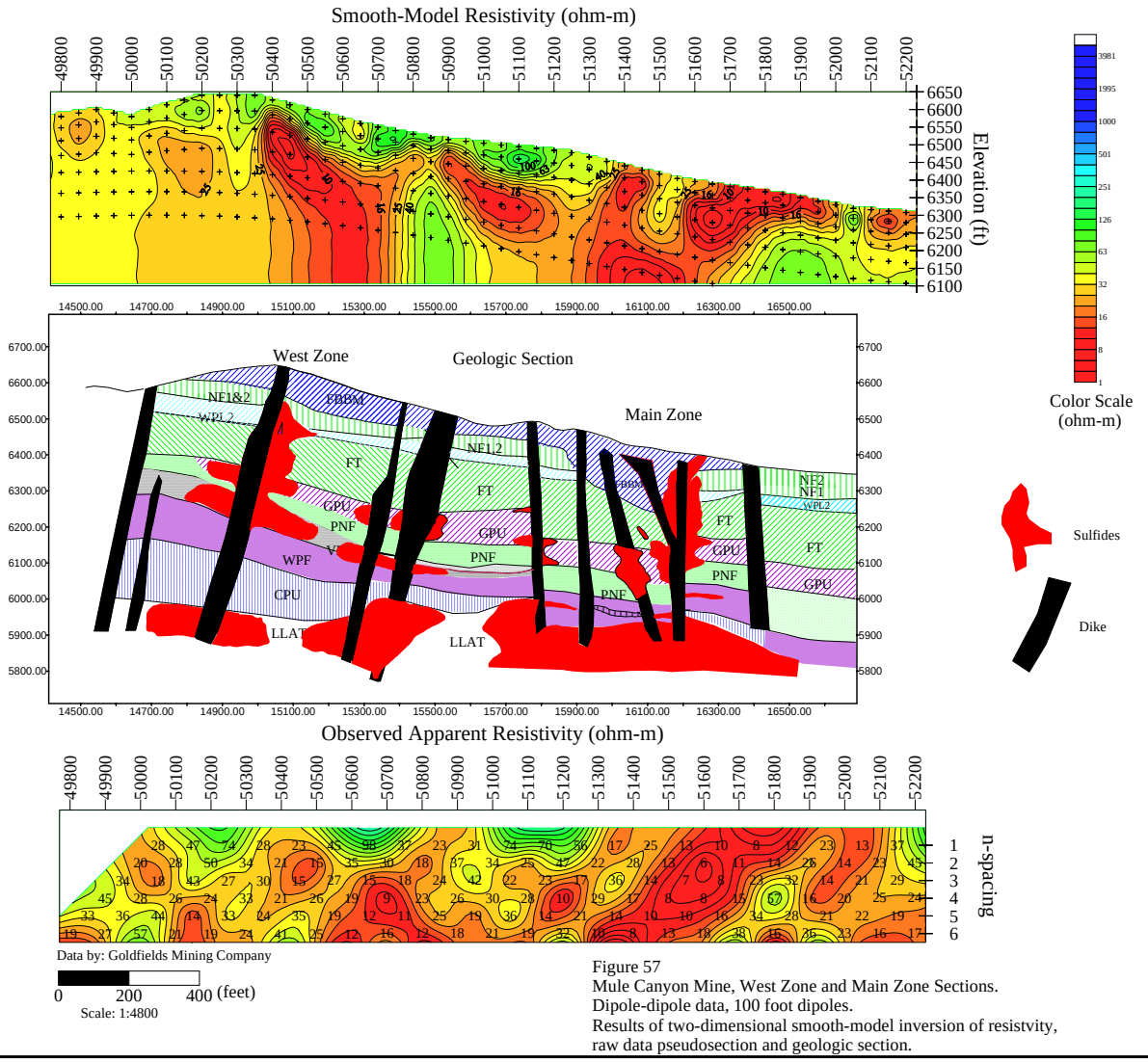

Figure 57
Mule Canyon Mine, West Zone and Main Zone Sections.
Dipole-dipole data, 100 foot dipoles.
Results of two-dimensional smooth-model inversion of resistvity, raw data pseudosection and geologic section.

This Page Left Blank